AN ABSTRACT OF THE THESIS OF

DAVID CAMPBELL JUNGE (Name) for the Ph. D. (Degree)

in MECHANICAL ENGINEERING (Major) presented on MAY 3, 1971 (Date)

Title: AN INVESTIGATION OF THE EFFECTS OF RADIAL ACCELERATION ON A FLUIDIZED BED USED FOR FILTRATION OF AIR-BORNE PARTICULATE OF SUB-MICRON SIZE

Redacted for privacy

Abstract approved: R. W. Boubel

The mechanisms which are involved in filtration of air-borne particulate matter have been established and reported in the literature. It has also been established that fluidized beds can act effectively as filters to remove air-borne particulate. Rotating fluidized beds have been studied but not in relation to their filtration characteristics.

In this experiment rotating fluidized beds were used to investigate the effects of radial acceleration on fluidized beds used for filtration of air-borne particulate of sub-micron size. Glass spheres with a mean diameter of 15 microns were used as the bed material and sodium chloride aerosols were used as the particulate matter. Level of radial acceleration was varied from 44 to 417 G's. Other independent variables included volumetric flow rate of gas through the bed and shape of the bed retainer. The dependent variable was filtration efficiency and accumulated running time on the bed was used

as a concomitant observation. The mass of the bed material was held constant for all tests.

The results indicate that the level of radial acceleration, the volumetric flow rate of gas through the bed, and the shape of the bed retainer all have a statistically significant effect on filtration efficiency at the 5% level of significance. The bed shape by flow rate interaction effect is also statistically significant at the 5% level. Further analysis of the data indicate that efficiency is related to the independent variables as follows:

$$\text{Eff.} = 1.25(V)^{-0.903}(\text{G-level})^{-0.1588}\left(\frac{H}{S}\right)^{-1.8531}\left(\frac{D_f\rho}{\mu}\right)^{-0.903}$$

Where:

V = Gas velocity at the discharge end of the fluidized bed cm/sec

G-level = Level of radial acceleration unitless

H = Operating bed height of fluidized bed cm

S = Diameter of the bed retainer at the discharge end of the bed cm

$D_f$ = Mean diameter of the bed material cm

$\rho$ = Density of the gas $gm/cm^3$

$\mu$ = Viscosity of the gas gm/cm-sec

Consideration of the mechanisms of filtration indicate that with respect to this experiment the predominant mechanisms are direct interception, Brownian diffusion, and electrostatic precipitation. Further research in the area of rotating fluidized bed filters is recommended.

# An Investigation of the Effects of Radial Acceleration on a Fluidized Bed Used For Filtration of Air-borne Particulate of Sub-micron Size

by

David Campbell Junge

A THESIS

submitted to

Oregon State University

in partial fulfillment of
the requirements for the
degree of

Doctor of Philosophy

June 1971

APPROVED:

Redacted for privacy

Professor of Mechanical Engineering
in charge of major

Redacted for privacy

Head of Department of Mechanical Engineering

Redacted for privacy

Dean of Graduate School

Date thesis is presented MAY 3, 1971

Typed by Mary Jo Stratton for David Campbell Junge

## ACKNOWLEDGEMENTS

I wish to express my thanks to the members of my doctoral committee for their efforts in regard to my graduate program. Their guidance and help has been greatly appreciated.

I also wish to acknowledge the following for particular contributions: the United States Public Health Service for financial assistance under fellowship 1 F3 AP 38, 718-01; the Oregon State University Computer Center for their financial support with respect to computer services; Jack Kellogg, mechanician, for his assistance in constructing the test equipment; Dr. Norbert Hartmann for his help with the statistical design and analyses of the data; and Mr. Robert D. Junge for his help in preparing this report.

Special thanks are offered to Dr. Richard W. Boubel for his guidance as my major professor, and to Professors James Knudsen and Octave Levenspiel for their help with respect to fluidized beds.

Doctoral Committee: R. W. Boubel, J. G. Mingle, F. D. Schaumburg, L. D. Calvin, T. E. Stitzel and G. Beecroft.

TABLE OF CONTENTS

Page

# LIST OF TABLES

LIST OF FIGURES

# AN INVESTIGATION OF THE EFFECTS OF RADIAL ACCELERATION ON FLUIDIZED BEDS USED FOR FILTRATION OF AIR-BORNE PARTICULATE OF SUB-MICRON SIZE

## I. INTRODUCTION

### The Problem

During the late 1940's it was established by Meissner and Mickley (10) that fluidized beds could serve to remove mists and dusts from air. More recent work carried out by Anderson and Silverman (2) in the mid 1950's and by Black (3) in 1966-67 has shown that fluidized beds can act as high efficiency filters for sub-micron size particulate matter suspended in air when they are operated under the proper conditions of bed height and superficial gas flow velocities. The electrostatic charge characteristic of the bed media is also an important variable.

Gas-solid phase fluidized beds are particularly adaptable to situations in which it is important to carry out a physical or chemical process on the bed material without removing the bed from operation. Because of this property, fluidized beds are commonly used in continuous catalytic cracking operations in the petroleum industry where it is necessary to regenerate the catalyst without taking the unit "off the line."

The regenerative capability of fluidized beds and their

applicability as filters for sub-micron size particulate suggest several important possible applications. For example, in space travel where we may soon be building space laboratories, manned moon laboratories, etc., it will be important to have available an efficient filtration system which can operate without interruption for extended periods of time, say several months or even years. It is not likely that such a system will be able to use "throwaway" filter elements; regenerative capability of the filter will be important.

Travel in space, however, may subject any system used for filtration to less than one "G" of gravitational force. Such a reduction could have an adverse effect on the operation of a fluidized bed unless it were counteracted by imposing some other force on the bed. One might, for example, place a bed of the appropriate material in a magnetic field. A second alternative would be to exert a centrifugal force on the bed by rotating the bed about its own axis or about an axis perpendicular to the axis of the bed.

The decision to counteract the loss of gravitational force on the bed by either of these methods requires some consideration of how much force to apply. Should one attempt to keep the bed under a combined effective influence of 980 $cm/sec^2$ at all times or is there some other mean acceleration value which might be applied to the bed which would optimize filtration efficiency?

This, in brief, is the problem. It has been established that

fluidized beds can act effectively as filters for sub-micron size particulate and that such beds do have regenerative capabilities. Thus, they may be useful as filters in space laboratories where these characteristics are desirable. In space travel, however, the bed may have to be subjected to radial acceleration forces to replace the "normal" gravitational forces found on Earth. It is not currently known what effect radial acceleration forces will have on a fluidized bed used for filtration of air-borne sub-micron size particulate matter. Such forces may serve to increase filtration efficiency or to decrease it. This is discussed in the Review of the Literature. The primary purpose of this study is to investigate the effects of radial acceleration on fluidized beds used as filters for sub-micron size particulate. The effects of varying the volumetric flow rate of gas through the bed and varying the shape of the bed retainer are also studied, since they are directly tied to fluidization characteristics under increasing radial acceleration levels.

# II. REVIEW OF THE LITERATURE

## Fluidized Beds

### History

The history of fluidization might be considered to date back to the sixteenth century when, according to a woodcut illustrated in Leva's text (8), the process was used in handling ore. The first patent using the process was issued in 1910 to Phillips and Bulteel in England and involved a fluidized catalyst in a reaction chamber. World War II fostered a need for high octane aviation gasoline in large quantities and this need brought about refinements in the art of fluidization in catalytic cracking processes. Research at the Massachusetts Institute of Technology by Professors W. K. Lewis and E. R. Gilliland contributed substantially to the field.

Currently fluidization is used in many applications such as heat exchangers, mass transport systems, mixing systems, drying and coating devices, roasting ovens, and absorption systems, to name a few. As Kunii and Levenspiel (7) point out, in these applications the principle reason for using fluidized bed operations is that relatively large quantities of solids can be treated in some way (i.e., transported, dried, or heated) and the fluidized bed provides a more efficient, convenient, and economical way for doing this than alternate

methods. Fluidization is also used in synthesis reaction control and other chemical processes where close temperature control of the reaction is necessary.

## Terminology

It would be well at this point to establish the terminology of this subject in order to avoid confusion of the terms used. Kunii and Levenspiel (7) have suggested the following definitions in their introductory remarks:

Fixed bed: A case in which a fluid is passing upward through fine particles at a low flow rate. The fluid merely percolates through the void spaces between stationary particles.

Incipiently fluidized bed or minimum fluidization: At the point where the fluid velocity is such that the particles are all just suspended in the upward flow the bed is considered to be just fluidized. At this point the frictional force between a particle and the fluid counterbalances the weight of the particle, the vertical component of the compressive force between adjacent particles disappears, and the pressure drop through any section of the bed about equals the weight of fluid and particles in that section.

Particulately, homogeneously, smoothly, or liquid fluidized bed: In liquid-solid systems an increase in flow rate above minimum fluidization usually results in a smooth, progressive expansion of the

bed. Gross flow instabilities are damped and remain small, and large scale bubbling or heterogeneity is not observed under normal conditions.

Aggregative, heterogeneous, bubbling fluidized bed: In gas-solid systems the nature of fluidization is generally quite different compared to liquid-solid systems. With an increase in flow rate beyond minimum fluidization, large instabilities with bubbling and channeling of gas are observed. At higher flow rates agitation becomes more violent and movement of solids is more vigorous. In addition, the bed does not expand much beyond its volume at minimum fluidization. In a few rare cases liquid-solid systems will not fluidize smoothly and gas-solid systems will not bubble.

Dense-phase fluidized beds: Both gas and liquid fluidized beds are considered to be in dense-phase as long as there is a fairly clearly defined upper limit or surface to the bed.

Disperse, dilute, or lean-phase fluidized beds: At a sufficiently high fluid flow rate through the bed, the terminal velocity of the solids is exceeded and the upper surface of the bed disappears, entrainment becomes appreciable, and solids are carried out of the bed with the fluid stream.

Slugging: A phenomenon strongly affected by the vessel geometry. Gas bubbles coalesce and grow as they rise. In a deep enough bed they may become large enough to spread across the vessel.

Thereafter the portion of the bed above the bubble is pushed upward as by a piston. Particles rain down from the slug and it finally disintegrates. Slugging is usually undesirable since it increases the problems of re-entrainment and lowers the performance potential of the bed for both physical and chemical operations. It is especially serious in long, narrow fluidized beds.

## Advantages

The major advantages of fluidized systems listed by Leva(8) are:

1. Continuous operation. Spent solids are easily removed from the system to be reactivated and returned to the system.
2. Flat temperature profiles. These result from intense particle and gas mixing.
3. High heat transfer coefficients.
4. Relatively low pressure drops through fluidized beds.
5. No special catalyst size preparation required.

Thus, a fluidized bed provides unique characteristics that may enhance many commercial applications.

Work done by many investigators in the field of fluidization has resulted in reasonably well established principles of operation of fluidized beds in terms of such parameters as pressure differential across the bed, minimum fluidizing velocities, and maximum velocities which can be achieved before re-entrainment. A substantial amount

of effort has also gone into the determination of mathematical models for fluidized beds to evaluate heat and mass transfer properties and bubble formation.

## Filtration

The object of filtration is to separate suspended matter from the carrier medium. For the case of small aerosols in a gas stream, seven mechanisms of filtration are recognized. These are discussed in detail in a report published by the American Petroleum Institute (1) and include the following:

1. Direct Interception
2. Inertial Impaction
3. Brownian Diffusion
4. Electrostatic Precipitation
5. Gravitational Settling
6. Thermal Precipitation
7. Sieving

For the situation of the rotating fluidized bed, the last two mechanisms do not apply. Thermal precipitation requires a thermal gradient which does not exist in a fluidized bed and sieving can only occur when the filter elements are fixed and sufficiently close so that the suspended particles cannot pass between them.

On the other hand, the first five mechanisms may apply to a

rotating fluidized bed. Black (3), in his work with fluidized beds used as filters, considered the significance of the first four with respect to his experimental results and concluded that direct interception was the key mechanism involved. He did not give more than passing mention to the gravitational settling mechanism, apparently feeling that it was not significant in his work.

The API report notes that collection efficiency due to gravitational settling is a direct linear function of the level of gravitational acceleration. If this applies to a rotating fluidized bed filter, then at 400 G's, one would expect filtration due to this mechanism to be 400 times more effective than at 1 G.

Considering the other mechanisms, the report indicates that gravitational terms are not involved in the mathematical models. Thus, any increase in G-level would not affect filtration efficiency due to direct interception, inertial impaction, Brownian diffusion, or electrostatic precipitation.

Under conditions of increasing radial acceleration in a fluidized bed, it is necessary to increase the velocity of the gas stream through the bed in order to keep the bed fluidized. In the mathematical models for filtration mechanisms, the gas velocity term frequently appears. Table 1 lists the filtration mechanisms and indicates the relationship of any gas velocity terms present to the filtration efficiency attributed to each of the mechanisms.

Table 1. Velocity terms found in the mathematical models of filtration mechanisms.

| Mechanism | Relationship of velocity term to filtration efficiency |
|---|---|
| Direct Interception | Not applicable |
| Inertial Impaction | Direct - linear |
| Brownian Diffusion | Inverse - linear |
| Electrostatic Precipitation | Inverse - linear |
| Gravitational Settling | Inverse - Cubic |

From Table 1 it can be seen that any increase in gas velocity through the bed would increase the effectiveness of the inertial impaction mechanism. At the same time, it would decrease the effectiveness due to the mechanisms of Brownian diffusion, electrostatic precipitation, and gravitational settling.

In summary of the preceding discussion, the effect on filtration efficiency due to increasing only G-level (holding all other operating parameters constant) should be to increase filtration efficiency (due to the gravitational settling mechanism). But increasing G-level requires that gas velocities also be increased if the bed is to remain fluidized. Three of the five mechanisms for filtration are related inversely to gas velocity while only inertial impaction is directly related. Therefore, net filtration efficiency may decrease with increasing gas velocity. This is dependent upon the relative influence of the filtration mechanisms involved.

It is recognized that the net filtration action is a summary effect of all of the mechanisms involved. Furthermore, one or more of the mechanisms may be involved at the same time, but it is not necessary that all mechanisms be involved. Silverman (2) has offered a general guide to situations where the mechanisms apply:

| Mechanism | Particle Size (in microns) |
|---|---|
| Direct Interception | >1 |
| Inertial Impaction | >1 |
| Brownian Diffusion | <0.01 to 0.5 |
| Electrostatic Precipitation | <0.01 to 5.0 |
| Gravitational Settling | >1 |

It should be noted, however, that Silverman's summary was not directly connected with conditions of a rotating fluidized bed. Nor was it established specifically to include a bed of glass beads with a mean diameter of 25 microns used to filter sub-micron sized sodium chloride aerosols. Therefore, care should be exercised in applying his guide to this particular experiment.

Another factor is involved in filtration in fluidized beds. If the flow rate through the bed is high and/or the geometry of the bed is incorrect, slugging may result as well as a general increase in the bubbling or aggregative mode of fluidization. This would have a tendency to reduce the contact of the bed material with particles passing through the bed and, therefore, would reduce filtration. However,

Hatch (5) found a definite tendency toward bubble suppression in his investigations of fluidized beds operating under high centrifugal loads. So for the higher G-levels, it is possible that this factor will not have a negative influence on filtration.

## Fluidized Bed Filters

A search of the available literature has resulted in only limited findings of the works of authors concerning fluidized beds used as filters. As previously mentioned, Meissner and Mickley (10) reported the results of laboratory experiments in which they investigated the use of fluidized beds for removal of mists and dusts. Their work deals with the removal of acid droplets in the 2 to 14 micron diameter range and involves bed materials of aluminum silicate, silica gel, and alumina. Collection efficiencies approaching 90% were attained for short periods of time.

Using the findings of Meissner and Mickely as a starting point, Anderson and Silverman (2) carried out an extensive study entitled, "Mechanisms in Electrostatic Filtration of Aerosols with Fixed and Fluidized Granules," in which fluidized beds were used to filter particles from an air stream. This study was divided into three parts: (1) An investigation of the electrostatic chargeability of certain high polymers both by batch and by continuous means; (2) A study of the filtration characteristics of packed beds of granules (both highly

insulating and conducting) in the fixed and fluidized states with emphasis on the electrostatic mechanisms involved; and (3) An analysis of the energy requirements (especially resistance to flow) of such beds as a function of their filtration ability.

In the second part of their study, the fluidized media tested were Koppers Dylene-polystyrene beads ranging from 250 to 590 microns in diameter. Using what was described as "indoor atmospheric dust" as a challenging aerosol in the initial tests, filtration efficiencies were measured in the range of 97% to 98%. Later tests were conducted in which Gentian Violet was chosen as the test aerosol and efficiencies up to 98% were observed. Independent variables in the experiments included gas velocity through the bed, electrostatic charge on the bed media, and the length of time in which the bed had been in service.

As a result of their tests, Anderson and Silverman concluded that an electric charge could be generated within a fluidized bed due to a phenomenon known as "triboelectrification," or the acquisition of a net electrostatic charge on a bed due to contacts of the fluidized media with conducting surfaces interspersed throughout the bed. Such a net charge is extremely influential in filtration efficiency. For example, in one series of tests a twelvefold increase was noted in collection efficiency due to the use of electrostatically charged filter media.

Black (3) also carried out a study regarding the effectiveness of a fluidized bed in filtration of airborne particulate of sub-micron size. In this it is found that filtration efficiency is primarily a function of the bed height-to-diameter ratio and the superficial gas velocity. This is expressed as:

$$\text{Eff.} = 0.565 \frac{h^{0.4}}{V_o^{0.1}} \qquad (1)$$

Under the conditions of his experiment, no effective changes in filtration efficiencies of the fluidized bed were found as a result of bed age or changes in challenging aerosol concentration. It should be noted that the bed material was glass spheres with a geometric mean diameter of 25 microns and the challenging aerosol was sublimated ammonium chloride particulate. Concentrations of aerosol ranged from 0.03 to 8.3 mg per cubic meter.

While there have been no other investigations reported in the literature on the use of fluidized beds as filters for particulate matter, there have been a substantial number of articles published concerning their use as "filters" for gases. Most of these units involve adsorption systems or catalyzed chemical reactions in which a fluidized bed provides an efficient, physical environment for the reactions to take place.

In addition to studies of the use of fluidized beds as filters, a substantial amount of work has been going on during the past 16 years

on the development of fluidized beds in general. Most of this work centers about heat and mass transfer studies and is being carried on extensively in the United States, England, and Russia. A list of books and journals dealing with this subject matter is presented in Appendix D.

## Rotating Fluidized Beds

In reviewing various texts, journals, etc., the writer has found that work dealing with rotating fluidized beds has been undertaken on at least three separate occasions. In 1960, Gel'perin (4) published a paper in Russian entitled "Apparatus with Fluidized Beds of Free-flowing Materials in Centrifugal Fields" in which is described a fluidized bed using granular material in a centrifugal force field on the inner surface of a rotating cylindrical screen. Figure 1 shows a sketch of the apparatus with a centrifugally "compressed" fluidized bed.

The fluidizing gas is fed into the shell (1) and passes from the periphery to the axis of the apparatus through the screen-like side walls of the cylindrical rotor (2), fluidizing the material which is thrown against the inner surface of the screen by the centrifugal force. Material is fed into the apparatus through the hollow shaft (3). The effluent gas leaves through the second hollow shaft (4). The baffle plate (5) prevents the material being fed in through (3) from passing

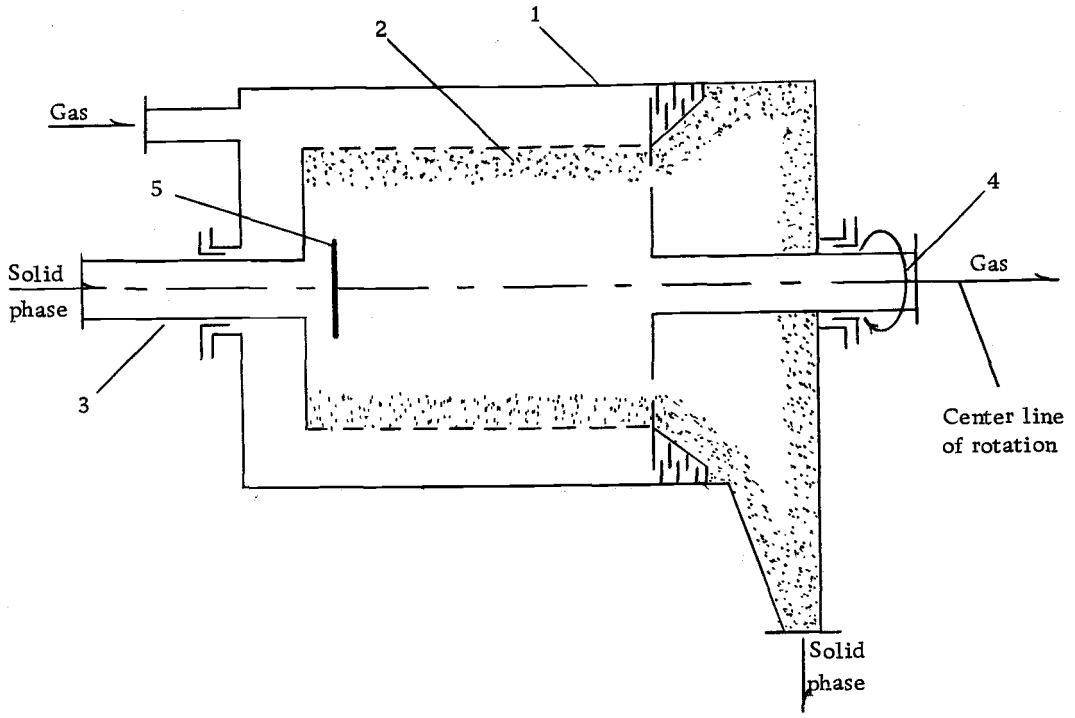


Figure 1. Apparatus used by Gel'perin in studies of fluidized beds operating in centrifugal fields.

directly into (4) and facilitates the spreading of the particles on the screen.

Gel'perin notes that in this type of equipment it is easy to achieve a marked increase in the gas throughput per unit area of bed compared with ordinary fluidized beds at the same gas pressure and material particle size. The limit to the throughput is set by the critical velocity of entrainment of the particles from the bed. For an ordinary bed, this cannot exceed the velocity of free fall of the particles in a gravitational force field. However, in this rotating design, entrainment is opposed by a centrifugal acceleration which

may be several times larger than that due to gravity when the rotor is spinning rapidly. The drawbacks of this equipment, according to the author, are the relative complexity of the apparatus and the presence of massive rotating parts.

A second study of rotating fluidized beds was undertaken at the Los Alamos Scientific Laboratory in 1962-63 (9). In this work two designs of rotating beds were used. The first is shown in Figure 2.

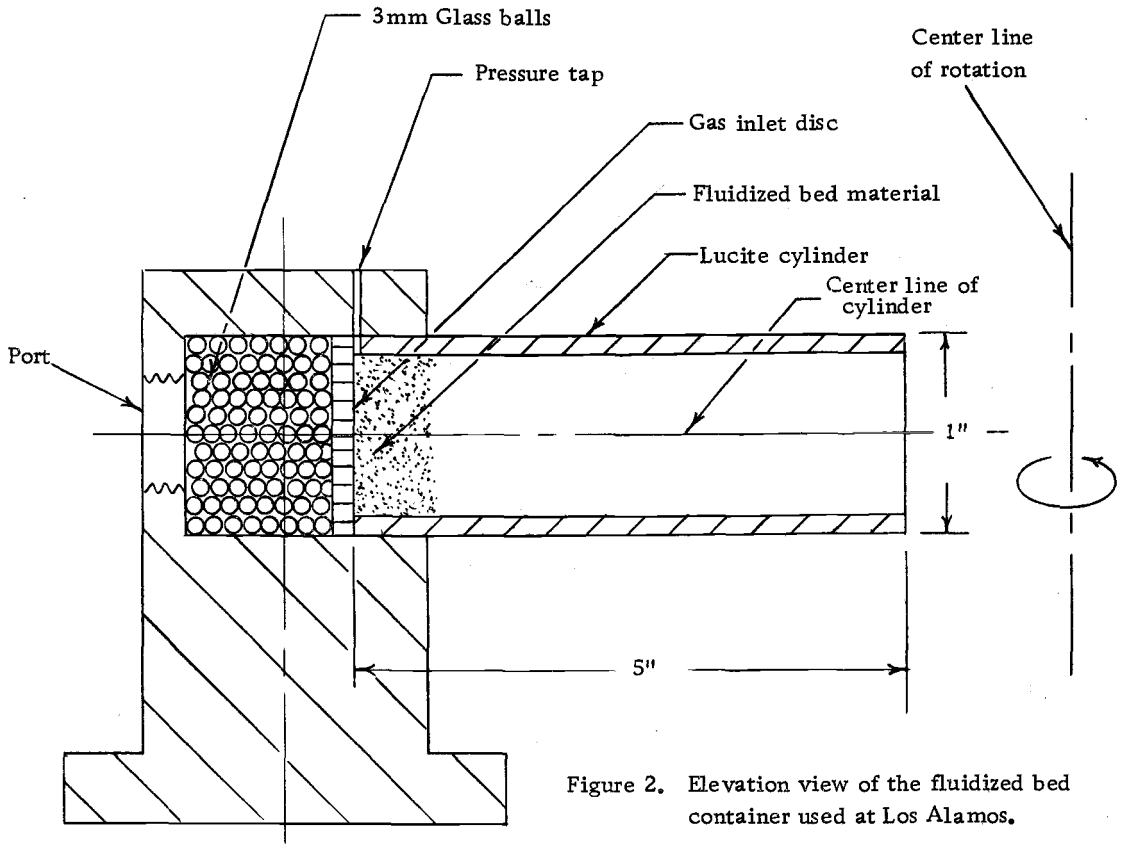


Figure 2. Elevation view of the fluidized bed container used at Los Alamos.

This container was fastened to a wheel with a vertical axis, so that it moved in a horizontal plane. The radius of rotation at the base of the bed was approximately 51 centimeters and the angular velocity was controlled to provide radial accelerations up to 147 G's. The

independent variables in the study included the type of fluidizing gas, bed material, radial acceleration level, gas flow rate, and bed depth. Of primary interest were the mechanical aspects of minimum fluidization in the rotating bed such as pressure differentials, bubble formation, and modes of fluidization.

The second design of rotating fluidized bed used at Los Alamos is shown in Figure 3. In this unit the bed was distributed about $360^{o}$ and could be operated up to 150 G's at the outside diameter of the 112 centimeter rotating assembly. The bed itself was 1.27 centimeters thick and consisted alternately of sand, steel shot, glass balls, and alumina bubbles. Other independent variables in the tests included gas flow rate, particle sizes, bed depths and radial acceleration level. Again the prime concern of the tests was to investigate the nature of fluidization in a rotating system. Note that considerable effort was expended to be able to photograph the bed during operation. This was quite successful from the standpoint of being able to observe bubble formation, bed voidage, and modes of fluidization in a rotating bed.*

Following the completion of the work at Los Alamos, the Nuclear Engineering Department of the Brookhaven National Laboratory in New York undertook further studies of rotating fluidized beds under the direction of Hatch (5). Their initial work dealt with a bed design very

---

*Films of the rotating bed in operation are available and are listed in the Los Alamos report (9).

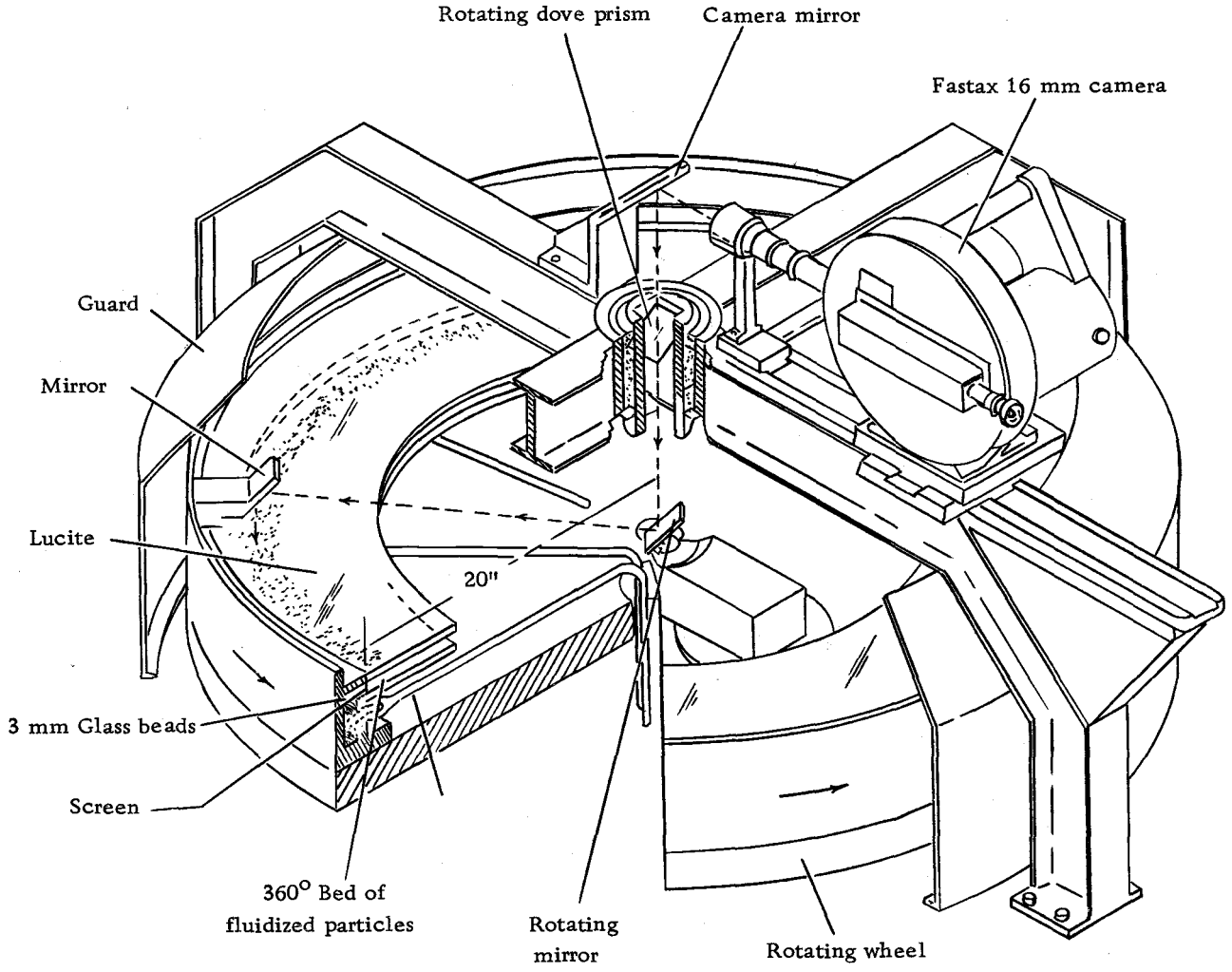


Figure 3. A cutaway perspective view of the 360° fluidized bed and associated machinery.

similar to that used in the first runs at Los Alamos. That is, the axis of the cylindrical bed was perpendicular to the vertical axis of rotation as shown in Figure 4.

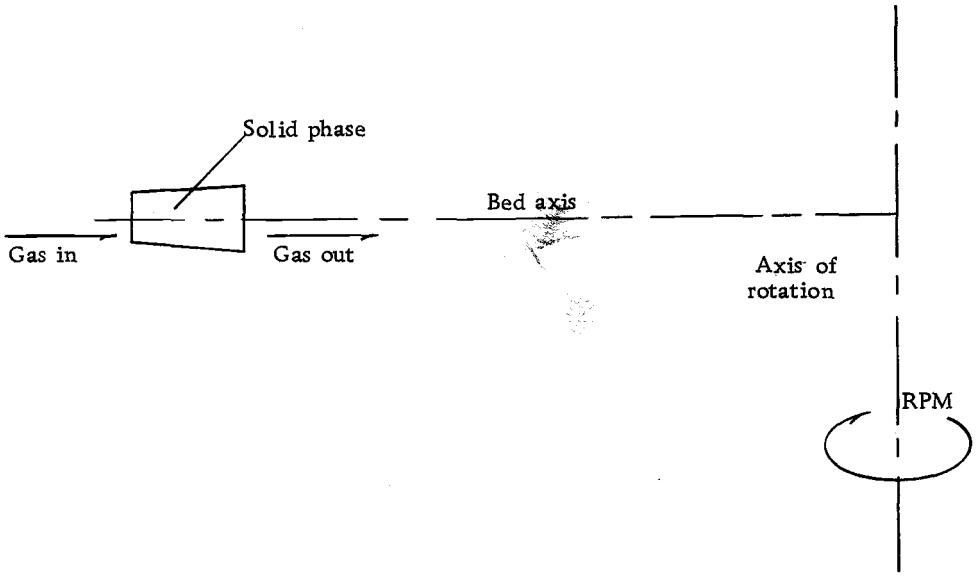


Figure 4. Apparatus used initially by Hatch in studies of fluidized beds in centrifugal fields.

No report was published concerning this work. According to Hatch this early experimentation convinced him that it would serve his needs better to go to a design similar to that used by Gel'perin. The Brookhaven Laboratory at that time was working with mass and heat transfer research for nuclear reactors with support from the AEC. Accordingly, they proceeded to the design shown in Figure 5, which is very much like that used by Gel'perin, except that in this design the granular material remains in the bed rather than flowing through the bed continuously.

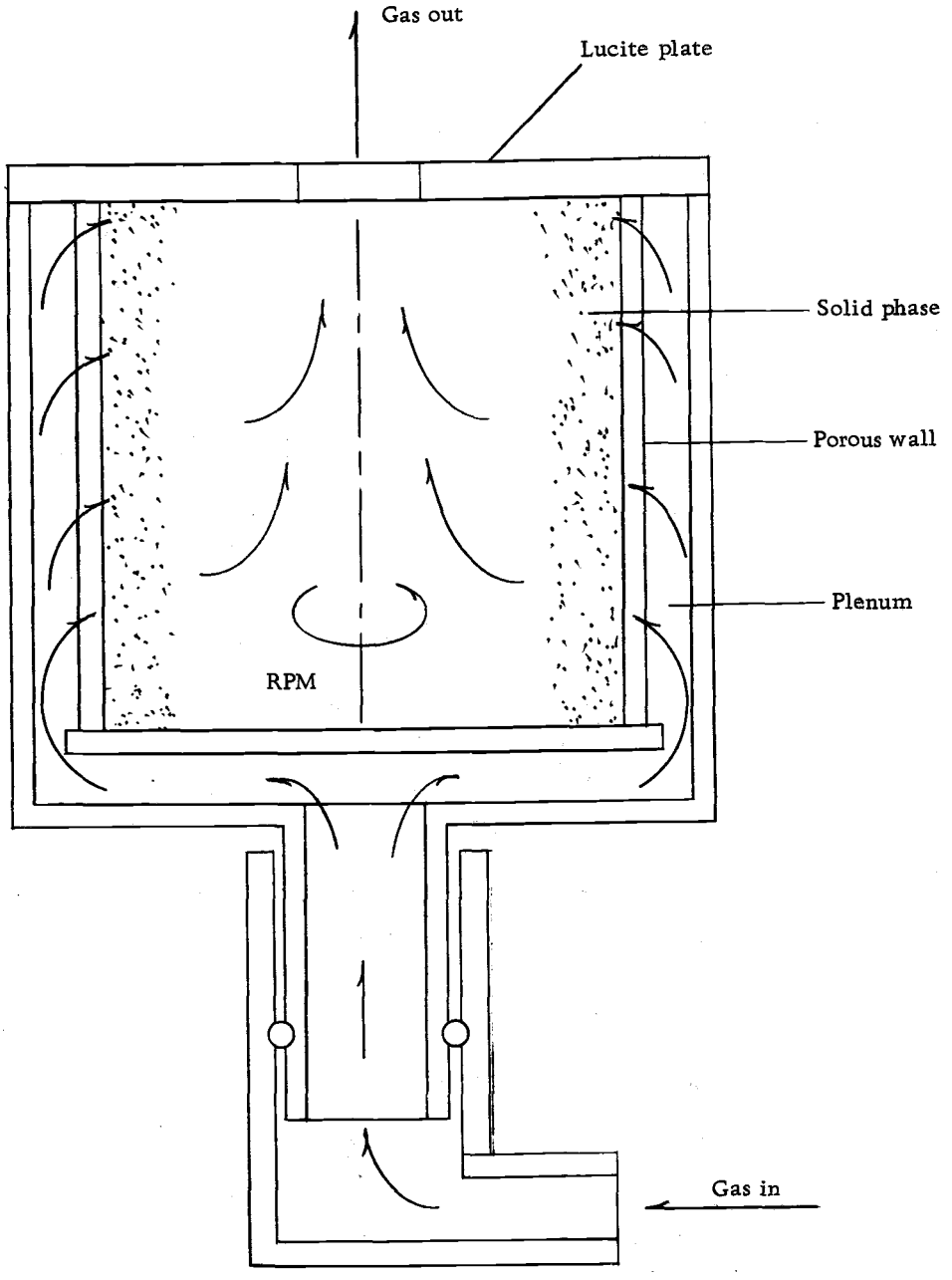


Figure 5. Apparatus used by Hatch to study fluidized beds in centrifugal fields where the bed is rotated about its own axis.

In the original equipment (Figures 4 and 5), Hatch had achieved radial accelerations up to 3500 G's. In the second arrangement accelerations up to 10,000 G's were planned. However, at the time the report was written experiments had been carried out only to 2000 G's. The main thrust of their work was to observe the beds in high gravity fields and to note their behavior, mainly with respect to gas bubble formation. Here they observed a definite tendency of the apparatus to inhibit bubble formation while operating at high radial accelerations. According to Hatch, the tests were never completed due to lack of financial support.

# III. EXPERIMENTAL PROGRAM

## Objectives

The objective of the experimental program was to investigate the effect of radial acceleration on fluidized beds used for filtration of airborne particulate of sub-micron size. Within this broad category were the following more specific objectives:

(1) To investigate the effect on filtration efficiency of three independent variables:

   a. Radial acceleration,

   b. Volumetric gas flow rate through the fluidized bed,

   c. Mode of fluidization as controlled by the shape of the bed retainer.

(2) To investigate interaction effects of the three independent variables shown above on filtration efficiency.

(3) To investigate the general behavior of a fluidized bed operating under high radial acceleration loads.

## Description of the Equipment

In order to meet the objectives noted above, experimental equipment was designed and constructed according to the following criteria:

(1) A fluidized bed must be constructed in which changes can be

made in the following:

a. Level of radial acceleration;

b. Rate of flow of the gas stream through the bed;

c. Shape of the bed retainer.

(2) The fluidized bed must rotate about an axis perpendicular to the axis of the bed. It must also rotate in a horizontal plane to maintain a constant resultant gravitational and radial acceleration force for any given angular velocity.

(3) Changes to the angular velocity of the system should be relatively simple and quick to make. Once the velocity for the system is established, it must be held constant.

(4) The rotating system must be easily balanced for smooth operation at high angular velocities.

(5) Air must be supplied to the bed in order to fluidize it in the rotating condition.

(6) The air stream to the bed must be reasonably dry, free of undesirable contaminants such as rust, oil, etc., and controllable with regard to pressure and flow rate.

(7) Aerosols must be generated and injected into the fluidizing air stream in order that studies can be conducted on the removal of such aerosols by the fluidized bed. The aerosols must be reasonably consistent in terms of size and concentration.

(8) The bed must be visible during operation in order that observations can be made on the modes of fluidization.

(9) The bed retainer must be of sufficient strength to withstand the stresses placed on it due to internal pressure and radial acceleration loads. It must also be easily removable from the system for cleaning and changing.

(10) It must be possible to remove the bed material from the system and replace it easily.

(11) It must be possible to collect a representative sample of the aerosol concentrations entering and leaving the fluidized bed.

(12) Sufficient instrumentation must be provided to measure temperatures, flow rates, pressure, and other pertinent parameters of the bed operation.

A schematic diagram of the system used in shown in Figure 6. A discussion of each of the system components follows.

Note that in describing this equipment, engineering units are used predominantly rather than metric units. This was done to avoid confusion. For example, 1-1/4" valves are mentioned rather than 3.17 cm valves. Much of the data taken is also in engineering units corresponding to the scales used on pressure gages, thermometers, and manometers. Filter weights are recorded in grams, corresponding to the scale on the laboratory balance. However, in order to maintain consistency in units, all of the data are converted to metric

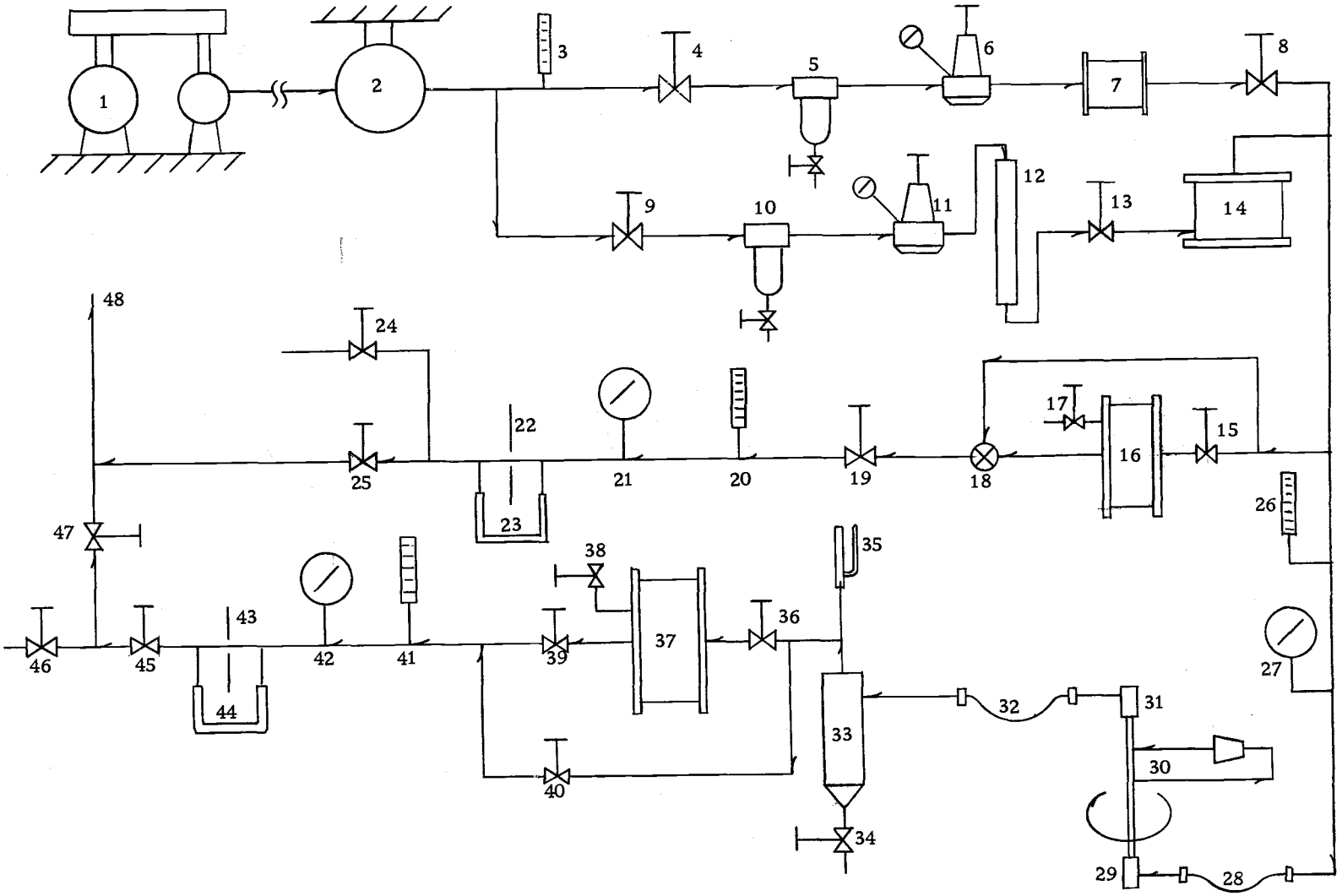


Figure 6. Schematic diagram of the system components involved in the rotating fluidized bed. Descriptions of these items appear in the pages following.

units in a basic data reduction computer program.

| No. | Description | Purpose |
|---|---|---|
| 1. | Two stage air compressor | To supply compressed air to the system to fluidize the bed. |
| 2. | Air receiver tank | To store compressed air and reduce pressure pulsations in the air supply system. |
| 3. | Thermometer | To measure air temperature into the system. |
| 4. | Globe valve, 1-1/4" | To isolate the system from the air compressor. |
| 5. | Air filter, std. 1" | To remove condensate from the air line feeding the system. |
| 6. | Pressure reducing valve, 1" | To maintain constant air pressure entering the fluidized bed unaffected by pressure fluctuations at the air receiver tank. |
| 7. | Packed fiberglass filter | To remove oil droplets and other unwanted particulate matter from the air stream to the bed. |
| 8. | Multiple vee-port flow control valve, 1-1/4" | To control the flow rate of the air to the fluidized bed. |
| 9. | Gate valve, 1/4" | To shut off the air to the aerosol generator. |
| 10. | Air filter, std. 3/8" | To remove condensate from the air to the aerosol generator. |

| | | |
|---|---|---|
| 11. | Pressure reducing valve, 3/8" | To maintain constant air pressure to the aerosol generation unit. |
| 12. | Air dryer | To remove water from the air for better aerosol generation. |
| 13. | Plug valve, 1/4" | To shut off the air supply to the aerosol generation unit. |
| 14. | Aerosol generator | See discussion of the design of this unit on page 45. |
| 15. | Gate valve, 1" | To isolate the inlet aerosol sampling unit from the air supply system. |
| 16. | Inlet aerosol sampling unit | To hold the glass fiber filters used to sample the concentration of aerosols to the fluidized bed. |
| 17. | Gate valve, 1/4" | This is a bleed valve used to bleed air from the inlet sampling box during filter changes. |
| 18. | Three-way plug valve, 1/2" | To direct air flow on the inlet sampling unit either through the sampler or through the bypass around the sampler. |
| 19. | Gate valve, 3/8" | To control pressure in the flow measurement system downstream of the inlet sampling unit. |
| 20. | Thermometer | To measure temperature of the air flowing through the inlet sampling unit. |

| | | |
|---|---|---|
| 21. | Pressure gage | To measure pressure of the air flowing through the inlet sampling unit. |
| 22. | Orifice, 1/2" Ø | To provide a pressure drop for measurement of the flow through the inlet sampling unit. |
| 23. | Water manometer | To measure the pressure differential across the orifice for determining the flow rate through the inlet sampling system. |
| 24. | Gate valve, 1/2" | To control the flow rate through the flow measurement system during periods of orifice calibration. |
| 25. | Gate valve, 1/2" | To control the flow rate through the flow measurement system during normal operation of the system. |
| 26. | Thermometer | To measure temperature of the air to the rotating fluidized bed assembly. |
| 27. | Pressure gage | To measure pressure in the air system to the rotating fluidized bed assembly. |
| 28. | Flexible hose, 1" | To allow adjustment in the V-belts driving the rotating assembly. |
| 29. | Rotating high pressure air seals | To transfer air from a fixed pipe to a hollow, rotating shaft. |

| | | |
|---|---|---|
| 30. | Rotating fluidized bed assembly | See discussion of the design of this unit on page 32. |
| 31. | See (28) above. | |
| 32. | See (27) above. | |
| 33. | Cyclone separator | To remove any bed material which might have become entrained in the air stream and prevent such material from entering the discharge air sampling filter. |
| 34. | Ball valve, 1/2" | To drain any material collected by the cyclone separator. |
| 35. | Safety relief valve, 3/4", set at 58 PSIG | To prevent a pressure buildup on the discharge side of the system in excess of the safe limits of the apparatus. |
| 36. | Ball valve, 1-1/4" | Shut-off valve to isolate the discharge aerosol sampling unit from the discharge air lines. |
| 37. | Discharge aerosol sampling unit | To hold the glass fiber filters used to sample the concentration of aerosols coming out of the fluidized bed. |
| 38. | Gate valve, 1/4" | To bleed the air from the discharge sampling unit during filter changes. |
| 39. | Globe valve, 1-1/4" | Same as (35) above. |
| 40. | Ball valve, 1-1/4" | To control air flow through the bypass line around the discharge air sampling unit. |

| | | |
|---|---|---|
| 41. | Thermometer | To measure temperature of the air going to the discharge air flow rate measuring unit. |
| 42. | Pressure gage | To measure air pressure in the discharge air flow rate measuring unit. |
| 43. | Orifice, 11/16" Ø | To provide a pressure differential for measurement of the flow rate through the discharge sampling system. |
| 44. | Water manometer | To measure the pressure differential across the orifice for determining the flow rate through the discharge sampling system. |
| 45. | Multiple vee-port flow control valve, 1-1/4" | To control the flow rate of air through the rotating fluidized bed and the discharge air sampling system. |
| 46. | Globe valve, 3/4" | To direct the air flow into equipment used to calibrate the orifice (42). |
| 47. | Globe valve, 1-1/4" | To direct the air flow into the exhaust header normally used for this system. |
| 48. | Line to exhaust header, 1-1/4" | To carry all of the discharge air into an exhaust header and thereby control the noise level around the experimental unit. |

The individual items shown in Figure 6 and described above are components of six distinct systems:

(1) Rotating bed assembly

(2) Power train

(3) General air handling system

(4) Aerosol generation system

(5) Aerosol sampling system

(6) Flow measurement system

Each of these is discussed with respect to its design details.

## Rotating Bed Assembly

The rotating bed assembly consists of a bed "retainer" supported by the apparatus shown in Figures 7 and 8. As indicated in Figure 7, compressed air enters through a vertical, hollow shaft and is directed through pipes into the base of the bed. Moving through the bed of glass beads toward the center of rotation, the air acts to fluidize the bed material. After the air leaves the bed operating region it flows into a "disengaging zone." Here the velocity is low enough to allow any of the bed material which may have been transported out of the operating region to "drop" back into it. Air leaves the disengaging zone through the top section of the vertical, hollow shaft.

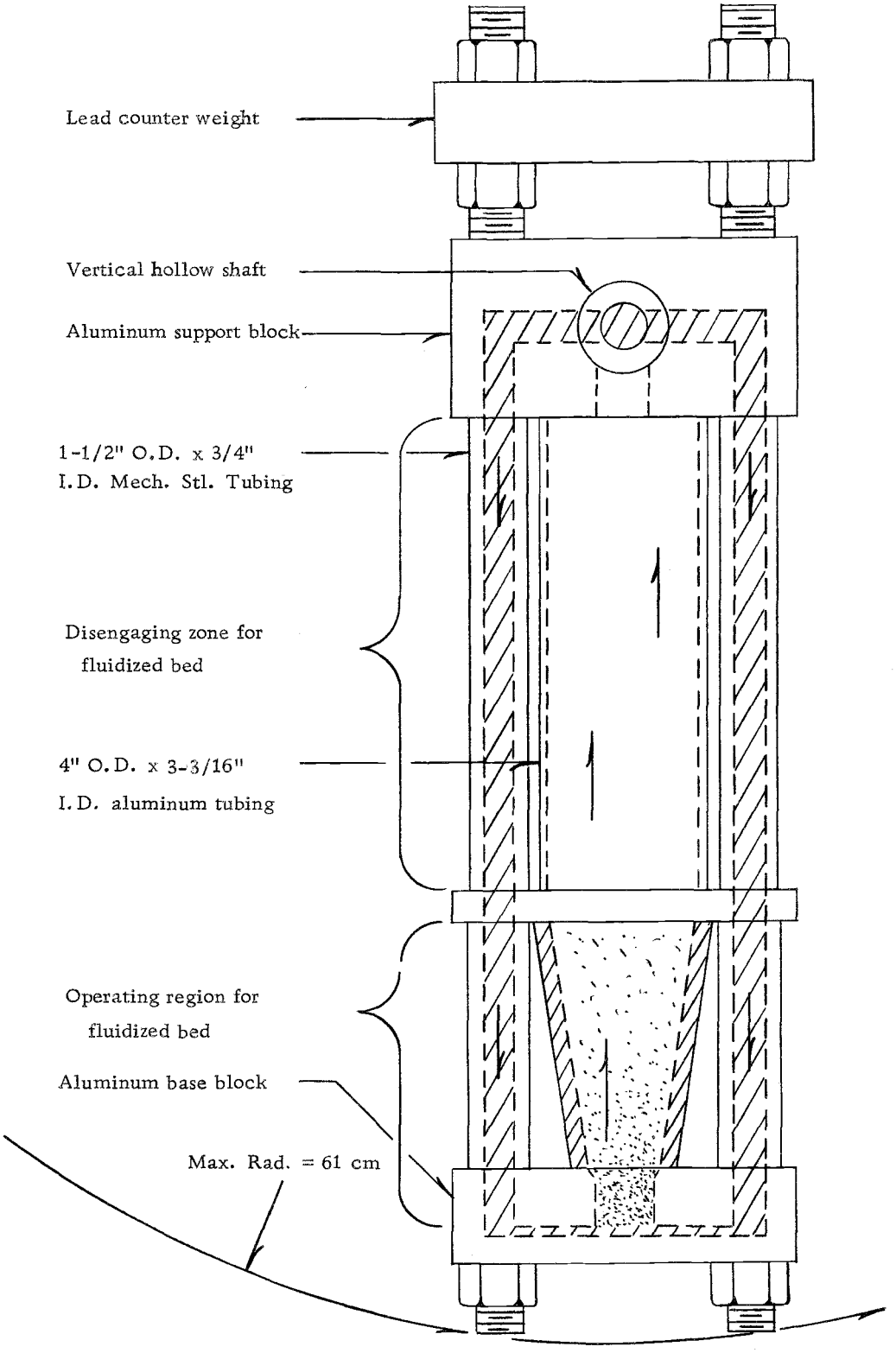


Figure 7. Cross sectional view of the rotating assembly.

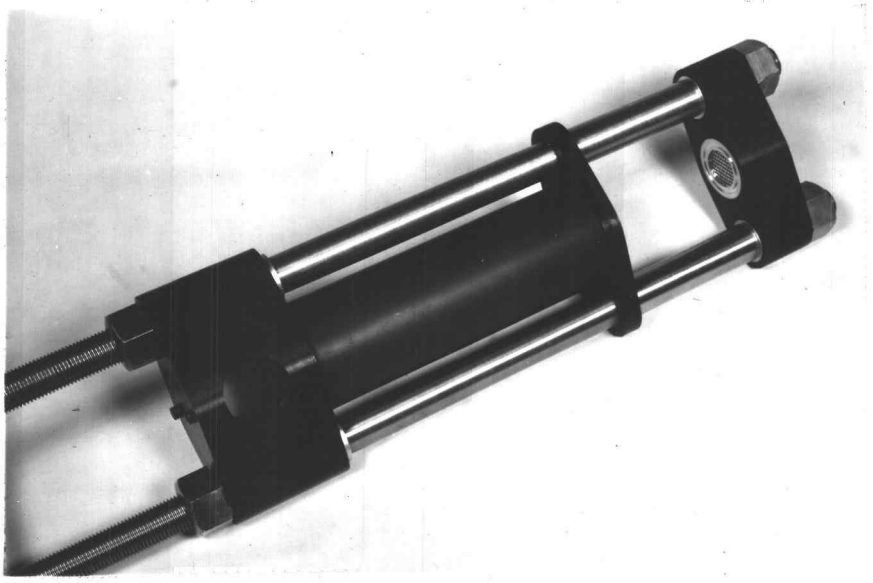

Figure 8. Photograph of rotating assembly shown in cross section in Figure 7. Bed retainer is not in place in this picture.

The bed retainer received special design consideration. Operating under high radial acceleration loads, it had to withstand stresses due to these accelerations as well as due to pressure inside the vessel. For example, at 417 G's, the inlet pressure at the base of the retainer was approximately 6.5 atmospheres. Furthermore, it was desirable to have a transparent bed retainer in order that the fluidized bed could be observed during operation. To meet these requirements of strength and visibility, clear polyester casting resin was chosen to make the retainers. Molds were constructed of cold rolled steel shaft stock which was shaped and polished in a lathe. Both the male and female parts of the molds were chrome plated to insure a smooth, glossy surface on the bed retainers. Numerous problems arose in the

actual casting process. Bubbles, cracks and voids were the main concern initially. However, these were overcome with experience. Cracking of the retainers in the process of removing them from the molds was also a major problem.

Three shapes were used for the interior of the bed ratainer in order to vary the mode of fluidization in the bed. The first shape, a straight cylinder, was used to produce a condition of smooth fluidization at the base of the bed, changing to an aggregative mode at the top of the bed. The change in mode is brought about by the pressure drop through the bed with resultant high velocities in the low pressure region at the top of the bed. Note that the radial acceleration at this point is less than that experienced by the bed material at the bottom of the bed. The combination of lower radial forces and higher gas velocities produces an aggregative mode of fluidization.

The second bed shape was designed such that the velocity of the gas stream moving through the bed was proportional to the G-level experienced by the bed at that point. The design was a compromise since it was not possible to construct the shape so that it worked equally well for all G-levels and all flow rates. The objective was to provide a common mode of fluidization throughout the bed, either all smooth or all aggregative. Based upon the pressure differentials recorded during testing, the design was effective in achieving this result.

The third bed shape was a cone with an interior angle of $18^{o}40'$. The objective here was to increase the cross sectional area of the bed faster than the corresponding change in pressure as the gas stream moved through the bed. It was hoped that in this manner the bed could operate in an aggregative mode at its inlet and in a smooth mode at its outlet, assuming moderate gas flow rates through the system.

The three shapes are illustrated in Figure 9. The external shape of the beds is common to all in order to use the same mounting structure for all three beds. Note that Shape I has a large flat surface on the top of the bed retainer area. During testing, bed material which was blown out of the retainer into the disengaging zone fell back onto this surface and collected there instead of returning to the cylindrical region. To overcome this difficulty, an aluminum funnel was installed in the rotating system as shown in Figure 10.

In order to test the integrity of the cast beds before they were actually put into operation, a bed of Shape II was placed in a compression testing machine. A total axial force of 43,000 pounds was applied before a failure occurred. Based on this, it was felt that the cast resin bed retainers were sufficiently strong to withstand operating stresses at radial acceleration levels of up to 1000 G's without difficulty.

Figure 11 below is a photograph of the bed retainer Shape II, mounted in the rotating assembly. The picture is taken through a

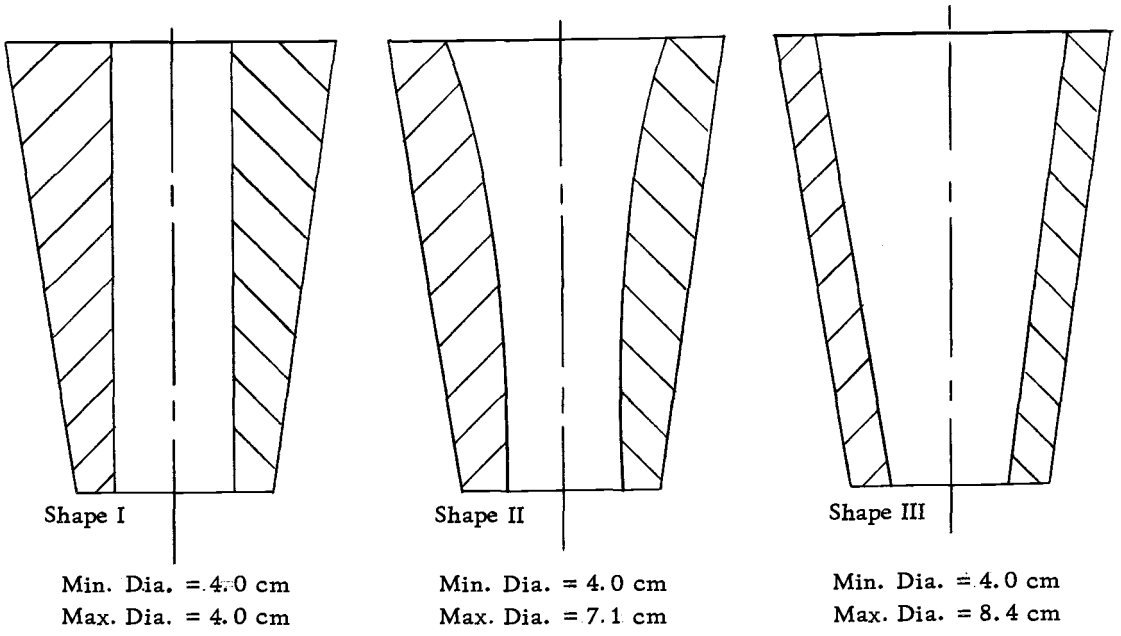


Figure 9. Schematic cross sectional views of bed retainer shapes.

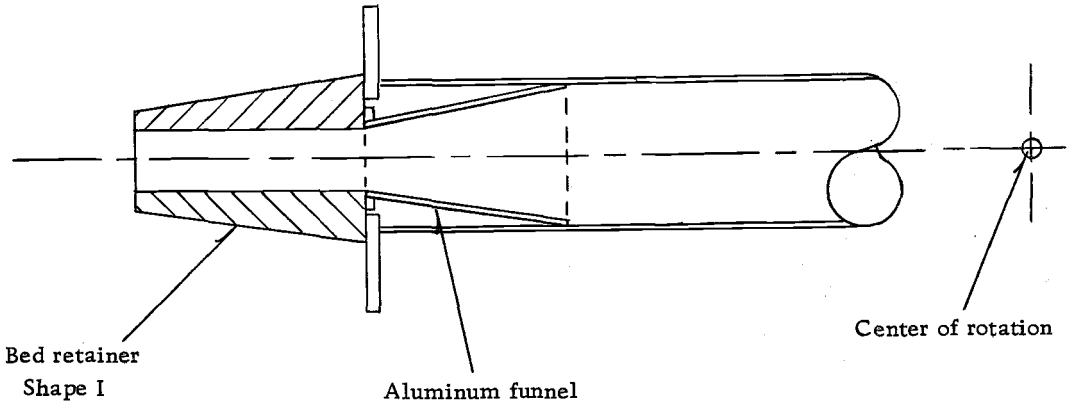


Figure 10. Schematic diagram showing the location of the aluminum funnel used in conjunction with bed retainer Shape I.

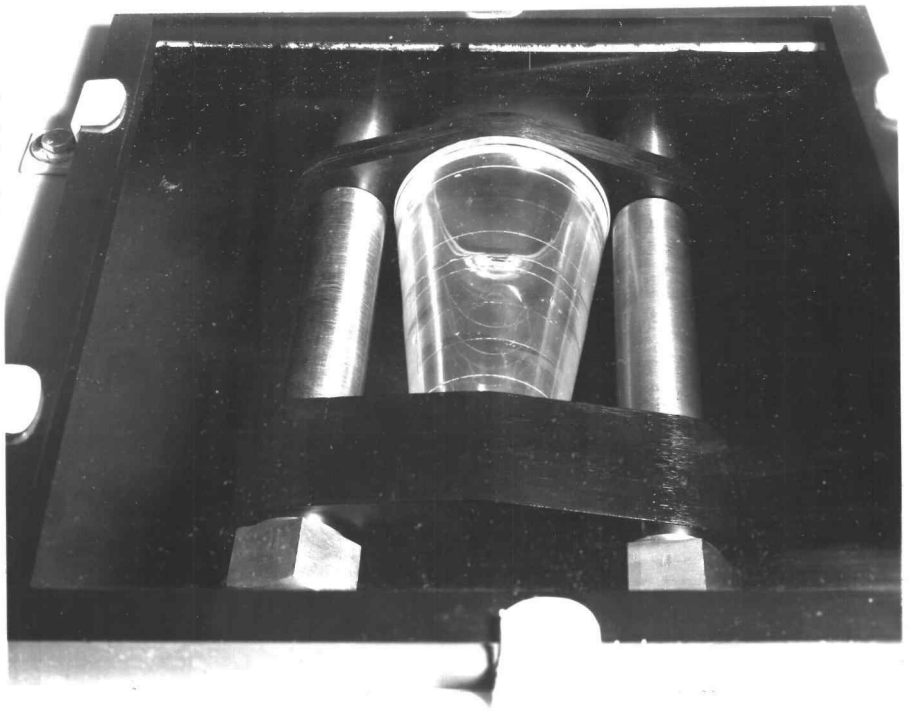

Figure 11. Photograph of bed retainer Shape II mounted in the rotating assembly.

plexiglass window located on the top of the bed guard. Note the high degree of visibility of the bed retainer and also the grooves in the interior of this retainer. These are spaced axially at 2 cm intervals and are used to judge bed operating height when the bed is in operation.

As noted previously, the rotating fluidized bed assembly was mounted on a vertical shaft. This shaft was supported by two pillow block mounted spherical roller bearings bolted to a heavy backing plate (Figure 12). This backing plate was, in turn, bolted to a seven ton, reinforced concrete foundation. Note that the backing plate is slotted to allow for sideways movement of the shaft. This was necessary to allow for belt tension adjustment in the vee-belt drive on

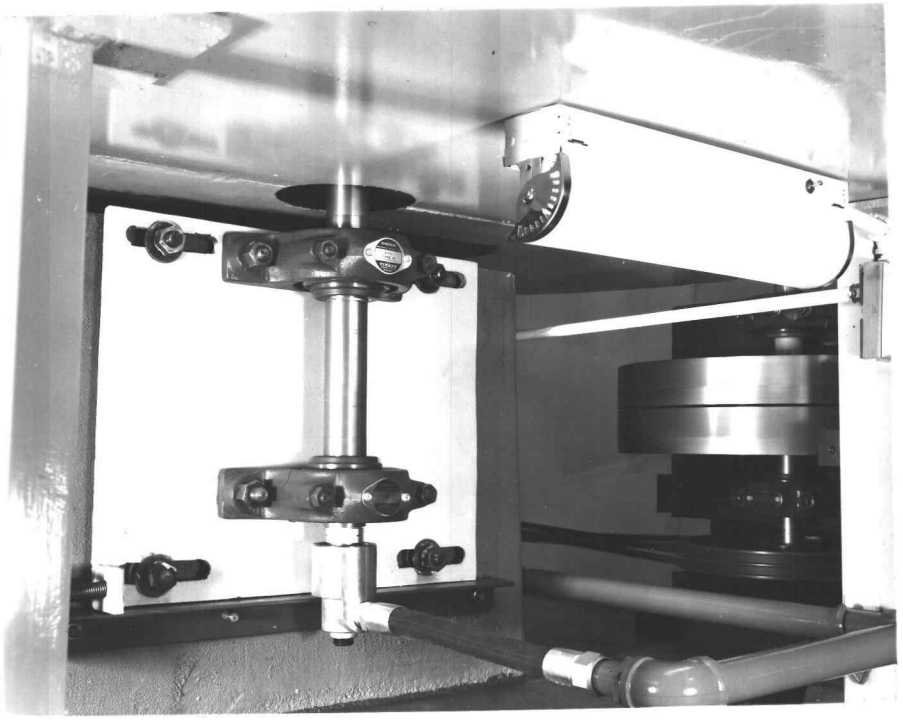

Figure 12. Photograph showing the mounting arrangement for the vertical shaft of the rotating assembly.

the top of the shaft. A position adjustment screw can be seen in the bottom left hand corner of the backing plate.

To guard against damage or physical injury in the event of a mechanical failure, the rotating assembly was completely enclosed in the housing shown below in Figure 13. Under the carpeted area lies an eight inch thick by ten inch high reinforced concrete "donut." This is encased, inside and out, by steel plate. The top and bottom of the housing are made of 3/16" thick steel plate. A window of one inch thick plexiglass was placed in the top so that the bed could be viewed while in operation. The vee-belt drive for the rotating assembly can also be seen in this picture.

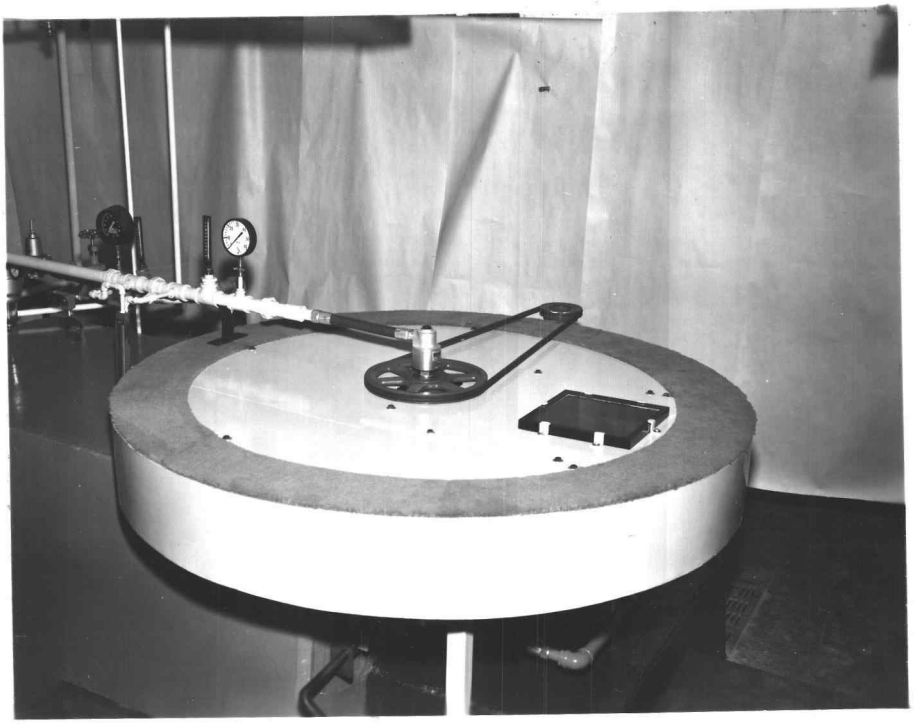

Figure 13. Photograph of the protective housing placed around the rotating assembly.

## Power Train

The power train used to drive the rotating fluidized bed is illustrated schematically in Figure 14. A five horsepower, 1750 RPM induction motor transmits power to a vertical jack shaft through a Dodge Flexidyne coupling. Located in the center of the jack shaft is a flywheel weighing approximately 400 pounds. It is used to maintain constant angular velocity of the rotating system despite minor fluctuations in line voltage at the induction motor. The Flexidyne coupling is exceptionally reliable in bringing the rotating assembly up to its operating speed without overloading the motor.

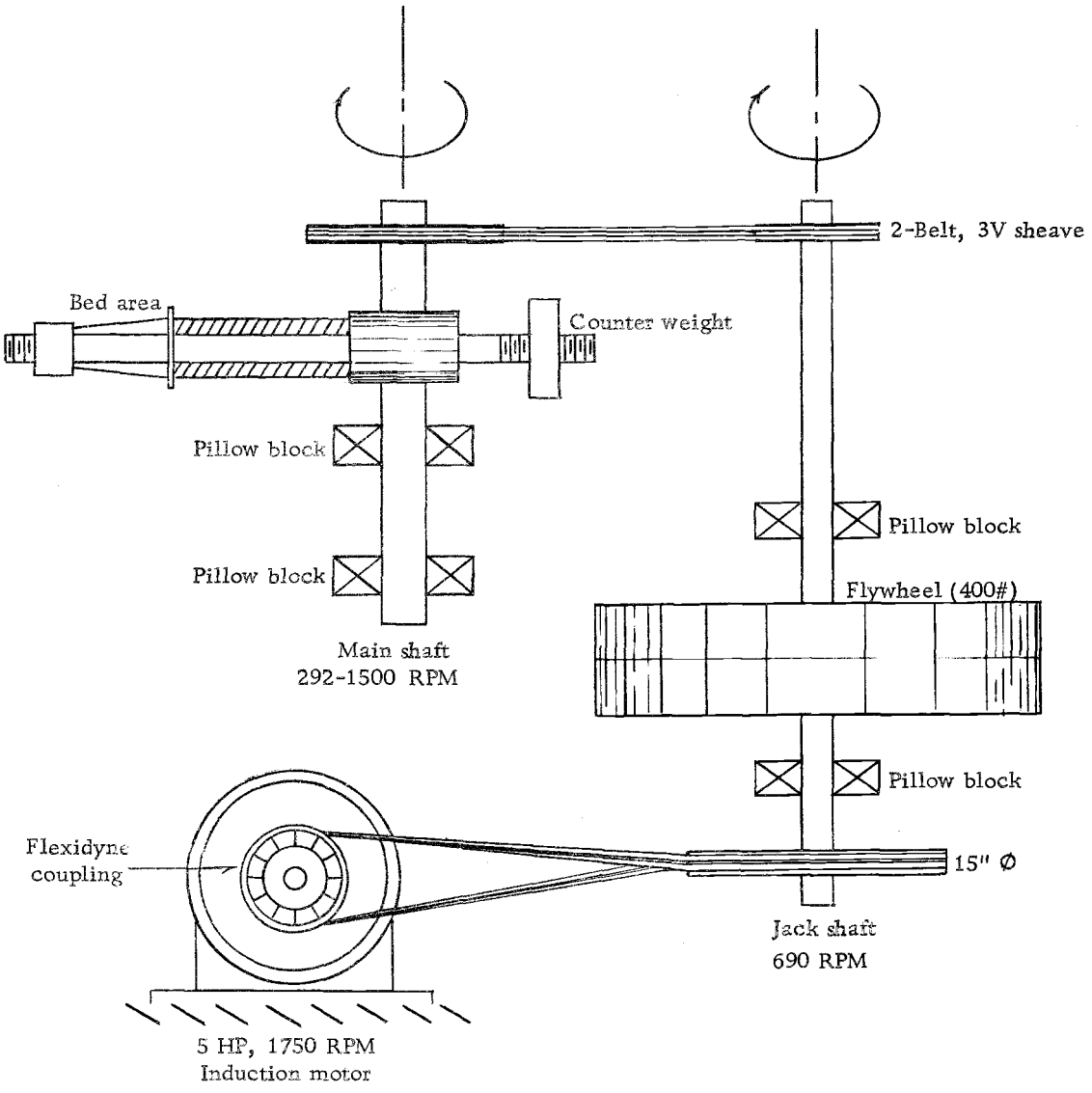


Figure 14. Schematic diagram of power transmission system for rotation of the fluidized bed assembly.

The jack shaft operates at a constant speed of 690 RPM and is driven by two A-section vee-belts. The center distance between the motor shaft and the jack shaft is approximately seven feet--sufficient to allow the belts to turn through $90^{o}$ without undue wear against the sheaves. Two pillow block mounted spherical roller bearings support the jack shaft in a steel housing.

Power is transmitted from the jack shaft to the rotating bed shaft via two 3V-section vee-belts. Using six interchangeable sheaves it is possible to obtain 21 different speeds on the rotating bed shaft in the range from 292 to 1400 RPM. The jack shaft is fixed securely in its housing, but the rotating bed shaft is mounted on a movable backing plate to permit drive belt tension adjustment.

The five horsepower motor is adequate to handle the power requirements of the system up to the maximum operating level tested. The high starting torque results in a peak output from the motor of 25 HP sustained for approximately 11 seconds with no apparent damage to the windings. The 220v, 3 ph circuit is fully protected with circuit breakers and fuses.

Figure 15 below shows the actual power train installation in operation. The cover has been removed from around the flywheel. Note the twist in the drive belts leaving the flexidyne coupling.

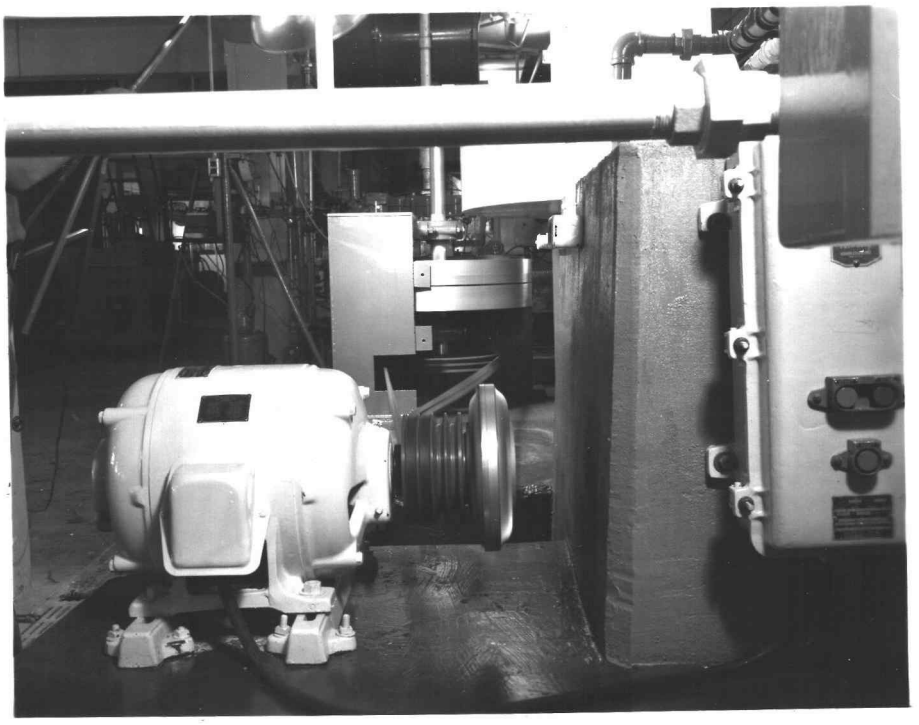

Figure 15. Photograph of the drive train including the starter, motor, coupling, jack shaft, and flywheel.

General Air Handling System

The general air handling system is illustrated in Figure 16. A two stage air compressor supplies compressed air to a receiver tank located near the experimental apparatus. A shut-off valve is used to isolate the apparatus from the receiver tank. Condensate from the incoming line is removed in a standard Norgren air filter and the system pressure is controlled with a standard Norgren air pressure control valve. Initial tests indicated that the air filter was not effective in removing rust, scale, and other particulate matter suspended in the incoming air stream. Therefore, a packed fiberglass

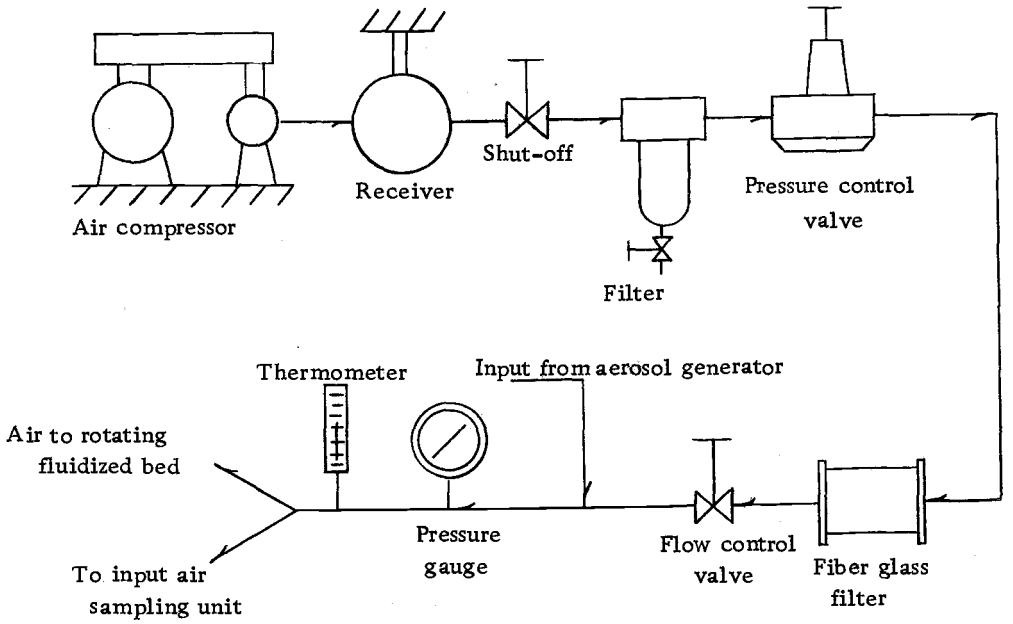


Figure 16. Schematic diagram of the general air handling system.

filter was constructed and installed downstream from the pressure control valve.

A multiple vee-port flow control valve was installed next to control the volumetric flow rate to the fluidized bed. The output from the aerosol generator enters the gas stream just downstream from the flow control valve. Pressure and temperature of the particulate laden air are measured just prior to entering the rotating fluidized bed. A commercial bourdon tube pressure gage and standard industrial thermometer are used. Schedule No. 40 black iron pipe and fittings are adqauate to handle the pressures involved.

Problems with rust from the system piping became apparent early in the testing program. The solution was to paint the interior of all of the system piping downstream from the packed fiberglass filter with two coats of epoxy base paint. This proved quite effective despite the use of the sodium chloride aerosol.

Note that no after cooler is used in the system downstream from the air compressor. This did not present any serious problems due to moisture in the air lines until tests were run in the 417 G-level at high flow rates. Under these conditions, condensation in the air lines did occur and limited the data collection. Fortunately, sufficient data were collected in the lower G-levels and flow rates without condensation difficulties and hence reasonable conclusions could be made. Tests carried out above 417 G's should be conducted with an after-cooler in the line to limit condensation problems.

## Aerosol Generation System

It was determined that for sampling purposes at least 25 mg of aerosol should be collected on both the inlet and outlet sampling filters. Assuming that the fluidized bed and the related piping would remove 90% of the aerosols, this required that a minimum 275 mg of aerosol should be generated for each sampling period. Using sodium chloride as the aerosol material with an average diameter of 0.7 microns it was estimated that approximately 750 trillion particles per

sampling period would meet the generation requirements.

Figure 17 illustrates the apparatus used. In this a saturated solution of sodium chloride dissolved in water was placed inside a pressure vessel containing a manifold of ten atomizers. Dry compressed air was used to atomize the salt solution into droplets. The large droplets impinged on the interior surface of the pressure vessel and ran down the walls to be re-atomized. The smaller droplets lost their moisture through evaporation leaving sub-micron salt particles suspended in the air stream. Any large droplets that left the pressure vessel impinged on the walls of the piping and were recirculated as liquid back into the generator.

The operating pressure of the aerosol generator was the same as the input pressure to the rotating fluidized bed. Thus it ranged from 2.2 Atm to 5.3 Atm. During each test a pressure differential of approximately 2.7 Atm was maintained across the atomizer manifold. Output concentrations of aerosol varied according to the operating pressure level with higher concentrations found at the lower pressures.

To limit corrosion due to the saturated salt solution, the entire pressure vessel was painted with two coats of a zinc base corrosion inhibiting paint. Galvanized pipe was used for recirculation, fill, and drain lines. The manifold was constructed of copper tubing and the valves were brass.

Substantial difficulties were encountered in attempting to

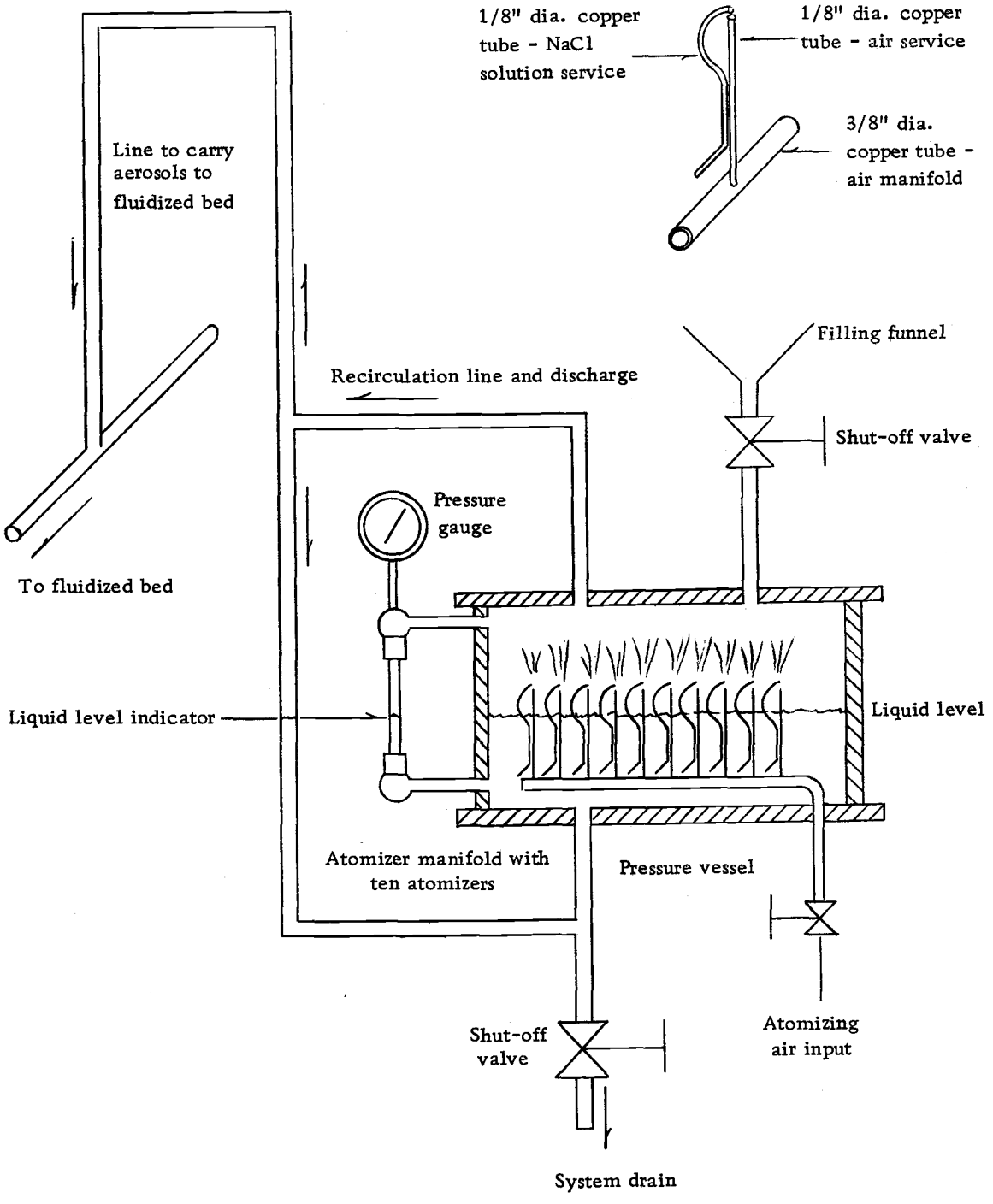


Figure 17. Schematic diagram of the aerosol generation system.

generate sufficient aerosols for testing purposes, partially in terms of maintaining consistent rates of generation without plugging the atomizers. Recirculation lines, a liquid level indicator, and the use of a dessicant dryer on the incoming air line all helped to overcome these difficulties.

## Aerosol Sampling Systems

In order to determine the filtration efficiency of the rotating fluidized bed, it was necessary to sample both the incoming and outgoing aerosol concentrations. Preliminary tests indicated that the aerosol generation system could not be counted on to deliver unvarying concentrations of aerosols to the rotating assembly. Therefore, it was necessary to measure the incoming and outgoing aerosol concentrations simultaneously.

Two separate systems were used. For the incoming sampling system (illustrated in Figure 18) a portion of the total flow of particulate laden air entering the fluidized bed was drawn off in a "Y" and carried to a pressure vessel containing a glass fiber filter . These filters (Gelman Type A) are very effective in removing fine particulate from a gas stream with a relatively low pressure drop. "Clean air" leaving the filter holders was reduced in pressure and its volumetric flow rate determined in a calibrated orifice system.

The portion of the gas stream which did not enter the inlet

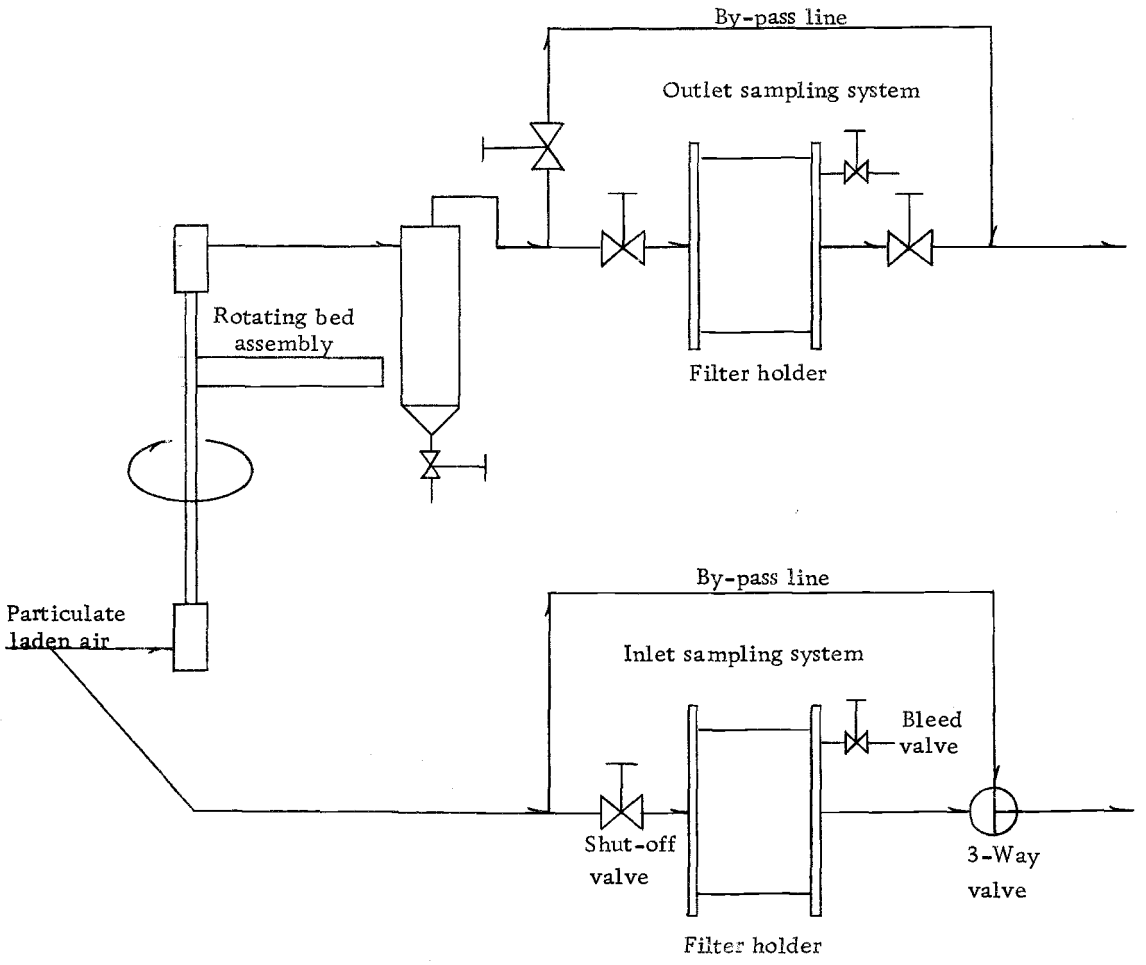


Figure 18. Schematic diagram of the aerosol sampling system.

sampling system passed into the rotating assembly. There most of the particulate matter was removed in the fluidized bed and related piping. Leaving the rotating assembly, the gas stream passed through a cyclone separator. Its purpose was to remove any large particles such as bed material (glass beads) which might have been carried out of the rotating assembly. Under conditions of high flow rates this

frequently occurred. Note that the purpose of the outlet sampling system was to measure concentrations of suspended sub-micron size particulate. If the filter had gathered glass beads as well, it would make particulate measurements very difficult if not impossible. Therefore, the cyclone separator was used to avoid this problem. The collection characteristics of this particular cyclone were such that the sub-micron aerosols were not captured while the larger glass beads were effectively removed from the air stream. Microscopic examination of the glass fiber filters showed no beads present on them.

A flow bypass was supplied for both the inlet and outlet sampling systems. This was done so that the flow through the rotating fluidized bed could be adjusted and the system brought to an equilibrium state before the actual sampling was begun. At the end of each sampling period, the bypasses were opened and the filter holders isolated from the flow systems. In this manner samples could be collected and filters changed without interrupting the operation of the fluidized bed.

The filter retainers were constructed as shown in Figure 19. Leakage around the filter and crushing of the filter material in the retainer were major problems which were overcome by this design. Ease of changing filters was also an important consideration since it had to be done over 100 times during the tests. As it turned out, both the inlet and outlet filters could be changed in seven minutes once the system was in operation.

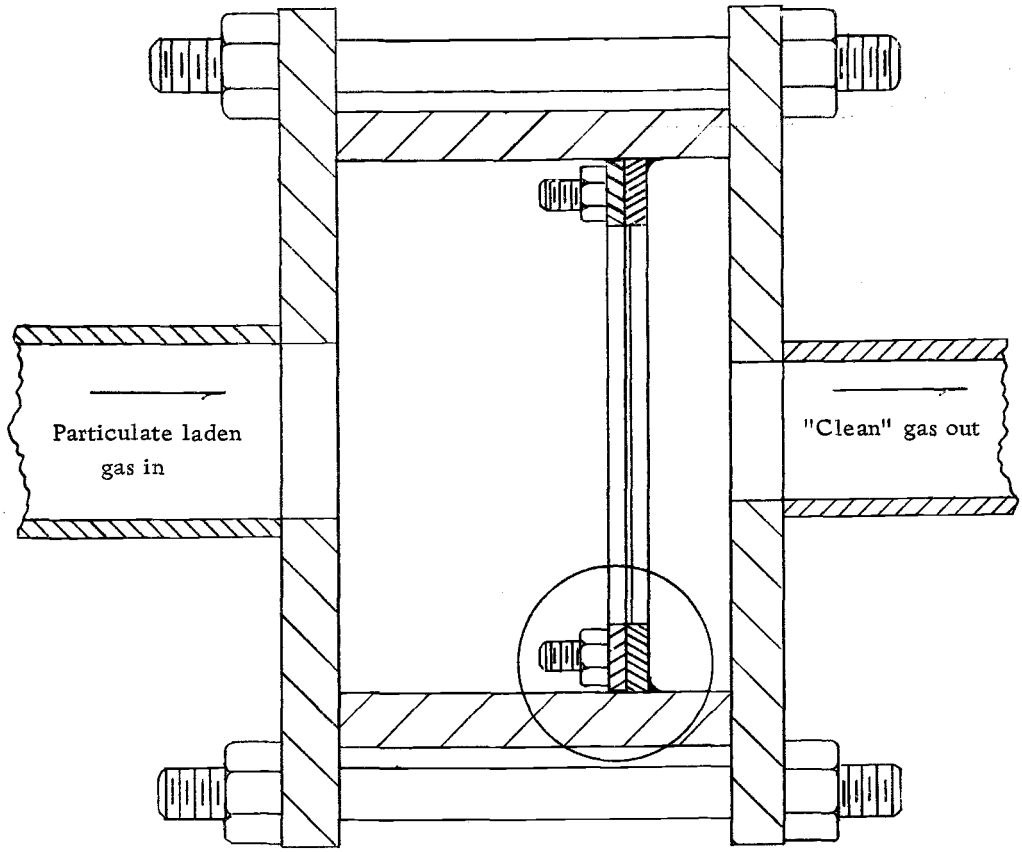


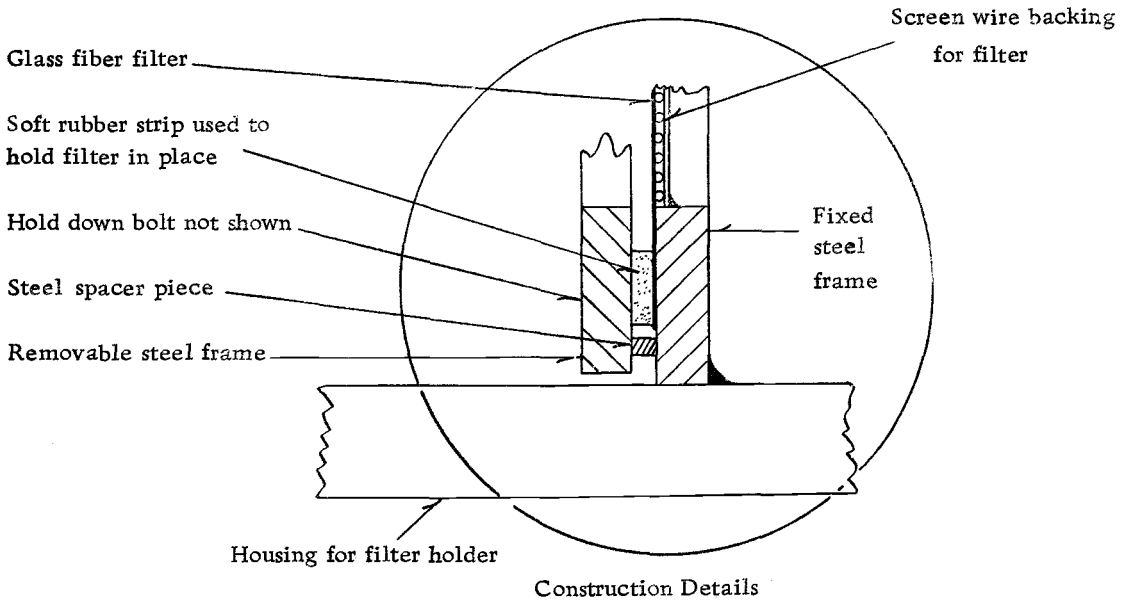


Figure 19. Cross sectional view of filter holder.

Figures 20 and 21 are photographs of the inlet and outlet sampling systems respectively. Note that each complete filter is made of two parallel plates with the filter holder bolted between. By loosening eight bolts the center box could be removed to change filters. Both units were constructed as pressure vessels and were tested up to a static pressure of 21 Atm, well above the maximum operating pressures involved during tests.

In Figure 21 the cyclone separator can be seen in the right hand side of the photograph. The valve on the bottom could be opened to remove collected bed material. On the top of the separator a pressure relief valve was installed to prevent overpressuring the system. Since the entire experimental apparatus involved some 31 valves, the possibility always existed of opening the wrong valve and damaging the system. The pressure relief valve was a safety device in the event that this situation occurred.

## Flow Measurement Systems

Accurate volumetric flow rate determination was important in determining the inlet and outlet aerosol concentrations. Two separate but similar systems were used, each involving a calibrated orifice as shown in Figure 22.

The operating pressure of the inlet sampling system was the same as the input pressure to the rotating assembly. Thus, it varied

Figure 20. Photograph of the inlet sampling system showing the filter holder and related piping.

Figure 21. Photograph of the outlet sampling system showing the cyclone separator, the filter holder, piping bypass, and control valves.

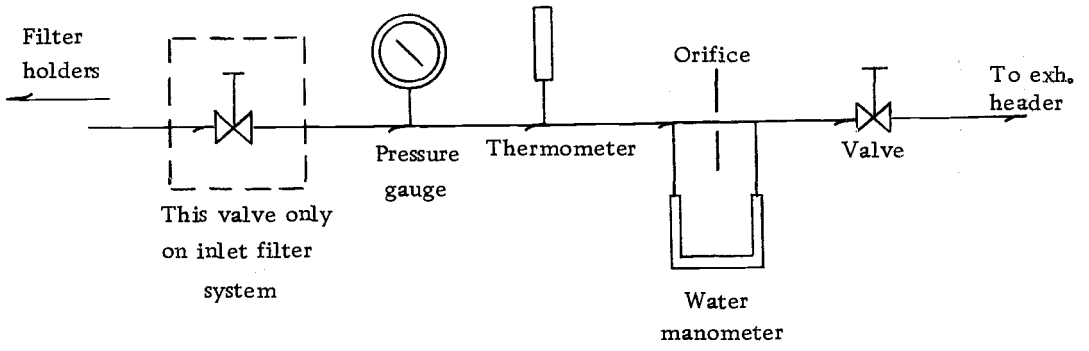


Figure 22. Schematic diagram showing the flow measurement system.

for each level of radial acceleration, flow rate, and bed retainer shape. In order to measure the volumetric flow rate through the sampler, it was necessary to reduce and control the pressure at one level as it passed through the orifice system. Thus, for the inlet system, a gate valve was installed in the line as shown above. The use of this valve in conjunction with the valve downstream of the orifice made it possible to control both the rate of flow through and the pressure within the flow measurement system.

For the outlet sampling system, all tests were conducted with a discharge pressure of 3 Atm leaving the rotating assembly. This pressure and the rate of gas flow through the system were controlled by the flow control valve mentioned earlier (see discussion of General

Air Handling System) and the valve downstream of the orifice (Figure 22).

For each of the two systems, one orifice was adequate to measure the full range of flows involved. Orifice calibration curves were developed by adjusting the flow levels and measuring the time required to fill a large plastic bag of known volume. The curves are presented in the Appendix. Standard water manometers were used to measure the pressure differentials across the orifices.

Since each system was calibrated by the technique described, there was no need for concern about location of orifice pressure taps, calculated orifice coefficients, etc. This greatly simplified the task of accurate volumetric flow measurement. Note, however, that it was necessary to measure flows at the same pressures used to develop the calibration curves. Corrections were made for differences in temperatures.

The gas streams leaving the flow measurement systems were connected to an exhaust header. This helped to reduce the noise level in the area of the experimental apparatus.

## Experimental Design

As noted previously, the first two objectives of this experiment were:

(1) To investigate the effect on filtration efficiency of three

independent variables:

a. Radial acceleration (G-level)

b. Volumetric gas flow rate through the fluidized bed

c. Mode of fluidization as controlled by the shape of the bed retainer.

(2) To investigate interaction effects on filtration efficiency of the three independent variables.

In order to meet these objectives an experiment was planned and executed involving the independent variables in 27 treatment combinations. Five levels of radial acceleration and three levels of flow rate for each of the three shapes were combined as illustrated in Figure 23.

| | G-level | 44 | 98 | 204 | 319 | 417 |
|---|---|---|---|---|---|---|
| Gas flow rate level | 1 | X | X | X | | |
| | 2 | | X | X | X | X |
| | 3 | | | | X | X |

Figure 23. Diagrammatic representation of the conditions under which data were collected for all three bed shapes. "X" indicates data collected.

Initial investigations showed that it was not possible to use each flow level at each level of radial acceleration. At the low G-levels, a high flow level would carry the bed material out of the rotating system. Conversely, at the high G-levels the low flow rate was not sufficient to

fluidize the bed. The treatment combinations shown were used for all three bed shapes.

Throughout the investigation, the dependent variable of interest was filtration efficiency of the fluidized bed. This is defined as follows:

$$\text{Filtration Eff.} = \frac{\text{Conc. of aerosols in - Conc. of aerosols out}}{\text{Conc. of aerosols in}}$$

The experimental unit was the rotating fluidized bed. The G-levels were measured at the top (discharge end) of the bed in the fluidized state. The observation units were the glass fiber filters in the inlet and outlet aerosol sampling systems.

The experimental design might be described as an unbalanced 5 x 3 x 3 factorial design with missing cells, unbalanced in the sense that the same number of replications was not applied in each cell. In the majority of treatment combinations three replications were used. However, in two cells, only two replications were used and in some cells, more than three were used. Note that the replications were not "true replications" of the treatment combinations. In order to take into account any effects due to the amount of time that the bed had been in operation, data were taken for each treatment combination approximately at the time intervals shown in Figure 24. Note that Figure 24 indicates a normal sampling time of 30 minutes with 10 minute intervals during which no sampling took place. While this situation applied to most of the experiment there were some deviations. For

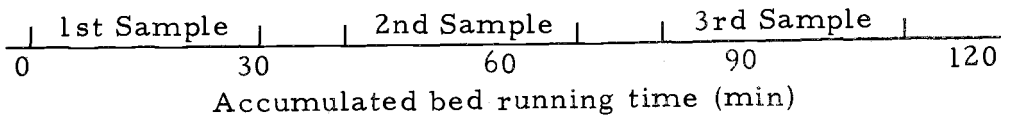


Figure 24. Diagram showing spacing of sampling time intervals to determine filtration efficiency.

example, at the 44 G-level, it was found that 20 minutes was often adequate to collect samples, and that 30 minute sampling periods resulted in destruction of the sampling filters due to clogging and subsequent breakage.

With this design, one might have considered accumulated running time on the bed as a fourth independent variable, with no replication involved. As an alternative, however, accumulated running time was used as a covariate. This was based on Black's work and on initial investigations which indicated that accumulated time was not an important factor in fluidized bed filtration efficiency.

The sequence in which treatment combinations were applied was neither completely random nor completely ordered. In general treatments were applied in a manner which required the least number of changes of G-level and bed shape. Such changes involved several hours of "down time" for the apparatus and were avoided whenever possible. There are possible disadvantages, however, in failing to completely randomize the treatment combinations. In doing so, the assumption is made that no systematic uncontrolled variations affecting the response are present. This assumption requires a subjective

evaluation of the experiment and may not be entirely correct. Any uncontrolled systematic variations may affect both the estimate of errors and the estimate of treatment effects.

The raw data collected were input to a brief computer program which converted them into concentrations of aerosols with appropriate corrections for temperatures, flows, etc. These data were then analyzed using the General Linear Hypothesis Testing Program (*BMD-05V), a statistical analysis library program on public file at the Oregon State University Computer Center. Seven hypotheses were tested involving the covariate, main effects and interactions of the independent variables, in each case through the use of the "F" statistic.

It was initially intended to use two different types of aerosols in the study, namely sodium chloride and ammonium chloride. The first was selected because of the ease of generation and handling and low cost. The second was selected with the thought that since Black had used ammonium chloride in his work, it would make a comparison of results more direct and valuable. Initial investigations with ammonium chloride did not prove successful, however. It reacted chemically with the aerosol generator and destroyed the generating manifold in a few hours. Further studies with it were discontinued and sodium chloride was used as the only aerosol for this investigation.

Mention should also be made concerning the choice of volumetric

gas flow rate through the system as an independent variable. In much of the literature dealing with fluidized beds, the term "superficial gas velocity" is used in describing an important variable of bed operation. This is the relative velocity of the gas moving through the bed with respect to the bed material. For a fixed bed, operating in a normal condition of "one G," the superficial gas velocity is easily determined and controlled if the pressure differential across the bed is on the order of only 0.1 Atm. In a rotating fluidized bed, subjected to 417 G's, however, the pressure differential across the bed approached 3.5 Atm. This resulted in substantial variations of superficial gas velocity within the bed. Under these conditions, it seemed more reasonable to measure and control the volumetric flow rate through the bed as an independent variable. This simplified both the measurement and the control of the variable.

In his work Black had shown that filtration was directly related to the amount of bed material present, greater efficiencies being possible with more bed material. Hence for purposes of this study it was not deemed necessary to include bed mass as an independent variable. Therefore, it was held constant. Furthermore, it was found experimentally that too little bed material (less than 70 grams) resulted in poor fluidization characteristics and that too much material (greater than 150 grams) resulted in excessive carry-over problems for the system, that is, the material was literally blown out of the

rotating bed assembly. Since either of these conditions would tend to distort experimental results concerning efficiency, the bed mass was held constant for all runs and equaled 100 grams.

Black also found that the concentration of the incoming aerosol had very little effect on filtration efficiency. Because this was established, no attempt was made to control the concentration of the incoming aerosol. Note that for each experimental run the concentration was measured, but not controlled.

In this experimental design, six basic assumptions were made:

(1) Each response measured was assumed to be the sum of a quantity depending only on the fluidized bed plus a quantity depending on the treatment applied to the bed plus a random error component. This is referred to as the assumption of additivity.

(2) The effects on filtration efficiency of the treatments applied to the fluidized bed were constant throughout the experiment.

(3) There were no interferences; conditions of previous tests did not affect the results of the test under consideration.

(4) The errors were independent of each other.

(5) The errors were normally distributed.

(6) There was no interaction effect of the three independent variables (i.e., G x F x S).

## Data Collection Procedures

The following process was used to collect data concerning filtration efficiency in the rotating fluidized bed:

(1) Glass fiber filters for the inlet and outlet sampling systems were cut to the right dimensions and placed in manila folders. These were set up in racks with spaces between them to permit air to circulate. They were allowed to equilibrate in a humidity controlled laboratory for a minimum period of two hours before their initial weights were taken.

(2) Weights of both the filters and their protective folders were recorded to 0.1 mg using a Mettler laboratory balance.

(3) The filters were placed in the aerosol sampling system and the treatments applied to the rotating fluidized bed.

(4) At the end of each test, the filters were removed from the sampling system and placed in their protective folders.

(5) Following the conclusion of a series of tests (usually one day's testing) the filters were returned to the spacing racks in the laboratory and allowed to equilibrate. Again a minimum of two hours was allowed before final weights were recorded.

(6) Final weights for both filters and their holders were determined. The difference between the initial and final

weights indicated the amount of aerosol collected on each filter.

(7) For each series of tests, a minimum of four inlet and four outlet filters were used as blanks or control filters. These were processed just like the sample filters except that they were not placed in the sampling systems to collect aerosols. Initial and final weights were recorded and the mean values of the weight changes for both the inlet and the outlet filters were calculated. These respective mean values were used to correct the test observations for changes in relative humidity. During the course of the testing, changes in filter weights up to 70 mg resulted from relative humidity and temperature variations.

(8) In addition to the observations made on the glass fiber sampling filters, data were collected regarding pressures, temperatures, and manometric readings for each test. These data were used to calculate flow rates and to control the operating variables of the system.

Additional corrections were made to the observations. The fluidized bed was not the only unit which removed aerosols from the gas stream. Initial investigations showed that substantial amounts of aerosols were removed by the piping used in the system. In effect the sampling system was similar to that shown in Figure 25. It was

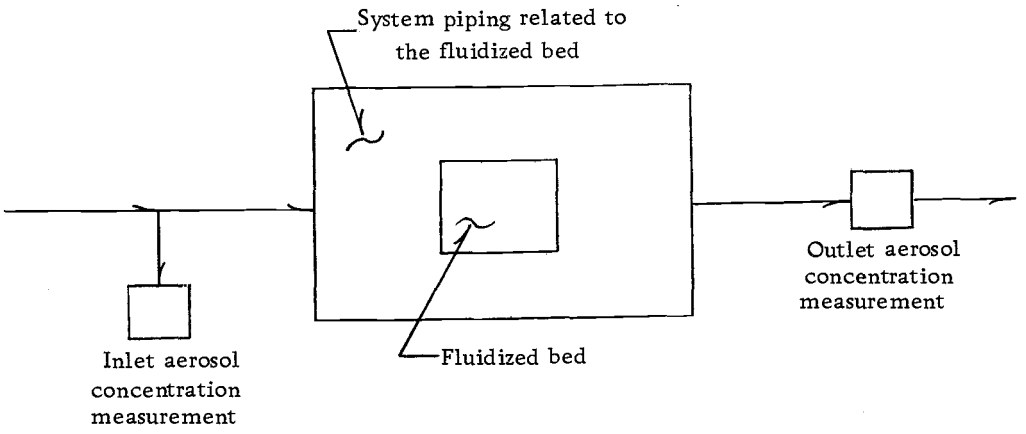


Figure 25. Diagram showing the relationship of the aerosol sampling system to the fluidized bed.

possible to measure only what went into the overall system and what came out of the overall system.

In an effort to determine the amount of aerosols removed by the fluidized bed alone, tests were run in which the glass beads were removed from the bed retainer. Observations were then made on the system collection efficiency for each condition of bed shape and flow rate. Three replications were made and the mean values calculated for each of the nine treatment combinations involved (three flow levels x three bed retainer shapes). These data were then used to calculate the collection efficiency of the fluidized bed as follows:

Fluidized bed collection efficiency = Total system collection efficiency - Collection efficiency of the system piping

## Data Collected

The raw data collected during the tests included the items shown in Figure 26.

Items numbered (1) through (15) in Figure 26 were transferred to data punch cards and input to a computer program for basic reduction. Items (16) through (22) were not used except to operate the system during testing. All of the raw data are included in the Appendix and tabulated according to the day on which the tests were performed. Thus, the blanks shown for a particular day are used to correct the test filters for that day.

The output from the data reduction computer program listed the items shown in Figure 27. Sample calculations indicating the nature of the data reduction are offered in the Appendix. Note that in collecting the raw data, both engineering and metric units were used (i. e., pressures in PSIG, temperatures in $^{o}$F, and weights in grams). This was done for convenience in taking the readings directly from the instruments involved. However, the computer program converts and outputs all data in metric units.

In order to make calculations concerning flow rates, the computer program had to use the data from the orifice calibration curves. Recall that these were developed for both the inlet and outlet sampling systems. Data from these curves were included in the program and are given in the Appendix.

| No. | Symbol | Description |
|---|---|---|
| 1. | Run no. | The number of the particular run for that test day |
| 2. | S | Bed shape -- 1, 2, or 3 |
| 3. | RPM | The RPM of the rotating assembly |
| 4. | Mass | Bed material present or not -- 100 = present; 0 = not |
| 5. | Blk | Filters used as blanks or not -- 0 = not; 1 = blank |
| 6. | IWI | Initial inlet filter weight -- grams |
| 7. | FWI | Final inlet filter weight -- grams |
| 8. | IWO | Initial outlet filter weight -- grams |
| 9. | FWO | Final outlet filter weight -- grams |
| 10. | H1 | Manometer reading on inlet sampling system -- tenths of an inch of $H_2O$ |
| 11. | H2 | Manometer reading on outlet sampling system -- hundredths of an inch of $H_2O$ |
| 12. | P3 | Inlet pressure to the fluidized bed -- PSIG |
| 13. | T3 | Inlet sampling system temperature -- $^oF$ |
| 14. | T4 | Outlet sampling system temperature -- $^oF$ |
| 15. | Time | Duration of the test -- minutes |
| 16. | P1 | Inlet pressure to the entire system -- PSIG |
| 17. | P2 | Pressure at the pressure control valve -- PSIG |
| 18. | P4 | Pressure within the inlet sampling flow measurement system -- PSIG |
| 19. | P5 | Pressure within the outlet sampling flow measurement system -- PSIG |
| 20. | P6 | Input pressure to the aerosol generator -- PSIG |
| 21. | T1 | Temperature of the air entering the general system -- $^oF$ |
| 22. | T2 | Temperature of the air entering the rotating fluidized bed -- $^oF$ |

Figure 26. List of the items included in the raw data collected for each test.

| No. | Symbol | Description |
|---|---|---|
| 1. | Date | Date on which tests were performed |
| 2. | Run | The number of the test run for a particular day |
| 3. | RPM | The RPM of the rotating assembly |
| 4. | G | The G-level affecting the top portion of the rotating fluidized bed -- in "G's" |
| 5. | S | The bed shape -- 1, 2, or 3 |
| 6. | Mass | Bed material present or not -- 100 = present; 0 = not |
| 7. | WTI | Weight of aerosols collected on the inlet filter corrected for the changes in the blank filters -- grams |
| 8. | WTO | Weight of aerosols collected on the outlet filter corrected for the changes in the blank filters -- grams |
| 9. | VOLI | Volume of the gas sampled in the inlet gas sampling system -- liters |
| 10. | VOLO | Volume of the gas sampled in the outlet gas sampling system -- liters |
| 11. | CONCI | The calculated concentrations of aerosols entering the rotating fluidized bed assembly -- micro grams/liter |
| 12. | CONCO | The calculated concentrations of aerosols leaving the rotating fluidized bed assembly -- micro grams/liter |
| 13. | Eff | The overall collection efficiency of the system -- % |

*The program also calculated velocities at various points in the system, Reynolds Number at the inlet to the fluidized bed, and the theoretical pressure differential across the bed during operation. These data, however, are somewhat extraneous to the purposes of this investigation.

Figure 27. List of the items included in the output of the computer program used for basic data reduction.

This program worked equally well for data reduction regardless of whether the bed material was included in the bed retainer or not. Thus, it could calculate system efficiencies for the piping related to the fluidized bed as well as total system efficiencies.

# IV. RESULTS

## Data Evaluation Procedure

The evaluation of the data collected in this experiment involves three separate steps. First, the data are presented in summary form as a table of means (Table 2) and graphically (Figures 28 and 29) so that one can visually observe the effects of the independent variables upon the dependent variable. Second, the data are evaluated in the statistical sense to determine which of the main effects and interaction effects are statistically significant with respect to the dependent variable. Third, the method of dimensional analysis is used in conjunction with linear regression analysis to develop a mathematical relationship between the dependent and independent variables.

## Experimental Data

Using the equipment and techniques described in Chapter III experimental data were collected and evaluated to determine filtration efficiencies for a fluidized bed subjected to the various treatments. A total of 84 replications were made involving 27 treatment combinations. Table 2 is a table of means summarizing the data collected. The values shown are expressed as percent filtration efficiency. The raw data are presented in the Appendix.

The main objective of this experiment is to investigate the effects

Table 2. Table of means summarizing the data collected from the experiment. The values shown are expressed as percent filtration efficiency.

| G-level | Flow levels | | | | | |
|---|---|---|---|---|---|---|
| | 1 | No. reps. | 2 | No. reps. | 3 | No. reps. |
| | | | Shape I | | | |
| 44 | 64.53 | 4 | | | | |
| 98 | 56.27 | 4 | 23.43 | 3 | | |
| 204 | 55.90 | 3 | 25.86 | 3 | | |
| 319 | | | 26.07 | 3 | 15.64 | 2 |
| 417 | | | 22.71 | 3 | 13.24 | 3 |
| Means | 59.17 | 11 | 24.52 | 12 | 14.20 | 5 |
| Shape I mean = 36.29<br>No. replications = 28 | | | | | | |
| | | | Shape II | | | |
| 44 | 52.32 | 3 | | | | |
| 98 | 55.59 | 3 | 32.74 | 3 | | |
| 204 | 49.03 | 3 | 29.45 | 3 | | |
| 319 | | | 28.00 | 3 | 19.65 | 3 |
| 417 | | | 29.07 | 3 | 13.37 | 3 |
| Means | 52.31 | 9 | 29.82 | 12 | 16.51 | 6 |
| Shape II mean = 34.36<br>No. replications = 27 | | | | | | |
| | | | Shape III | | | |
| 44 | 50.28 | 3 | | | | |
| 98 | 48.40 | 4 | 25.30 | 3 | | |
| 204 | 43.18 | 3 | 19.76 | 5 | | |
| 319 | | | 19.18 | 3 | 8.96 | 3 |
| 417 | | | 22.19 | 3 | 4.68 | 2 |
| Means | 47.40 | 10 | 21.34 | 14 | 7.25 | 5 |
| Shape III mean = 27.90<br>No. replications = 29 | | | | | | |
| Flow level means | 53.19 | 30 | 25.02 | 38 | 12.89 | 16 |
| Grand mean = 32.77<br>Total replications = 84 | | | | | | |

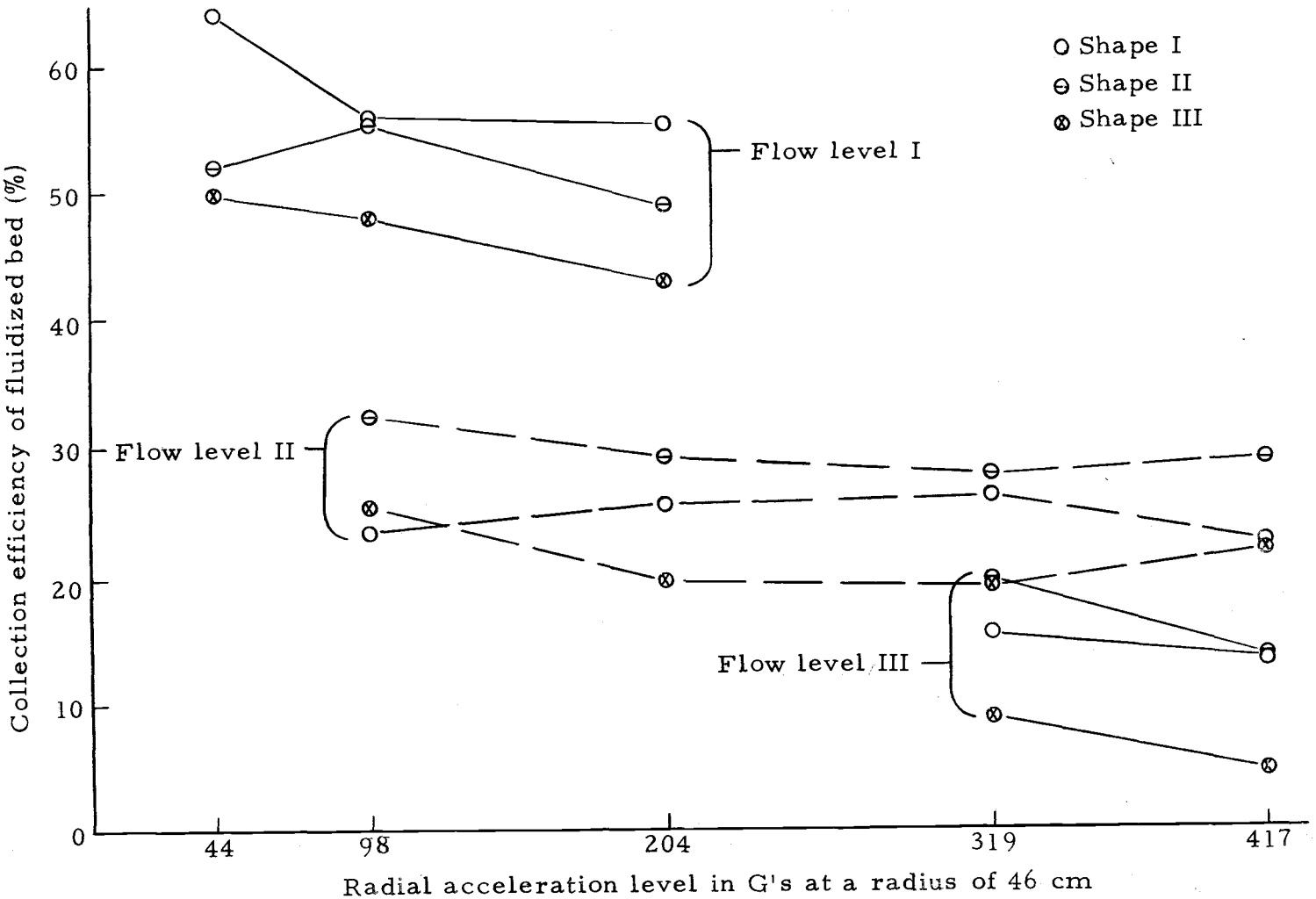


Figure 28. Plot of the data showing the relationship of collection efficiency in the fluidized bed to increasing levels of radial acceleration imposed on the bed for three levels of flow rate and three bed retainer shapes.

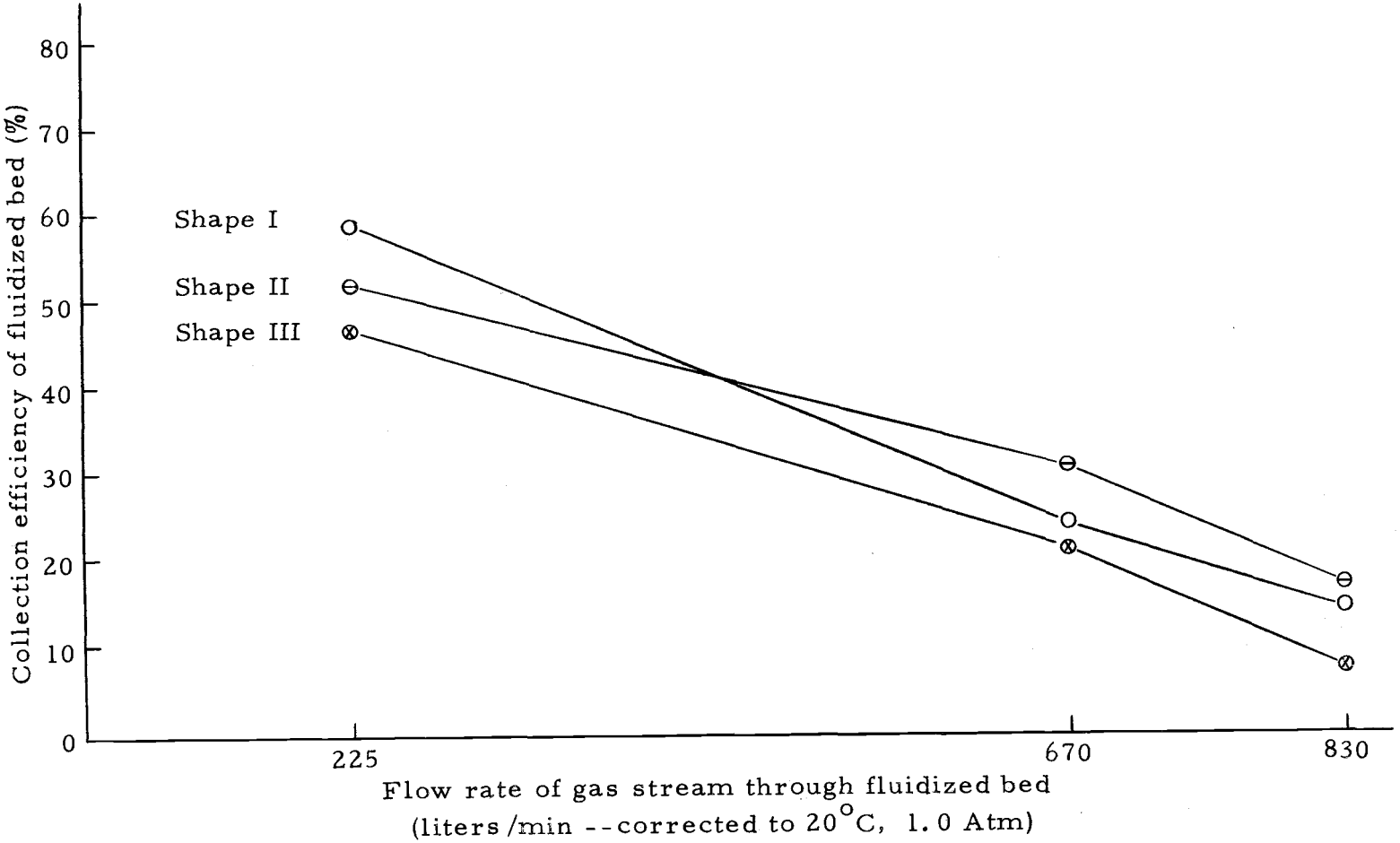


Figure 29. Plot of the data showing the relationship of collection efficiency in a fluidized bed to increasing levels of flow rate through the bed, for three bed retainer shapes.

of radial acceleration on a fluidized bed used as a filter. To show the relationship graphically, filtration efficiency is plotted versus radial acceleration in Figure 28 using the data from Table 2. Note that within each condition of flow level and bed shape there is a slight decrease in collection efficiency as the level of radial acceleration increases. For the nine cases plotted in Figure 28, the average slope of the line is -0.0304. Thus, with all other factors held constant (i.e. flow level and shape) filtration efficiency does decrease as G-level increases.

The second independent variable in this experiment is volumetric gas flow rate through the fluidized bed. Figure 29 shows the relationship of this variable to filtration efficiency for each bed shape using the data from Table 2. Note, however, that Figure 29 does not distinguish between levels of radial acceleration. Values shown are the averages for each flow level over all levels of radial acceleration used. The decrease in filtration efficiency with increasing volumetric flow rate is quite apparent.

The third independent variable in this experiment is the shape of the bed retainer. By considering the relative values of the average filtration efficiencies for each of the three bed shapes it can be observed that Shape I provides the most efficient filter configuration while Shape III is the least efficient.

| Bed retainer shape | I | II | III |
|---|---|---|---|
| Average filtration efficiency (%) | 36.24 | 34.36 | 27.90 |

## Results of the Statistical Analyses

In order to fully evaluate the experimental data, it is necessary to determine which of the main effects and interaction effects are statistically significant with respect to filtration efficiency. The experimental design provides sufficient "overlap" of the treatment combinations to make such investigations possible through the use of the General Linear Hypothesis Testing Program (*BMD-05V). With this program, seven hypotheses are tested using the "F" statistic at the 5% level of significance. The first of these is stated as follows:

Ho: The covariate cannot be used to adjust treatment means and reduce residual errors.

Hi: The covariate can be used to adjust treatment means and reduce residual errors.

The next six hypotheses have the same general form and can be stated as:

Ho: There is no difference in the response of the dependent variable due to changes in the independent variable.

Hi: There is a difference in the response of the dependent variable due to changes in the independent variable.

This form of the hypotheses applies equally well in testing the significance of both main effects and interaction effects.

The results of these seven hypothesis tests are summarized in Table 3. In tests two through seven the treatment means are adjusted

Table 3. Summary of the results of the seven hypothesis tests involved in the statistical analysis of the data.

| Test number | Factor tested | Significant at 5% level |
|---|---|---|
| 1 | Covariate (accumulated running time) | Yes |
| 2 | G-level | Yes |
| 3 | Volumetric flow rate | Yes |
| 4 | Bed retainer shape | Yes |
| 5 | G-level x Volumetric flow rate | No |
| 6 | G-level x Bed retainer shape | No |
| 7 | Volumetric flow rate x Bed retainer shape | Yes |

for accumulated running time on the bed. The third order interaction effect (i. e., G-level x Bed retainer shape x Volumetric flow rate) is assumed to be non-existent and is lumped with the error term.

The General Linear Hypothesis Testing Program is well adapted to analyzing the experimental data. Recall that the design included both unequal replications and missing cells. This precluded use of the library program written for analysis of covariance. The program is not without limitation, however. Development of the control cards used to analyze the data is a major undertaking. Also it is not possible to include the third order interaction in the hypotheses tested.

The data input to the program includes only two factors: (1) the values of the covariate; (2) the corresponding values of filtration efficiency of the fluidized bed. The program control cards are used

to distinguish the levels of the independent variables.

## Results of Dimensional Analysis

The third step in evaluating the experimental data involves the use of dimensional analysis methods in conjunction with linear regression analysis. Table 4 summarizes the independent variables of this experiment which may have influenced the dependent variable.

Table 4. Summary of the independent variables of this experiment.

| Independent variable | Symbol | Dimensions |
|---|---|---|
| Velocity* | V | cm/sec |
| G-level | G | Unitless |
| Bed shape | S | cm |
| Bed height | H | cm |
| Accumulated running time | T | sec |
| Gas density | $\rho$ | $gm/cm^3$ |
| Gas viscosity | $\mu$ | gm/cm· sec |
| Aerosol size | $D_p$ | cm |
| Bed material size | $D_f$ | cm |

*As discussed previously the actual experimental variable is volumetric flow rate. However, the bed shape is characterized by its diameter at the outlet. Since this is constant for each bed shape, velocity at the outlet it directly proportional to volumetric flow rate at the outlet. This makes a direct substitution of velocity for volumetric flow rate possible.

Using these items, the dimensionless relationships shown in Equation 2 are developed.

$$\text{Eff.} = \emptyset\ (N_{Re},\ \text{G-level},\ H/S,\ TV/D_p) \tag{2}$$

where $N_{Re}$ = Reynold's number = $\frac{VD_f\rho}{\mu}$

An additive model is then assumed of the following form:

$$\text{Eff.} = \text{Const.} \times (N_{Re})^a(\text{G-level})^b(\frac{H}{S})^c(\frac{TV}{D_p})^d \tag{3}$$

Using the experimental data to evaluate the basic parameters and the Stepwise Multiple Linear Regression Analysis Program (*Step) of the Oregon State University Statistical Library to estimate the constant and the exponents, Equation 4 is developed.

$$\text{Eff.} = 1.25(N_{Re})^{-0.9030}(\text{G-level})^{-0.1588}(\frac{H}{S})^{1.8519} \tag{4}$$

Note that the last dimensionless term of Equation 3 is not found in Equation 4. Its presence in Equation 4 increases the percentage of variation explained by regression by only 0.4%. Therefore, it is not included.

In order to evaluate the effects on filtration efficiency due to varying G-level, volumetric flow rate, and/or bed shape, Equation 4 is rewritten in the form of Equation 5.

$$\begin{aligned}\text{Eff.} = {} & \text{Constant} \times (\text{G-level})^{-0.1588} \times (\text{Volumetric flow rate})^{-0.9030} \\ & \times (\text{Bed shape})^{-1.8519} \times (\text{Bed height})^{1.8519} \times (\text{Dia. bed} \\ & \text{material})^{-0.9030} \times (\text{Gas density})^{-0.9030} \times (\text{Gas} \\ & \text{viscosity})^{0.9030}\end{aligned} \tag{5}$$

As would be expected from observing Figure 28, efficiency decreases with increasing G-level and with increasing flow rate. The bed shape is characterized by the diameter of the bed retainer at the discharge end of the bed. As this diameter increases (for a constant bed mass) the filtration efficiency decreases.

It should be noted that to correctly use the method of dimensional analysis all of the variables affecting the response should be considered. It is pointed out in the Review of the Literature that the electrostatic charge characteristics of the fluidized bed and of the aerosols being collected do have an effect on the response measured. However, these variables are not measured in this experiment. Therefore, they are not included in the dimensional analysis. This results in a regression equation which accounts for only 64% of the total variation observed.

## Interpretation of the Results

It has been noted in the preceding discussion that filtration efficiency in a fluidized bed is decreased by (1) increasing the level of radial acceleration and (2) increasing the volumetric flow rate (hence the velocity) through the bed. By referring to the discussion of filtration mechanisms (Chapter II) insight can be gained as to why these effects were observed.

In the mathematical models for the mechanisms involved in filtration, only the mechanism of gravitational settling contains a

gravitation term. Filtration efficiency associated with this mechanism is considered to be a direct, linear function of the G-level. Since overall filtration efficiency of the fluidized bed is assumed to be a cumulative function of all of the mechanisms involved, theory predicts that increasing only the G-level would result in increasing the overall filtration efficiency.

The fact that this effect is not observed in this experiment is attributed to two things. First, the mechanism of gravitational settling does not play an important part in overall filtration efficiency of a fluidized bed. If it did, then the large range over which G-level was varied in this experiment would have resulted in large changes in efficiency. Second, the method in which filtration efficiency is measured is subject to systematic errors. These are discussed in detail under Discussion of Errors. Error No. 13 (p. 89) is thought to have resulted in the basic differences between the theoretical efficiencies and the observed efficiencies under conditions of increasing G-level.

The effects observed on filtration efficiency due to increasing the volumetric flow rate may indicate which of the filtration mechanisms predominate in this experiment. Noting that inertial impaction was the only mechanism in which filtration efficiency is directly related to velocity, the conclusion can be made that inertial impaction is not a dominant mechanism in rotating fluidized bed filtration. If it were a dominant mechanism, then increases in velocity would result

in increased filtration efficiency.

The models for gravitational settling, Brownian diffusion and electrostatic precipitation mechanisms all relate filtration efficiency inversely to velocity. Since gravitational settling has already been established as not being an important mechanism in this experiment, that leaves Brownian diffusion and electrostatic precipitation as possible alternatives. Both mechanisms relate filtration efficiency linearly and inversely to velocity.

Referring again to the Review of the Literature, Anderson and Silverman (2) established the existence of the "triboelectrification" effect and noted that charging of the bed material did have a strong influence on filtration efficiency in fluidized beds. This phenomenon was observed in this experiment, as noted by the charged beads adhering to the disengaging zone walls after each series of tests. (See discussion of this in Chapter V). Therefore, it is reasonable to assume that the mechanism of electrostatic precipitation did play a strong part in the overall filtration efficiencies observed since (1) the electrostatic charge was observed and (2) the efficiency decreased with increasing velocity in keeping with the mathematical model for this mechanism.

In evaluating his results Black (3) concluded that direct interception was the dominant mechanism but that Brownian diffusion was also involved. This conclusion was based upon analyses of the

so-called "target efficiencies" calculated for each of the filtration mechanisms. Since Black's bed material was approximately the same size and since the size of the aerosols was also similar, it is reasonable to assume these two mechanisms also apply to filtration in a rotating fluidized bed.

No further attempt is made to evaluate the relative influence of the filtration mechanisms for this experiment. However, they are summarized in Table 5.

Table 5. Summary of the relative importance of the mechanisms of filtration as they apply to this experiment.

| Mechanism | Relative importance in filtration efficiency for this experiment |
|---|---|
| Direct interception | Most important based on Black's evaluation of efficiency due to this mechanism in terms of the relative size of the bed material and the challenging aerosol. |
| Inertial Impaction | Not important |
| Brownian diffusion | Probably has some effect. This is based on (1) Black's evaluation of this mechanism and (2) the inverse relationship of efficiency to velocity expressed in the model for this mechanism. |
| Electrostatic precipitation | Probably has some effect, based on (1) Anderson and Silverman's findings and (2) the observed electrostatic charge on the bed material. |
| Gravitational settling | Not important |
| Thermal precipitation | Not applicable |
| Sieving | Not applicable |

In concluding this discussion of the experimental results, a comparison is made between Black's findings with a "stationary" fluidized bed filter and the results of this experiment. Recall that the bed material used for both studies was approximately the same size. However, Black used ammonium chloride aerosols, whereas sodium chloride aerosols were used in this experiment. Black found that for the conditions of his tests filtration efficiency could be expressed as:

$$\text{Eff.} = 0.454 \left(\frac{H}{S}\right)^{0.4} V^{-0.1}$$

In comparison, efficiency for a rotating fluidized bed under the condition of this experiment is expressed as:

$$\text{Eff.} = 1.25\ V^{-0.9030} (\text{G-level})^{-0.1588} \left(\frac{H}{S}\right)^{1.8519} (D_f \rho/\mu)^{-0.9030}$$

Apparently both velocity and bed height to diameter ratio become more important in the rotating fluidized bed filter system. However, this may be due in part to the difference in the type of challenging aerosol. For each case efficiency and velocity are inversely related and efficiency and bed height to diameter ratio are directly related.

# V. CONCLUSIONS AND DISCUSSION OF ERRORS

## Conclusions

From the evaluation and interpretation of the data the following conclusions can be drawn:

(1) At the 5% level of significance radial acceleration has a statistically significant effect on filtration efficiency of a fluidized bed used to filter sub-micron particulate. With increasing G-levels filtration efficiency decreases.

(2) At the 5% level of significance the gas flow rate through a rotating fluidized bed has a significant effect on filtration efficiency. Increasing the gas flow rate decreases filtration efficiency.

(3) At the 5% level of significance variations in the shape of the bed do exhibit a significant influence on filtration efficiency. When the shape is characterized by the diameter of the bed retainer at the discharge end of the bed, then efficiency is inversely related to bed diameter for a given bed mass.

(4) At the 5% level of significance there is a significant interaction effect on filtration efficiency between gas flow rate and the shape of the bed retainer.

(5) We do not have sufficient data to say at the 5% level of significance that interaction effects between gas flow rate

and G-level and between bed retainer shape and G-level are significant in their effect on filtration efficiency.

(6) The above mentioned relationships can be expressed mathematically as follows:

$$\text{Eff.} = 1.25(N_{Re})^{0.9030}(\text{G-level})^{-0.1588}\left(\frac{H}{S}\right)^{1.8519}$$

(7) From evaluation of the data for this experiment and from the findings of other authors it would appear that the most dominant mechanism of filtration involved in this experiment is direct interception. Brownian diffusion and electrostatic precipitation are also thought to be involved to a lesser extent.

## Discussion of Errors

There are many sources of errors involved in this experiment. Generally speaking they can be grouped into two categories: (1) Errors of measurement; (2) Miscellaneous errors.

### Errors of Measurement

(1) Two temperature readings were involved with each test. The range on the thermometers was 30-240$^{o}$F and readings could be made to within $\pm$ 1$^{o}$F. Since these data were used to correct flow rates in the flow measurement systems, such errors would not affect the results by more than 0.2%.

(2) Pressure readings were not involved in the calculation of filtration efficiency. Rather, they were used to monitor and control the system during testing. However, both the inlet and outlet sampling flow measurement systems were calibrated at specific pressures. Any deviations from these pressures would result in errors of flow measurement and, therefore, errors in calculating filtration efficiency. In each case, it was felt that pressures could be measured and controlled to within $\pm$ 0.068 Atm. (1 PSIG). For the inlet sampling system, this would result in errors up to 5%; for the outlet sampling system, 2%.

(3) Since manometers were used to measure pressure differentials across the orifices, errors in reading the manometers were introduced. During normal operation of the system, slight fluctuations in the water levels were observed. Values recorded were taken as "visual average" values of the manometer readings. Errors of this type were probably less than 2% for the inlet flow measuring system and 1% for the outlet flow measuring system.

(4) For each test, the calculations of incoming and outgoing aerosol concentrations involved a time measurement of the aerosol collection period. Errors in measuring time were small, probably less than 0.5%.

(5) The angular velocity of the system was measured with a "Strobotac" or a variable frequency strobe light. In the low RPM

range the instrument allows measurements to within ± 1 RPM, but in the higher ranges accuracy is reduced to ± 3 RPM. Thus errors were introduced in measuring the level of radial acceleration. It is estimated that the G-level determinations were influenced up to 2% by this factor.

(6) As noted previously, the bed mass in the rotating system was a constant and equaled 100 grams of glass beads. Small errors were introduced in weighing these beads and through loss of bed material while transferring it to the rotating system. Errors of this type were estimated at less than 1%.

(7) In the 84 tests of this experiment, approximately 350 individual glass fiber filters had to be weighed twice. Thus some 700 weights were recorded using a laboratory balance. Weights were taken to the nearest tenth of a milligram. Due to the high quality of the scale, it is estimated that errors in weight measurement were less than 0.01%.

Miscellaneous Errors

(8) The orifice calibration curves were developed by plotting measured flow rate versus the manometer readings. A smooth curve was drawn between the calibration points, not all of which fell on the curve. The data used in the computer program to calculate flows and efficiencies were taken from the smooth curve. Therefore, some

small errors may have been introduced. They are likely to be less than 1%.

(9) Timing sequence errors were also introduced. The sampling procedure for the system was as follows:

1. Fluidize the rotating bed and set all flow levels and pressures at the desired values. Do this with the sample filter holders bypassed.
2. Close the bypass on the inlet sampling system and open the flow path through the filter holder.
3. Repeat (2) for the discharge sampling system.
4. Collect samples for the required period of time.
5. Open the bypass on the inlet filter system and isolate the filter holder.
6. Repeat (5) for the discharge section.
7. Bleed the pressure off the filter holders and change the filters.
8. Keep the system operating so that the second and third samples can be taken following steps (2) through (7).

Note that in this procedure (steps 2 and 3) there is a time lapse after the inlet system starts collecting samples and before the discharge system starts. This time lapse is repeated at the end of the cycle (steps 5 and 6). The operating sequence is designed to minimize errors in sampling due to this lapse. Such errors probably do not

affect concentration measurements by more than 1%.

(10) As noted in (8) above, some 700 weights were recorded. In addition approximately 800 more data points were involved in the experiment. Transfer of these data from primary data collection forms to data punch cards undoubtedly involved some errors even though the cards were carefully proofread. It is estimated that transfer errors occurred three times for 1500 data points.

(11) The flywheel on the jack shaft was installed to control angular velocity fluctuations due to line voltage variations at the induction motor. In this regard it served its purpose well. However, the upper bearing on the jack shaft suffered some damage during installation and did not run smoothly. This resulted in minor RPM fluctuations probably not greater than $\pm$ 2 RPM. Such fluctuations did contribute to errors in determining G-level, since the system was not instrumented to detect these fluctuations.

(12) The object of this experiment was to investigate filtration efficiency for particulate matter of sub-micron size. Microscopic analysis of the sodium chloride particulate indicated that the individual aerosols were indeed of sub-micron size. A size distribution analysis was not made, however, because to do so would require an electron microscope and the related expenses. Junge (6) has pointed out that under conditions of relative humidity in excess of 70%, small particles tend to agglomerate, thus increasing their effective mass.

Unquestionably during the course of this experiment tests were made wherein relative humidities exceeded 70%. In fact, the tests were halted at the 417 G-level due to excessive moisture in the system. Microscopic examination of the bed material following tests at high G-levels showed agglomerated aerosols on the surface of the glass spheres. Whether such agglomeration occurred in the bed or prior to entering the bed is not determined. It is safe to assume, however, that conditions were conducive to agglomeration and that under some test conditions (particularly at the 417 G-level) the fluidized bed was filtering out micron sized aerosols. No estimate is offered of the magnitude of the errors involved due to this factor.

(13) As has been discussed, it was not possible to directly measure the filtration efficiency of the fluidized bed. Instead, the efficiency of the system was measured with and without the bed material. Mean values of filtration efficiency for the system without the bed were used to determine the "bed efficiency" for each condition of bed shape and flow rate.

This procedure for determining the filtration characteristics of the fluidized bed has a serious drawback. When the bed material is in place, pressure differentials across the bed ranged from 0.14 Atm at 44 G's to 3.04 Atm at 417 G's. For the lower pressure differential conditions the velocity of the gas stream entering the bed region is roughly the same with or without the presence of the bed

material. But for the higher pressure differential conditions, the velocities of the incoming gas stream are not the same. This is illustrated in Figure 30.

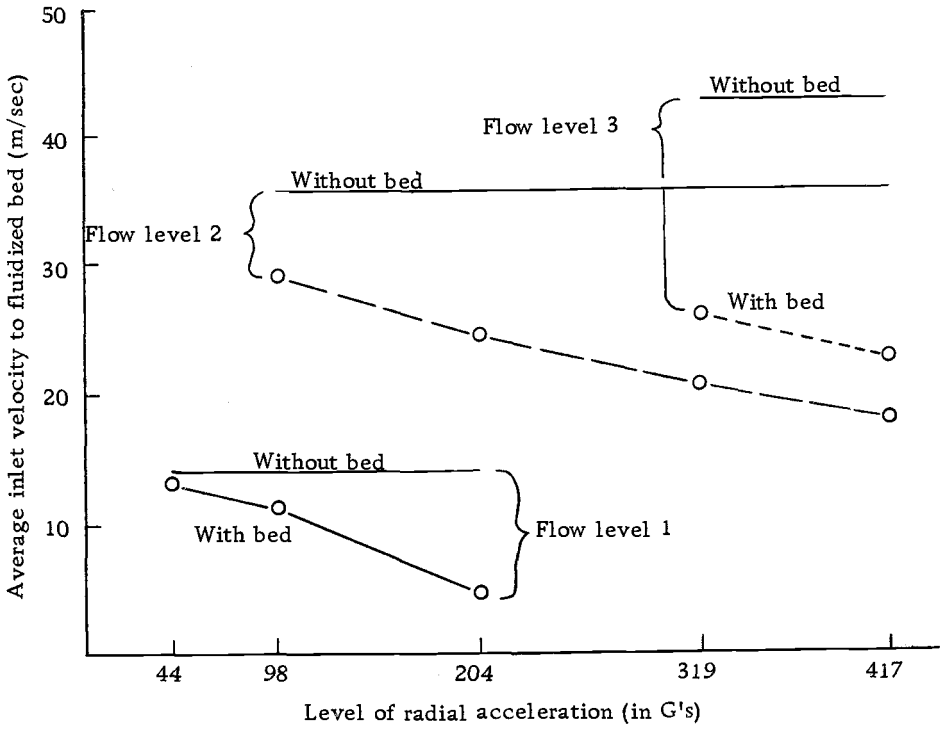


Figure 30. Plot showing the relationship of average inlet velocity to the fluidized bed versus G-level for the Shape II bed retainer and different flow conditions.

Now consider the means by which aerosols are removed in the "empty bed" system. The gas stream makes four sharp $90^{o}$ turns in the rotating piping system before it reaches the bed retainer. At higher velocities, greater amounts of aerosols will be removed by impaction at each of these turns. Therefore, if the velocities for the

"empty system" are higher than the corresponding velocities for the system with the bed in place, substantial errors in calculating actual "bed efficiency" are introduced.

Although they are difficult to estimate in magnitude, sizable errors are likely in calculating actual fluidized bed filtration efficiencies at the higher G-levels. The errors would, of course, be less at the lower G-levels where the pressure differentials are diminished. The trend of the errors would be to reduce the calculated "bed efficiency." Thus it is possible that bed efficiencies may tend actually to increase with increasing G-level rather than decrease as was shown in Figure 28.

(14) In any gas flow measurement system, if the gas leaks out of the system before it is measured, inaccuracies in measurement will result. For this particular project, it is felt that leakage at the unions, rotating couplings, and other seals was negligible. Some very minor leaks were observed. The loss of volumetric flow was probably less than 0.5% of the total. Thus, errors due to this factor were extremely small.

(15) For each day of testing, a minimum of four blank filters for both the inlet sampling system and the outlet sampling system were used to correct for changes in relative humidity. Naturally there was some variance in the weight changes on these blanks. This variance was not great but it was uncontrolled. Since the mean value

of the blank filter weight changes was used to correct each regular test filter, the variance of the blanks was not taken into account. It is difficult to estimate just how great this error is. In looking at the variance of the blanks, it is quite likely to be small.

(16) As Black has observed, the concentration of the incoming aerosols did not have a significant effect on the filtration efficiency of his system. That assumption was made for purposes of this experiment. In this experiment the incoming concentrations did vary substantially, however, ranging from 5 to 64 micrograms of aerosol per standard liter of gas. The concentration level appeared to be most strongly influenced by the pressure of the incoming gas stream and by the flow rate. At high pressures and high flow rates, the concentration of aerosols was very low. Under these same conditions which corresponded to high G-levels and high flows, the fluidized bed filtration efficiency was very low. Therefore, a high positive correlation exists between incoming concentrations and fluidized bed efficiency.

It may be that errors have arisen in the experiment by disregarding concentration variations. It is difficult to estimate the magnitude of such errors, however.

(17) Early in the experimental work, it was discovered that rust particles generated within the system were strongly influencing the measurement of aerosols in both the inlet and outlet sampling systems.

To solve this problem, the interior of all of the pipes from the initial fiber glass filter to the discharge of the output sampling unit were painted with two coats of epoxy base paint. Note, however, that the vertical shaft supporting the rotating assembly and the two parallel pipes on the rotating assembly did not receive this treatment. The material involved here was mechanical steel tubing which is subject to the corrosive action of the sodium chloride aerosols. This area of of the system is downstream from the inlet sampling system so any rust generated would not be sampled on the inlet side. It would show up on the discharge side, however, and would act effectively to (1) increase the loading on the bed; (2) show reduced filtration efficiencies for the bed.

As to the magnitude of the problem, it was probably very slight. It is true that rust particles did show up on the discharge filters, but they were very small (two to five microns) and very few in number. It is estimated that they did not account for more than 1% of the total loading on these filters.

(18) In some treatment combinations involving high flow rates and lower G-levels, some of the bed material was transported out of the bed. When this occurred, it was either carried out of the rotating assembly entirely, or it remained in the disengaging zone. (See discussion of the bed operating characteristics.) In either case, the effective mass of the bed was reduced to something less than 100 grams.

Black has observed that bed mass was directly related to filtration efficiency. On the assumption that this applied to a rotating bed as well as a static bed, then such losses of material would reduce the effectiveness of the bed as a filter. The analyses of the data do not account for such losses, however. It is assumed throughout that the bed mass remained constant. Thus errors were present due to loss of bed material. Again their magnitude was probably small. Losses of material are estimated at less than 5% or five grams for the normal series of tests. This is based on changes in pressure drop versus time while the system was operating.

(19) As is noted in the discussion covering the collection of data, the average sampling period during tests was 30 minutes. During this period slight changes in pressures and temperatures were observed as the system came to equilibrium conditions. The changes in pressure were corrected as soon as they were observed, but no temperature alterations could be made. Therefore, it was the practice to make all temperature and pressure measurements for the data log at a time midway in each test. Thus slight errors may have arisen due to lack of integration for temperature-time relationships. These are probably small in size, however, accounting for less than 2% errors in flow rates.

# VI. SOME OBSERVATIONS REGARDING FLUIDIZED BEDS OPERATING AT HIGH RADIAL ACCELERATION LOADS

As noted previously, only a few rotating fluidized beds have been constructed. Therefore, little has been published concerning their operating characteristics. The following discussion pertains to some areas of interest herein.

## Bed Material

Many materials have been used for rotating fluidized beds, i. e., bronze, aluminum, silica, glass beads, and steel shot. Black used glass spheres with a mean diameter of 25 microns, and achieved reasonable success in terms of filtration efficiency. Based on these findings, similar glass spheres were used for this investigation. These are manufactured by the Micro-Bead Division of Cataphote Corp. They ranged in size from 4 to 51 microns and were quite spherical with few blemishes. In the initial investigations, larger spheres were used ranging in size from 150 to 250 microns with a mean diameter of 174 microns. These worked satisfactorily at the 44 G-level of radial acceleration; however, they failed at the 204 G-level. Due to their higher settling velocities, much greater flow rates were required to fluidize the larger spheres. The higher superficial gas velocities coupled with the larger mass of the spheres resulted in high impact collisions between particles. After one hour of operation

at the 204 G-level, the beads were observed at 450X and were found to be severely damaged. Every sphere was broken and chipped. The small fragments of broken glass badly eroded the bed retainer and the inlet to the retainer. Further tests were discontinued with the larger spheres. All subsequent tests were run with the small beads.

## Bed Inlet

In a "normal" fluidized bed, the gas stream entering the operating region is usually fed through a distributor. This acts both as a support for the bed material and as a device to provide a constant velocity profile across the bed.

In the initial design for this rotating fluidized bed, a combination bed support and gas distributor was used. Unfortunately, it acted to remove substantial amounts of sodium chloride aerosols at the same time. Since this made reasonable data collection very difficult, the support was removed. In its final configuration, the inlet to the bed appeared as shown in Figure 31.

In this design, the incoming gas stream passed through a constricted area and, therefore, entered the base of the bed at high velocities. This accomplished two things: (1) it provided a turbulent condition to help in fluidizing the bed without "dead spots" or quiet zones in the bed; (2) it prevented the bed material from leaving the normal operating region by backing up into the constricted region.

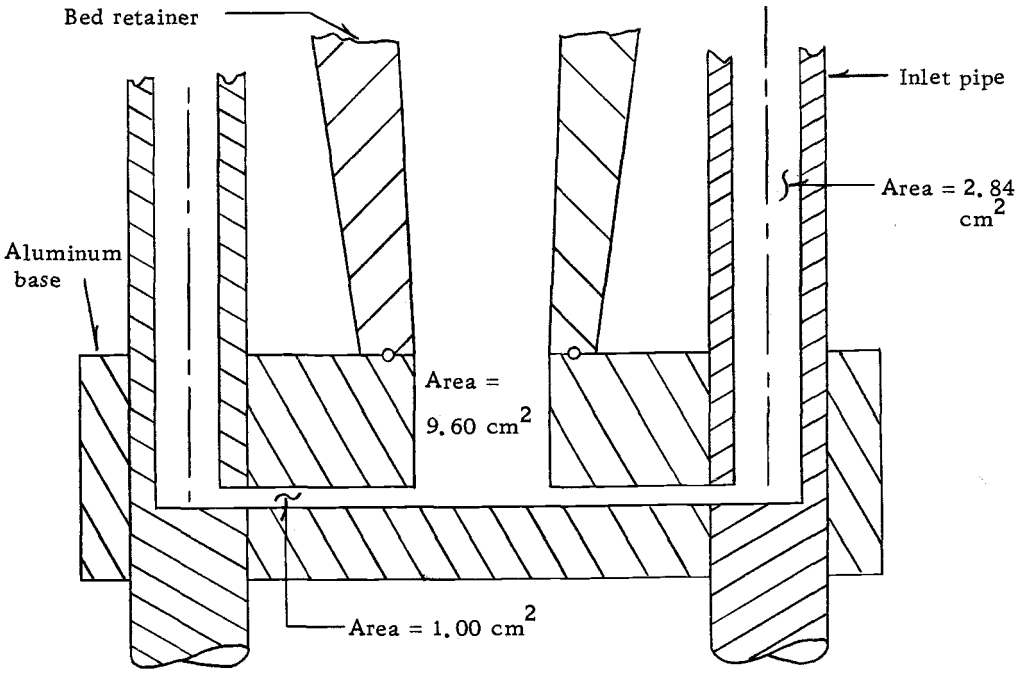


Figure 31. Diagram showing the configuration of the inlet to the fluidized bed operating region.

## Pressure Differential Characteristics

The pressure differential characteristics of a rotating fluidized bed may be of interest to some investigators. For this experiment all tests were conducted with the bed in a fluidized state. Therefore, no data were collected concerning the pressure drop in the non-fluidized state. Figure 32 is a plot of the actual pressure drop observed versus radial acceleration level.

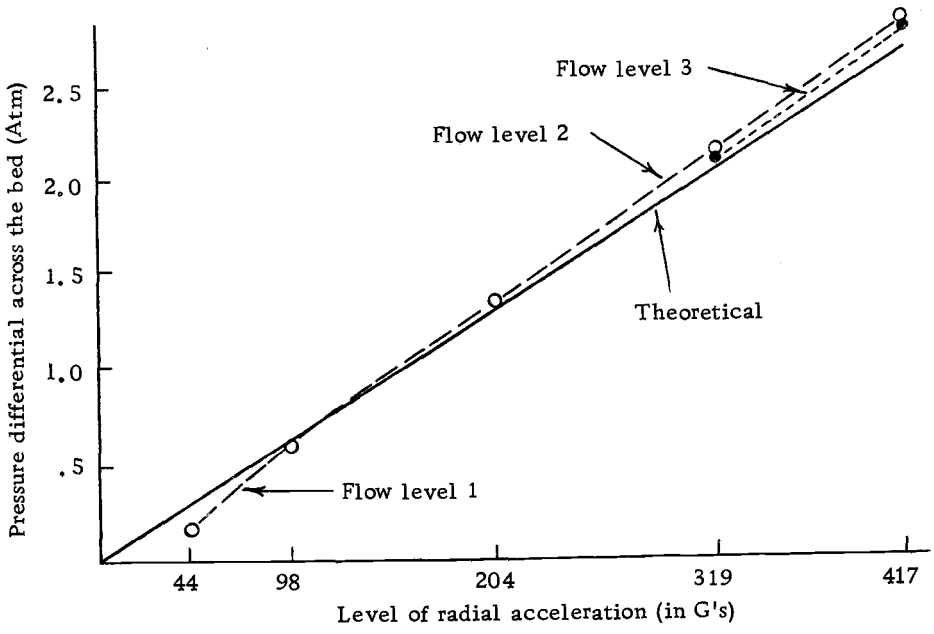


Figure 32. Plot of the actual and predicted pressure drops versus radial acceleration level for fluidized beds.

Kunii and Levelspiel (7) provide an equation relating pressure drop to G-level:

$$\Delta P = \frac{L_{mf}(1 - \epsilon_{mf})(\rho_s - \rho_g)g}{g_c} \qquad (6)$$

where $\Delta P$ = pressure drop, gm-wt/cm$^2$

$L_{mf}$ = bed height at min. fluidizing conditions, cm

$\epsilon_{mf}$ = void fraction of the bed, assumed equal to 0.63*

$\rho_s$ = density of the solid material, gm/cm$^3$

$\rho_g$ = density of the fluid (gas), gm/cm$^3$

$g$ = acceleration level, cm/sec$^2$

*7, p. 72.

$g_c = 980$ gm cm/gm-wt $sec^2$

This relation is also plotted in Figure 32 for comparative purposes. Note that the value of $\epsilon_{mf}$ is assumed for all conditions and that such an assumption may not be valid throughout the range of G-levels indicated. Furthermore, in the rotating condition the fluidized bed was generally unstable. Therefore, determination of an average value of $L_{mf}$ is difficult.

## Operating Characteristics

A description of the operating characteristics of the rotating bed may be appropriate. In general, for any given G-level and shape the bed responded to changes in flow rate in the same manner. Once the bed was brought up to its operating angular velocity, the air flow valves were opened gradually. The pressure would build up to a point where bubbles of air would be forced through the bed. For low flow rates, these bubbles could be seen emerging as small bumps or "teats" on the discharge end of the bed. As the flow rate increased slightly, the bed would expand somewhat and the surface would become "choppy" like the surface of a small lake affected by a light breeze. Further increases in flow rate would result in increased instability of the bed. Slugging conditions frequently occurred with relatively low flow rates, particularly at higher G-level.

Under moderately high flow rates, air bubbles could be seen

going up the side of the bed retainer wall. The extreme turbulence of the bed was quite obvious under these conditions. Still higher flow brought about dispersed fluidization and carryover of the bed material to the disengaging zone.

While some effects were observed due to the shape of the bed retainer, the system did not permit any visual observation of the differences in modes of fluidization due to this treatment. Certainly the beds looked different depending on which retainer was in use, but it was not possible to say, for example, whether a bed was quiescent on the top and aggregative on the bottom or vice-versa. In general, for most tests the bed was turbulent and unstable throughout, regardless of the bed shape.

Reference was made in the Review of the Literature to work by Anderson and Silverman concerning the phenomenon of triboelectrification. This is the acquisition of a net electrostatic charge on a bed due to contacts of the fluidized medium with conducting surfaces interspersed throughout the medium. The glass beads used as bed material did make frequent contact during fluidization with the conducting walls and supports for the disengaging zone. The aluminum base of the bed was a conductor, electrically contacting the disengaging zone via the parallel inlet pipes. This physical situation, in conjunction with the highly polar nature of glass beads resulted in triboelectrification.

Invariably at the end of each series of tests on one bed of material, it was observed that substantial amounts of the beads were strongly adhering to the walls of the disengaging zone. A vacuum (from an industrial vacuum cleaner) and vigorous brushing were required to remove these beads before a new bed could be placed in the system. As the beads were pulled through the vacuum hose, several sparks could be drawn between the hose and a ground source as the charge was dissipated.

Black did not report any similar effects. However, his bed retainer was of glass and did not involve any conductive surfaces. No measurements of the actual amounts of accumulated charge were made. It is felt, however, that this charging effect did improve the filtration efficiency of the system. It was frequently observed that filtration efficiencies did increase after the first test in the subsequent runs. This suggests that the charge was building up in the bed as a time function and that it offset tendencies toward lower filtration efficiencies caused by a removal of bed material from the operating region.

Following tests, several microscopic examinations were made of the bed material. Usually the beads would have a slightly grey appearance following tests as opposed to their "flour" white appearance as new beads. This change may have resulted from refractive variations due to particulate buildup on the spheres. It was not

common to see individual sub-micron particles on the spheres. In fact the particulate usually appeared as agglomerated clusters of the sub-micron aerosols. Furthermore, not all beads collected aerosols. Apparently due to polarity differences, some beads collected many aerosols and some beads collected none.

This concludes the discussion concerning the observations of the behavior of rotating fluidized beds.

# VII. SUMMARY AND RECOMMENDATIONS

## Summary

It has been established in the literature that fluidized beds can act effectively as filters for air-borne sub-micron size particulate. This fact in conjunction with the known regenerative capacity of fluidized beds suggests their applicability as filters for space laboratories. In space the change in the Earth's gravitational attraction would have to be offset by other combined forces in order to maintain fluidization of the bed material. One method of accomplishing this is to exert radial acceleration forces on the fluidized bed. In doing so it is possible to increase the level of radial acceleration substantially beyond one "G." As G-levels are increased, greater volumetric flow rates of gas through the bed can be attained.

Studies have been reported in the literature dealing with rotating fluidized beds. However, none of these have dealt with the filtration characteristics of fluidized beds subjected to radial accelerations above one "G." From the mathematical models used to describe the mechanisms of filtration, one cannot predict the effect on filtration efficiency due to increasing either G-levels or flow rate through the bed.

Therefore, experimental equipment was designed and constructed to evaluate this net effect. Glass spheres with a mean diameter of 15

microns were used as bed material and sodium chloride aerosols were used as particulate matter. Test data were collected in an experimental design in which G-level, gas flow rate, and shape of bed were considered as independent variables. The hypotheses tests indicated that each of the independent variables and the flow level by shape interaction significantly affected filtration efficiency at the 5% level of significance.

The estimated mathematical relationship between the variables is expressed as:

$$\text{Eff.} = 1.25\,(V)^{-0.903}(\text{G-level})^{-0.1588}\left(\frac{H}{S}\right)^{1.8531}\left(\frac{D_f \rho}{\mu}\right)^{-0.903}$$

Based on this relationship and the works of other investigators, it is suggested that under the conditions of this experiment the most important mechanisms of filtration are direct interception, Brownian diffusion, and electrostatic precipitation.

Since filtration efficiency is inversely related to G-level raised to the 1/6 power, one might vary G-level over a wide range without a large change in filtering efficiency. However, increasing the G-level requires a corresponding increase in the flow rate of gas through the bed in order to maintain a state of fluidization. Since filtration efficiency is almost linearly and inversely related to gas velocity, the net effect of flow rate increases is to decrease filtering efficiency.

As applied to future work in space travel, fluidized bed filtration systems certainly have possibilities. This experimental work indicates

that such filters should be subjected to relatively low levels of radial acceleration in order to reduce the gas flow rates required for fluidization to take place. This is not a severe restriction, however. Given a sufficient bed height to diameter ratio and a suitably large bed mass efficiencies in excess of 90% can easily be attained at radial acceleration levels up to 50 G's. Furthermore, the use of rotating fluidized beds as filters should not be restricted to space travel. Efficient filtration of sub-micron sized particulate matter has been a difficult task in many industrial situations, particularly those in which large volumetric flow rates are involved. By going to elevated levels of radial acceleration, greater flow rates can be handled in a fluidized bed of a given size. It is entirely conceivable that rotating fluidized bed filters could be built to handle flows in the range of 100,000 CFM with efficiencies in excess of 90%. Such beds could be continuously regenerated and the particulate matter recovered for recycling. Considering the cost of the present alternatives such filtration systems are certainly worth investigating.

## Recommendations

As a result of the current need for high efficiency, low cost, reliable filtration systems to handle pollutant emissions, it is recommended that this research work be continued in the following specific areas:

(1) Investigate the effectiveness of different fluidized bed materials in filtering specific sub-micron size particulate.

(2) Investigate the filtration characteristics of fluidized beds used to remove common pollutants such as:

a) Kraft mill recovery furnace emissions

b) Fossil fuel burning power boiler fly ash emissions

c) Municipal incinerator emissions.

(3) Investigate the effect of temperature on filtration efficiency in fluidized bed filters.

(4) Investigate the use of a fluidized bed of dolomite lime subjected to elevated G-levels in removing $SO_2$ from a gas stream.

(5) Expand the work in (4) to include high temperature and high humidity studies as well as continuous regeneration of the dolomite lime.

# BIBLIOGRAPHY

1. American Petroleum Institute. Removal of particulate matter from gaseous wastes, filtration. New York, 1961. 56 p.

2. Anderson, D. M. and L. Silverman. Mechanisms in electrostatic filtration of aerosols with fixed and fluidized granules. Boston, Massachusetts, Harvard University. 1958. 132 p.

3. Black, C. H. Effectiveness of a fluidized bed in filtration of air-borne particulate of submicron size. Ph. D. thesis. Corvallis, Oregon State University. 1967. 80 numb. leaves.

4. Gel'perin, N. I. et al. Apparatus with fluidized beds of free-flowing materials in centrifugal fields. (In Russian). Khim. Mashinostroenie, 1960, No. 3, 1-4.

5. Hatch, L. P. Proceedings of an Advanced Nuclear Propulsion Symposium. R. S. Cooper. (Los Alamos Scientific Laboratory. June 1, 1965)

6. Junge, C. E. Air chemistry and radioactivity. Academic Press. 1963. p. 133.

7. Kunii, D. and O. Levenspiel. Fluidization engineering. New York, Wiley. 1969. 534 p.

8. Leva, M. Fluidization. New York, McGraw-Hill. 1959. 327 p.

9. Los Alamos Scientific Laboratory of the University of California. Experimental studies relating to rotating fluidized bed reactors. Los Alamos, New Mexico. February, 1964. 38 p.

10. Meissner, H. P. and H. S. Mickley. Removal of mists and dusts from air by beds of fluidized solids. Industrial and Engineering Chemistry 41:1238-1242. 1949.

# APPENDICES

# APPENDIX A

## RAW DATA

| No. | Symbol | Description |
|---|---|---|
| 1. | Run no. | The number of the particular run for that test day |
| 2. | S | Bed shape -- 1, 2, or 3 |
| 3. | RPM | The RPM of the rotating assembly |
| 4. | Mass | Bed material present or not -- 100 = present; 0 = not |
| 5. | Blk | Filters used as blanks or not -- 0 = not; 1 = blank |
| 6. | IWI | Initial inlet filter weight -- grams |
| 7. | FWI | Final inlet filter weight -- grams |
| 8. | IWO | Initial outlet filter weight -- grams |
| 9. | FWO | Final outlet filter weight -- grams |
| 10. | H1 | Manometer reading on inlet sampling system -- in tenths of an inch |
| 11. | H2 | Manometer reading on outlet sampling system -- in hundredths of an inch |
| 12. | P3 | Inlet pressure to the fluidized bed -- in PSIG |
| 13. | T3 | Inlet sampling system temperature -- in $^{o}F$ |
| 14. | T4 | Outlet sampling system temperature -- in $^{o}F$ |
| 15. | Time | Duration of the test -- in minutes |
| 16. | P1 | Inlet pressure to the entire system -- PSIG |
| 17. | P2 | Pressure at the pressure control valve -- PSIG |
| 18. | P4 | Pressure within the inlet sampling flow measurement system -- PSIG |
| 19. | P5 | Pressure within the outlet sampling flow measurement system -- PSIG |
| 20. | P6 | Input pressure to the aerosol generator -- PSIG |
| 21. | T1 | Temperature of the air entering the general system -- $^{o}F$ |
| 22. | T2 | Temperature of the air entering the rotating fluidized bed -- $^{o}F$ |

| TEST DATE | RUN NO. | SHAPE NO. | RPM | BED MASS | BLK | H1 | H2 | P3 | T3 | T4 | TIME | IWI | FWI | IWO | FWO | P1 | P2 | P4 | P5 | P6 | T1 | T2 |
|---|---|---|---|---|---|---|---|---|---|---|---|---|---|---|---|---|---|---|---|---|---|---|
| 122970 | 0 | 0 | 0 | 0 | 1 | 0 | 0 | 0 | 0 | 0 | 0 | 8.4073 | 8.4040 | 13.1797 | 13.1797 | 0 | 0 | 0 | 0 | 0 | 0 | 0 |
| 0 | 0 | 0 | 0 | 0 | 1 | 0 | 0 | 0 | 0 | 0 | 0 | 8.5160 | 8.5140 | 13.0654 | 13.0656 | 0 | 0 | 0 | 0 | 0 | 0 | 0 |
| 0 | 0 | 0 | 0 | 0 | 1 | 0 | 0 | 0 | 0 | 0 | 0 | 8.6427 | 8.6399 | 13.2728 | 13.2724 | 0 | 0 | 0 | 0 | 0 | 0 | 0 |
| 0 | 0 | 0 | 0 | 0 | 1 | 0 | 0 | 0 | 0 | 0 | 0 | 8.3706 | 8.3677 | 13.0093 | 13.0086 | 0 | 0 | 0 | 0 | 0 | 0 | 0 |
| 0 | 0 | 0 | 0 | 0 | 1 | 0 | 0 | 0 | 0 | 0 | 0 | 8.5316 | 8.5300 | 13.1796 | 13.1790 | 0 | 0 | 0 | 0 | 0 | 0 | 0 |
| 0 | 0 | 0 | 0 | 0 | 1 | 0 | 0 | 0 | 0 | 0 | 0 | 8.4554 | 8.4550 | 13.0294 | 13.0283 | 0 | 0 | 0 | 0 | 0 | 0 | 0 |
| 122970 | 1 | 2 | 629 | 100 | 0 | 29 | 305 | 49.8 | 73 | 77 | 30 | 8.4893 | 8.5488 | 13.1011 | 13.1245 | 100 | 72 | 5 | 30 | 90 | 83 | 76 |
| 0 | 2 | 2 | 629 | 100 | 0 | 29 | 310 | 48.8 | 75 | 80 | 30 | 8.4721 | 8.5383 | 13.0843 | 13.1045 | 100 | 72 | 5 | 30 | 90 | 88 | 80 |
| 0 | 3 | 2 | 629 | 100 | 0 | 29 | 315 | 43.5 | 75 | 80 | 30 | 8.3200 | 8.4023 | 13.4946 | 13.5020 | 100 | 72 | 5 | 30 | 90 | 90 | 81 |
| 0 | 4 | 2 | 291 | 100 | 0 | 31 | 55 | 34.5 | 73 | 76 | 30 | 8.4491 | 8.5431 | 13.1609 | 13.1712 | 100 | 72 | 5 | 30 | 70 | 82 | 75 |
| 0 | 5 | 2 | 291 | 100 | 0 | 29 | 55 | 34.1 | 75 | 77 | 30 | 8.7545 | 8.8581 | 13.5450 | 13.5512 | 100 | 72 | 5 | 30 | 70 | 86 | 77 |
| 0 | 6 | 2 | 291 | 100 | 0 | 30 | 50 | 34.0 | 75 | 78 | 30 | 8.5300 | 8.6400 | 13.0187 | 13.0228 | 100 | 72 | 5 | 30 | 70 | 88 | 78 |
| 0 | 7 | 2 | 291 | 0 | 0 | 31 | 55 | 31.2 | 75 | 77 | 10 | 8.3650 | 8.4275 | 13.8182 | 13.8521 | 100 | 72 | 5 | 30 | 70 | 84 | 76 |
| 0 | 8 | 2 | 291 | 0 | 0 | 30 | 55 | 31.2 | 74 | 77 | 10 | 8.5320 | 8.5933 | 13.2702 | 13.3004 | 100 | 72 | 5 | 30 | 70 | 86 | 76 |
| 0 | 9 | 2 | 291 | 0 | 0 | 29 | 50 | 31.2 | 75 | 78 | 10 | 8.4239 | 8.4827 | 13.4728 | 13.5008 | 100 | 72 | 5 | 30 | 70 | 87 | 77 |

| TEST DATE | RUN NO. | SHAPE NO. | RPM | BED MASS | BLK | H1 | H2 | P3 | T3 | T4 | TIME | IWI | FWI | IWO | FWO | P1 | P2 | P4 | P5 | P6 | T1 | T2 |
|---|---|---|---|---|---|---|---|---|---|---|---|---|---|---|---|---|---|---|---|---|---|---|
| 10171 | 0 | 0 | 0 | 0 | 1 | 0 | 0 | 0 | 0 | 0 | 0 | 8.3498 | 8.3349 | 13.6409 | 13.6255 | 0 | 0 | 0 | 0 | 0 | 0 | 0 |
| 0 | 0 | 0 | 0 | 0 | 1 | 0 | 0 | 0 | 0 | 0 | 0 | 8.3155 | 8.3013 | 13.1291 | 13.1160 | 0 | 0 | 0 | 0 | 0 | 0 | 0 |
| 0 | 0 | 0 | 0 | 0 | 1 | 0 | 0 | 0 | 0 | 0 | 0 | 8.9541 | 8.9414 | 12.8997 | 12.8874 | 0 | 0 | 0 | 0 | 0 | 0 | 0 |
| 0 | 0 | 0 | 0 | 0 | 1 | 0 | 0 | 0 | 0 | 0 | 0 | 8.8811 | 8.8675 | 13.4846 | 13.4710 | 0 | 0 | 0 | 0 | 0 | 0 | 0 |
| 0 | 0 | 0 | 0 | 0 | 1 | 0 | 0 | 0 | 0 | 0 | 0 | 9.1645 | 9.1504 | 12.9515 | 12.9379 | 0 | 0 | 0 | 0 | 0 | 0 | 0 |
| 10171 | 1 | 3 | 291 | 100 | 0 | 29 | 50 | 35.0 | 73 | 76 | 30 | 8.3165 | 8.5931 | 13.0870 | 13.0873 | 100 | 72 | 5 | 30 | 71 | 80 | 73 |
| 0 | 2 | 3 | 291 | 100 | 0 | 15 | 55 | 35.0 | 74 | 77 | 30 | 8.4523 | 8.6701 | 13.0680 | 13.0648 | 100 | 72 | 5 | 30 | 71 | 83 | 74 |
| 0 | 3 | 3 | 291 | 100 | 0 | 14 | 50 | 35.0 | 75 | 78 | 30 | 8.4113 | 8.7133 | 13.4638 | 13.4685 | 100 | 72 | 5 | 30 | 71 | 84 | 75 |
| 0 | 4 | 3 | 291 | 0 | 0 | 15 | 50 | 31.0 | 74 | 77 | 10 | 8.3943 | 8.5322 | 13.1341 | 13.2198 | 100 | 72 | 5 | 30 | 70 | 80 | 74 |
| 0 | 5 | 3 | 291 | 0 | 0 | 14 | 50 | 31.0 | 74 | 77 | 10 | 8.5974 | 8.6295 | 13.5127 | 13.5308 | 100 | 72 | 5 | 30 | 70 | 83 | 74 |
| 0 | 7 | 3 | 629 | 0 | 0 | 15 | 50 | 31.0 | 74 | 76 | 10 | 8.3083 | 8.3333 | 13.8132 | 13.8237 | 100 | 72 | 5 | 30 | 70 | 79 | 73 |
| 0 | 8 | 3 | 629 | 0 | 0 | 15 | 50 | 31.0 | 74 | 77 | 10 | 8.5013 | 8.5300 | 13.2619 | 13.2733 | 100 | 72 | 5 | 30 | 70 | 82 | 73 |
| 0 | 9 | 3 | 629 | 0 | 0 | 15 | 50 | 31.0 | 74 | 78 | 10 | 8.2705 | 8.2953 | 13.4615 | 13.4688 | 100 | 72 | 5 | 30 | 70 | 83 | 74 |
| 0 | 10 | 3 | 629 | 0 | 0 | 15 | 300 | 32.5 | 74 | 79 | 10 | 8.3830 | 8.3930 | 13.1424 | 13.1520 | 100 | 72 | 5 | 30 | 70 | 85 | 75 |
| 0 | 11 | 3 | 629 | 0 | 0 | 15 | 305 | 32.5 | 74 | 80 | 9 | 8.4932 | 8.4961 | 13.0294 | 13.0330 | 100 | 72 | 5 | 30 | 70 | 87 | 76 |
| 0 | 12 | 3 | 629 | 0 | 0 | 15 | 305 | 32.5 | 74 | 80 | 10 | 8.6206 | 8.6263 | 13.2360 | 13.2396 | 100 | 72 | 5 | 30 | 70 | 87 | 77 |
| 0 | 14 | 3 | 629 | 100 | 0 | 15 | 50 | 52.0 | 71 | 76 | 30 | 8.5105 | 8.6029 | 13.1432 | 13.1500 | 100 | 72 | 5 | 30 | 91 | 79 | 72 |
| 0 | 15 | 3 | 629 | 100 | 0 | 15 | 50 | 52.0 | 72 | 77 | 30 | 8.4338 | 8.5375 | 12.9938 | 12.9933 | 100 | 72 | 5 | 30 | 91 | 80 | 73 |
| 0 | 16 | 3 | 629 | 100 | 0 | 15 | 300 | 52.0 | 72 | 78 | 30 | 8.5307 | 8.5524 | 13.2845 | 13.2962 | 100 | 72 | 5 | 30 | 91 | 83 | 74 |
| 0 | 17 | 3 | 629 | 100 | 0 | 27 | 300 | 52.0 | 73 | 79 | 30 | 8.5872 | 8.6197 | 13.3963 | 13.3960 | 100 | 72 | 5 | 30 | 91 | 87 | 78 |

| TEST DATE | RUN NO. | SHAPE NO. | RPM | BED MASS | BLK | H1 | H2 | P3 | T3 | T4 | TIME | IWI | FWI | IWO | FWO | P1 | P2 | P4 | P5 | P6 | T1 | T2 |
|---|---|---|---|---|---|---|---|---|---|---|---|---|---|---|---|---|---|---|---|---|---|---|
| 10771 | 0 | 0 | 0 | 0 | 1 | 0 | 0 | 0 | 0 | 0 | 0 | 8.5719 | 8.5682 | 12.9984 | 12.9865 | 0 | 0 | 0 | 0 | 0 | 0 | 0 |
| 0 | 0 | 0 | 0 | 0 | 1 | 0 | 0 | 0 | 0 | 0 | 0 | 8.9823 | 8.9800 | 12.7733 | 12.7574 | 0 | 0 | 0 | 0 | 0 | 0 | 0 |
| 0 | 0 | 0 | 0 | 0 | 1 | 0 | 0 | 0 | 0 | 0 | 0 | 8.9500 | 8.9510 | 13.5711 | 13.5516 | 0 | 0 | 0 | 0 | 0 | 0 | 0 |
| 0 | 0 | 0 | 0 | 0 | 1 | 0 | 0 | 0 | 0 | 0 | 0 | 8.9318 | 8.9306 | 12.8767 | 12.8635 | 0 | 0 | 0 | 0 | 0 | 0 | 0 |
| 0 | 0 | 0 | 0 | 0 | 1 | 0 | 0 | 0 | 0 | 0 | 0 | 8.8575 | 8.8563 | 13.4587 | 13.4463 | 0 | 0 | 0 | 0 | 0 | 0 | 0 |
| 0 | 0 | 0 | 0 | 0 | 1 | 0 | 0 | 0 | 0 | 0 | 0 | 9.1404 | 9.1380 | 12.9237 | 12.9135 | 0 | 0 | 0 | 0 | 0 | 0 | 0 |
| 10371 | 1 | 3 | 629 | 100 | 0 | 16 | 305 | 52.0 | 71 | 74 | 20 | 8.4193 | 8.4692 | 13.0269 | 13.0311 | 100 | 71 | 5 | 30 | 90 | 77 | 70 |
| 0 | 2 | 3 | 629 | 100 | 0 | 28 | 295 | 52.0 | 71 | 76 | 20 | 8.5624 | 8.6373 | 13.1830 | 13.1801 | 100 | 71 | 5 | 30 | 90 | 82 | 74 |
| 0 | 3 | 3 | 629 | 100 | 0 | 28 | 305 | 52.4 | 71 | 76 | 20 | 8.3500 | 8.4218 | 12.9382 | 12.9345 | 100 | 71 | 5 | 30 | 90 | 82 | 73 |
| 0 | 7 | 3 | 629 | 100 | 0 | 28 | 50 | 51.5 | 70 | 74 | 30 | 8.3803 | 8.5865 | 13.1097 | 13.1118 | 100 | 72 | 5 | 30 | 88 | 80 | 72 |
| 0 | 9 | 3 | 0 | 0 | 0 | 27 | 55 | 31.0 | 70 | 75 | 10 | 8.3861 | 8.5310 | 13.0460 | 13.1068 | 100 | 72 | 5 | 30 | 70 | 81 | 71 |
| 0 | 11 | 3 | 0 | 0 | 0 | 27 | 305 | 32.0 | 71 | 74 | 10 | 8.5493 | 8.6213 | 12.6087 | 12.6467 | 100 | 72 | 5 | 30 | 70 | 86 | 74 |
| 0 | 12 | 3 | 0 | 0 | 0 | 27 | 305 | 32.0 | 71 | 74 | 10 | 8.5475 | 8.6204 | 13.2296 | 13.2670 | 100 | 72 | 5 | 30 | 71 | 86 | 76 |
| 0 | 13 | 3 | 0 | 0 | 0 | 27 | 300 | 32.0 | 72 | 74 | 10 | 8.3083 | 8.3785 | 13.4602 | 13.4970 | 100 | 72 | 5 | 30 | 71 | 87 | 76 |

| TEST DATE | RUN NO. | SHAPE NO. | RPM | BED MASS | BLK | H1 | H2 | P3 | T3 | T4 | TIME | IWI | FWI | IWO | FWO | P1 | P2 | P4 | P5 | P6 | T1 | T2 |
|---|---|---|---|---|---|---|---|---|---|---|---|---|---|---|---|---|---|---|---|---|---|---|
| 10571 | 0 | 0 | 0 | 0 | 1 | 0 | 0 | 0 | 0 | 0 | 0 | 8.4527 | 8.4537 | 13.8288 | 13.8320 | 0 | 0 | 0 | 0 | 0 | 0 | 0 |
| 0 | 0 | 0 | 0 | 0 | 1 | 0 | 0 | 0 | 0 | 0 | 0 | 8.4489 | 8.4490 | 14.0314 | 14.0341 | 0 | 0 | 0 | 0 | 0 | 0 | 0 |
| 0 | 0 | 0 | 0 | 0 | 1 | 0 | 0 | 0 | 0 | 0 | 0 | 8.9663 | 8.9686 | 13.8806 | 13.8872 | 0 | 0 | 0 | 0 | 0 | 0 | 0 |
| 0 | 0 | 0 | 0 | 0 | 1 | 0 | 0 | 0 | 0 | 0 | 0 | 8.2319 | 8.2334 | 13.8030 | 13.8076 | 0 | 0 | 0 | 0 | 0 | 0 | 0 |
| 0 | 0 | 0 | 0 | 0 | 1 | 0 | 0 | 0 | 0 | 0 | 0 | 8.4757 | 8.4773 | 13.3937 | 13.3980 | 0 | 0 | 0 | 0 | 0 | 0 | 0 |
| 10571 | 1 | 1 | 290 | 100 | 0 | 25 | 50 | 36.0 | 69 | 73 | 30 | 8.7796 | 9.0685 | 13.8509 | 13.8785 | 100 | 72 | 5 | 30 | 72 | 75 | 70 |
| 0 | 2 | 1 | 290 | 100 | 0 | 25 | 50 | 35.8 | 69 | 74 | 20 | 8.9570 | 9.2301 | 13.9838 | 14.0060 | 100 | 72 | 5 | 30 | 72 | 78 | 71 |
| 0 | 3 | 1 | 290 | 100 | 0 | 25 | 50 | 35.5 | 70 | 74 | 20 | 8.7520 | 9.0171 | 13.7337 | 13.7537 | 100 | 72 | 5 | 30 | 72 | 80 | 72 |
| 0 | 4 | 1 | 290 | 100 | 0 | 25 | 50 | 35.5 | 70 | 74 | 20 | 8.8646 | 9.1776 | 13.7346 | 13.7580 | 100 | 72 | 5 | 30 | 72 | 80 | 72 |
| 0 | 5 | 1 | 0 | 0 | 0 | 26 | 50 | 31.0 | 70 | 74 | 10 | 9.0501 | 9.1772 | 13.7483 | 13.8335 | 100 | 72 | 5 | 30 | 72 | 82 | 72 |
| 0 | 6 | 1 | 0 | 0 | 0 | 27 | 50 | 31.0 | 70 | 74 | 10 | 9.0231 | 9.1778 | 13.7440 | 13.8357 | 100 | 72 | 5 | 30 | 72 | 81 | 72 |
| 0 | 7 | 1 | 0 | 0 | 0 | 26 | 50 | 31.0 | 70 | 74 | 10 | 8.8120 | 8.9752 | 13.8845 | 13.9816 | 100 | 72 | 5 | 30 | 72 | 81 | 72 |

| TEST DATE | RUN NO. | SHAPE NO. | RPM | BED MASS | BLK | H1 | H2 | P3 | T3 | T4 | TIME | IWI | FWI | IWO | FWO | P1 | P2 | P4 | P5 | P6 | T1 | T2 |
|---|---|---|---|---|---|---|---|---|---|---|---|---|---|---|---|---|---|---|---|---|---|---|
| 10671 | 0 | 0 | 0 | 0 | 1 | 0 | 0 | 0 | 0 | 0 | 0 | 8.8875 | 8.9093 | 13.9312 | 13.9666 | 0 | 0 | 0 | 0 | 0 | 0 | 0 |
| 0 | 0 | 0 | 0 | 0 | 1 | 0 | 0 | 0 | 0 | 0 | 0 | 8.5663 | 8.5884 | 13.7717 | 13.8059 | 0 | 0 | 0 | 0 | 0 | 0 | 0 |
| 0 | 0 | 0 | 0 | 0 | 1 | 0 | 0 | 0 | 0 | 0 | 0 | 8.9783 | 8.9971 | 13.8543 | 13.8900 | 0 | 0 | 0 | 0 | 0 | 0 | 0 |
| 0 | 0 | 0 | 0 | 0 | 1 | 0 | 0 | 0 | 0 | 0 | 0 | 8.9492 | 8.9692 | 14.1705 | 14.2077 | 0 | 0 | 0 | 0 | 0 | 0 | 0 |
| 0 | 0 | 0 | 0 | 0 | 1 | 0 | 0 | 0 | 0 | 0 | 0 | 8.9291 | 8.9478 | 13.7977 | 13.8327 | 0 | 0 | 0 | 0 | 0 | 0 | 0 |
| 10671 | 1 | 1 | 629 | 100 | 0 | 28 | 50 | 54.0 | 69 | 73 | 30 | 8.9278 | 9.1917 | 13.8812 | 13.9316 | 100 | 72 | 5 | 30 | 92 | 76 | 70 |
| 0 | 2 | 1 | 629 | 100 | 0 | 30 | 50 | 54.0 | 70 | 75 | 20 | 8.6365 | 8.8395 | 13.7340 | 13.7744 | 100 | 72 | 5 | 30 | 92 | 79 | 72 |
| 0 | 3 | 1 | 629 | 100 | 0 | 29 | 50 | 54.0 | 70 | 75 | 30 | 8.4022 | 8.6957 | 14.3283 | 14.3890 | 100 | 72 | 5 | 30 | 92 | 80 | 72 |
| 0 | 4 | 1 | 629 | 100 | 0 | 28 | 300 | 54.8 | 71 | 77 | 30 | 8.4212 | 8.5670 | 13.8670 | 13.9270 | 100 | 72 | 5 | 30 | 92 | 84 | 75 |
| 0 | 5 | 1 | 629 | 100 | 0 | 28 | 300 | 54.0 | 72 | 79 | 30 | 8.6448 | 8.7998 | 14.3041 | 14.3545 | 100 | 72 | 5 | 30 | 92 | 86 | 77 |
| 0 | 6 | 1 | 629 | 100 | 0 | 27 | 305 | 54.0 | 72 | 80 | 30 | 8.5307 | 8.6828 | 14.3620 | 14.4105 | 100 | 72 | 5 | 30 | 91 | 87 | 78 |
| 0 | 7 | 1 | 0 | 0 | 0 | 28 | 50 | 31.0 | 72 | 77 | 10 | 8.8252 | 9.0130 | 13.7895 | 13.9211 | 100 | 72 | 5 | 30 | 72 | 84 | 72 |
| 0 | 8 | 1 | 0 | 0 | 0 | 27 | 50 | 31.0 | 71 | 76 | 10 | 8.8664 | 9.0776 | 14.3167 | 14.4484 | 100 | 72 | 5 | 30 | 72 | 83 | 72 |
| 0 | 9 | 1 | 0 | 0 | 0 | 28 | 50 | 31.0 | 71 | 75 | 10 | 8.8860 | 9.1101 | 14.0121 | 14.1389 | 100 | 72 | 5 | 30 | 72 | 83 | 72 |
| 0 | 10 | 1 | 0 | 0 | 0 | 28 | 305 | 32.0 | 71 | 75 | 10 | 8.8707 | 8.9788 | 13.8597 | 13.9569 | 100 | 72 | 5 | 30 | 71 | 87 | 74 |
| 0 | 11 | 1 | 0 | 0 | 0 | 26 | 300 | 32.0 | 72 | 75 | 10 | 8.7873 | 8.9065 | 13.8243 | 13.9269 | 100 | 72 | 5 | 30 | 71 | 90 | 77 |
| 0 | 12 | 1 | 0 | 0 | 0 | 27 | 300 | 32.0 | 73 | 75 | 10 | 8.9688 | 9.0752 | 13.8268 | 13.9232 | 100 | 72 | 5 | 30 | 71 | 90 | 78 |

| TEST DATE | RUN NO. | SHAPE NO. | RPM | BED MASS | BLK | H1 | H2 | P3 | T3 | T4 | TIME | IWI | FWI | IWO | FWO | P1 | P2 | P4 | P5 | P6 | T1 | T2 |
|---|---|---|---|---|---|---|---|---|---|---|---|---|---|---|---|---|---|---|---|---|---|---|
| 10871 | 0 | 0 | 0 | 0 | 1 | 0 | 0 | 0 | 0 | 0 | 0 | 8.3876 | 8.4257 | 13.6754 | 13.7261 | 0 | 0 | 0 | 0 | 0 | 0 | 0 |
| 0 | 0 | 0 | 0 | 0 | 1 | 0 | 0 | 0 | 0 | 0 | 0 | 8.4177 | 8.4570 | 13.7967 | 13.8461 | 0 | 0 | 0 | 0 | 0 | 0 | 0 |
| 0 | 0 | 0 | 0 | 0 | 1 | 0 | 0 | 0 | 0 | 0 | 0 | 8.5686 | 8.6050 | 12.8047 | 12.8514 | 0 | 0 | 0 | 0 | 0 | 0 | 0 |
| 0 | 0 | 0 | 0 | 0 | 1 | 0 | 0 | 0 | 0 | 0 | 0 | 8.6355 | 8.6729 | 13.6040 | 13.6531 | 0 | 0 | 0 | 0 | 0 | 0 | 0 |
| 0 | 0 | 0 | 0 | 0 | 1 | 0 | 0 | 0 | 0 | 0 | 0 | 8.4989 | 8.5350 | 12.9113 | 12.9592 | 0 | 0 | 0 | 0 | 0 | 0 | 0 |
| 10871 | 1 | 1 | 900 | 100 | 0 | 29 | 300 | 78.5 | 72 | 78 | 30 | 8.8874 | 9.1039 | 13.9333 | 14.0090 | 130 | 92 | 5 | 30 | 117 | 84 | 75 |
| 0 | 2 | 1 | 900 | 100 | 0 | 27 | 300 | 78.5 | 73 | 81 | 30 | 8.9632 | 9.0973 | 13.4293 | 13.5012 | 130 | 92 | 5 | 30 | 117 | 90 | 79 |
| 0 | 3 | 1 | 900 | 100 | 0 | 26 | 300 | 78.5 | 75 | 83 | 30 | 8.9717 | 9.1118 | 13.8093 | 13.8807 | 130 | 92 | 5 | 30 | 117 | 93 | 81 |
| 0 | 8 | 1 | 0 | 0 | 0 | 27 | 605 | 33.9 | 73 | 80 | 10 | 8.4859 | 8.6078 | 13.8858 | 14.0196 | 135 | 78 | 5 | 30 | 72 | 97 | 80 |
| 0 | 9 | 1 | 0 | 0 | 0 | 26 | 605 | 34.0 | 76 | 80 | 10 | 8.4823 | 8.5970 | 14.0898 | 14.2214 | 135 | 78 | 5 | 30 | 72 | 99 | 85 |
| 0 | 10 | 1 | 0 | 0 | 0 | 29 | 600 | 33.9 | 78 | 82 | 10 | 8.4739 | 8.5863 | 14.1121 | 14.2430 | 135 | 78 | 5 | 30 | 72 | 101 | 86 |

| TEST DATE | RUN NO. | SHAPE NO. | RPM | BED MASS | BLK | H1 | H2 | P3 | T3 | T4 | TIME | IWI | FWI | IWO | FWO | P1 | P2 | P4 | P5 | P6 | T1 | T2 |
|---|---|---|---|---|---|---|---|---|---|---|---|---|---|---|---|---|---|---|---|---|---|---|
| 10971 | 0 | 0 | 0 | 0 | 1 | 0 | 0 | 0 | 0 | 0 | 0 | 8.8162 | 8.8356 | 13.0708 | 13.0958 | 0 | 0 | 0 | 0 | 0 | 0 | 0 |
| 0 | 0 | 0 | 0 | 0 | 1 | 0 | 0 | 0 | 0 | 0 | 0 | 9.0045 | 9.0224 | 13.0532 | 13.0802 | 0 | 0 | 0 | 0 | 0 | 0 | 0 |
| 0 | 0 | 0 | 0 | 0 | 1 | 0 | 0 | 0 | 0 | 0 | 0 | 8.9452 | 8.9643 | 14.0180 | 14.0454 | 0 | 0 | 0 | 0 | 0 | 0 | 0 |
| 0 | 0 | 0 | 0 | 0 | 1 | 0 | 0 | 0 | 0 | 0 | 0 | 8.6237 | 8.6428 | 13.8566 | 13.8856 | 0 | 0 | 0 | 0 | 0 | 0 | 0 |
| 0 | 0 | 0 | 0 | 0 | 1 | 0 | 0 | 0 | 0 | 0 | 0 | 9.0284 | 9.0477 | 13.9423 | 13.9645 | 0 | 0 | 0 | 0 | 0 | 0 | 0 |
| 10971 | 1 | 2 | 629 | 100 | 0 | 29 | 300 | 52.5 | 76 | 80 | 30 | 9.0113 | 9.1905 | 13.2528 | 13.3110 | 115 | 72 | 5 | 30 | 92 | 86 | 77 |
| 0 | 2 | 2 | 629 | 100 | 0 | 28 | 300 | 52.0 | 78 | 83 | 30 | 8.9835 | 9.1915 | 13.0012 | 13.0551 | 115 | 72 | 5 | 30 | 92 | 92 | 80 |
| 0 | 3 | 2 | 629 | 100 | 0 | 27 | 300 | 52.5 | 78 | 84 | 30 | 9.0066 | 9.2051 | 13.4969 | 13.5448 | 115 | 72 | 5 | 30 | 92 | 95 | 83 |
| 0 | 6 | 2 | 629 | 100 | 0 | 27 | 50 | 51.2 | 77 | 81 | 20 | 8.9299 | 9.1807 | 13.2554 | 13.3126 | 115 | 76 | 5 | 30 | 92 | 88 | 78 |
| 0 | 7 | 2 | 629 | 100 | 0 | 27 | 50 | 52.0 | 77 | 82 | 20 | 9.0933 | 9.3664 | 13.6110 | 13.6592 | 115 | 76 | 5 | 30 | 92 | 90 | 78 |
| 0 | 8 | 2 | 629 | 100 | 0 | 29 | 50 | 52.0 | 77 | 82 | 20 | 8.9606 | 9.2484 | 13.0763 | 13.1216 | 115 | 76 | 5 | 30 | 92 | 90 | 79 |
| 0 | 9 | 2 | 0 | 0 | 0 | 30 | 305 | 32.0 | 77 | 82 | 10 | 8.9325 | 9.0235 | 13.7381 | 13.8257 | 115 | 72 | 5 | 30 | 72 | 92 | 79 |
| 0 | 10 | 2 | 0 | 0 | 0 | 29 | 300 | 32.0 | 77 | 82 | 10 | 8.9232 | 9.0284 | 13.1845 | 13.2755 | 115 | 72 | 5 | 30 | 72 | 94 | 81 |
| 0 | 11 | 2 | 0 | 0 | 0 | 28 | 300 | 32.0 | 78 | 81 | 10 | 8.9818 | 9.0887 | 13.3100 | 13.3965 | 115 | 72 | 5 | 30 | 72 | 94 | 82 |

| TEST DATE | RUN NO. | SHAPE NO. | RPM | BED MASS | BLK | H1 | H2 | P3 | T3 | T4 | TIME | IWI | FWI | IWO | FWO | P1 | P2 | P4 | P5 | P6 | T1 | T2 |
|---|---|---|---|---|---|---|---|---|---|---|---|---|---|---|---|---|---|---|---|---|---|---|
| 11071 | 0 | 0 | 0 | 0 | 1 | 0 | 0 | 0 | 0 | 0 | 0 | 8.9359 | 8.8971 | 13.5143 | 13.4674 | 0 | 0 | 0 | 0 | 0 | 0 | 0 |
| 0 | 0 | 0 | 0 | 0 | 1 | 0 | 0 | 0 | 0 | 0 | 0 | 9.0326 | 8.9962 | 13.8630 | 13.8142 | 0 | 0 | 0 | 0 | 0 | 0 | 0 |
| 0 | 0 | 0 | 0 | 0 | 1 | 0 | 0 | 0 | 0 | 0 | 0 | 9.0764 | 9.0401 | 14.1513 | 14.1016 | 0 | 0 | 0 | 0 | 0 | 0 | 0 |
| 0 | 0 | 0 | 0 | 0 | 1 | 0 | 0 | 0 | 0 | 0 | 0 | 8.9248 | 8.8891 | 13.5650 | 13.5149 | 0 | 0 | 0 | 0 | 0 | 0 | 0 |
| 0 | 0 | 0 | 0 | 0 | 1 | 0 | 0 | 0 | 0 | 0 | 0 | 8.4403 | 8.4034 | 13.7444 | 13.6952 | 0 | 0 | 0 | 0 | 0 | 0 | 0 |
| 11071 | 1 | 2 | 900 | 100 | 0 | 30 | 295 | 74.5 | 75 | 80 | 30 | 8.9197 | 9.0148 | 14.0812 | 14.0642 | 115 | 87 | 5 | 30 | 111 | 87 | 78 |
| 0 | 2 | 2 | 900 | 100 | 0 | 29 | 300 | 74.5 | 77 | 83 | 30 | 9.0261 | 9.1371 | 14.2071 | 14.1719 | 115 | 87 | 5 | 30 | 111 | 92 | 81 |
| 0 | 3 | 2 | 900 | 100 | 0 | 29 | 300 | 74.5 | 78 | 84 | 30 | 8.8905 | 8.9942 | 13.9540 | 13.9252 | 115 | 87 | 5 | 30 | 111 | 94 | 82 |
| 0 | 4 | 2 | 900 | 100 | 0 | 30 | 505 | 76.5 | 77 | 83 | 30 | 9.0105 | 9.0570 | 13.9449 | 13.9320 | 115 | 83 | 5 | 30 | 111 | 94 | 83 |
| 0 | 5 | 2 | 900 | 100 | 0 | 30 | 505 | 74.5 | 78 | 85 | 30 | 9.1604 | 9.2093 | 13.9664 | 13.9412 | 115 | 83 | 5 | 30 | 111 | 97 | 85 |
| 0 | 6 | 2 | 900 | 100 | 0 | 29 | 505 | 74.0 | 79 | 86 | 30 | 9.1232 | 9.1739 | 13.8774 | 13.8599 | 115 | 83 | 5 | 30 | 111 | 98 | 86 |
| 0 | 7 | 2 | 0 | 0 | 0 | 29 | 490 | 32.5 | 76 | 82 | 10 | 8.9279 | 8.9493 | 14.0449 | 14.0375 | 115 | 83 | 5 | 30 | 72 | 94 | 78 |
| 0 | 8 | 2 | 0 | 0 | 0 | 29 | 500 | 32.5 | 76 | 80 | 10 | 9.0778 | 9.1055 | 14.0079 | 14.0025 | 115 | 83 | 5 | 30 | 72 | 96 | 82 |
| 0 | 9 | 2 | 0 | 0 | 0 | 29 | 495 | 32.5 | 78 | 80 | 10 | 8.8731 | 8.8972 | 13.9100 | 13.9047 | 115 | 83 | 5 | 30 | 72 | 96 | 84 |

| TEST DATE | RUN NO. | SHAPE NO. | RPM | BED MASS | BLK | H1 | H2 | P3 | T3 | T4 | TIME | IWI | FWI | IWO | FWO | P1 | P2 | P4 | P5 | P6 | T1 | T2 |
|---|---|---|---|---|---|---|---|---|---|---|---|---|---|---|---|---|---|---|---|---|---|---|
| 11271 | 0 | 0 | 0 | 0 | 1 | 0 | 0 | 0 | 0 | 0 | 0 | 8.6330 | 8.6425 | 13.6064 | 13.6137 | 0 | 0 | 0 | 0 | 0 | 0 | 0 |
| 0 | 0 | 0 | 0 | 0 | 1 | 0 | 0 | 0 | 0 | 0 | 0 | 8.5023 | 8.5059 | 12.9139 | 12.9210 | 0 | 0 | 0 | 0 | 0 | 0 | 0 |
| 0 | 0 | 0 | 0 | 0 | 1 | 0 | 0 | 0 | 0 | 0 | 0 | 8.3546 | 8.3576 | 13.4961 | 13.5045 | 0 | 0 | 0 | 0 | 0 | 0 | 0 |
| 0 | 0 | 0 | 0 | 0 | 1 | 0 | 0 | 0 | 0 | 0 | 0 | 8.3210 | 8.3240 | 12.9612 | 12.9708 | 0 | 0 | 0 | 0 | 0 | 0 | 0 |
| 11271 | 1 | 2 | 787 | 100 | 0 | 27 | 300 | 65.0 | 72 | 77 | 30 | 8.8546 | 8.9876 | 13.8273 | 13.8740 | 110 | 92 | 5 | 30 | 100 | 82 | 74 |
| 0 | 2 | 2 | 787 | 100 | 0 | 27 | 300 | 64.0 | 73 | 80 | 30 | 8.9261 | 9.0632 | 14.0838 | 14.1125 | 110 | 92 | 5 | 30 | 100 | 86 | 78 |
| 0 | 3 | 2 | 787 | 100 | 0 | 26 | 295 | 64.0 | 74 | 81 | 30 | 8.8225 | 8.9635 | 13.7852 | 13.8101 | 110 | 92 | 5 | 30 | 100 | 88 | 78 |
| 0 | 4 | 2 | 787 | 100 | 0 | 26 | 500 | 64.0 | 70 | 76 | 30 | 8.9339 | 9.0353 | 13.7965 | 13.8335 | 110 | 92 | 5 | 30 | 100 | 82 | 74 |
| 0 | 5 | 2 | 787 | 100 | 0 | 27 | 495 | 64.0 | 72 | 80 | 30 | 9.0835 | 9.1948 | 13.9217 | 13.9497 | 110 | 92 | 5 | 30 | 100 | 87 | 78 |
| 0 | 6 | 2 | 787 | 100 | 0 | 26 | 500 | 64.0 | 73 | 80 | 30 | 8.9932 | 9.0985 | 13.7125 | 13.7351 | 110 | 92 | 5 | 30 | 100 | 90 | 79 |
| 0 | 7 | 2 | 437 | 100 | 0 | 28 | 50 | 40.8 | 72 | 76 | 30 | 8.8613 | 9.2530 | 13.8694 | 13.8940 | 110 | 92 | 5 | 30 | 80 | 82 | 72 |
| 0 | 8 | 2 | 437 | 100 | 0 | 28 | 50 | 41.0 | 73 | 77 | 30 | 9.0003 | 9.4310 | 13.9028 | 13.9283 | 110 | 92 | 5 | 30 | 80 | 84 | 74 |
| 0 | 9 | 2 | 437 | 100 | 0 | 29 | 50 | 41.5 | 73 | 78 | 30 | 8.7584 | 9.1973 | 13.8654 | 13.8950 | 110 | 92 | 5 | 30 | 80 | 85 | 74 |
| 0 | 10 | 2 | 437 | 100 | 0 | 27 | 295 | 41.8 | 71 | 75 | 30 | 8.8856 | 9.0610 | 13.4535 | 13.4820 | 110 | 92 | 5 | 30 | 82 | 81 | 72 |
| 0 | 11 | 2 | 437 | 100 | 0 | 27 | 300 | 41.5 | 73 | 78 | 30 | 8.9856 | 9.1725 | 13.7997 | 13.8210 | 110 | 92 | 5 | 30 | 82 | 87 | 76 |
| 0 | 12 | 2 | 437 | 100 | 0 | 26 | 300 | 41.5 | 74 | 79 | 30 | 9.0298 | 9.2094 | 14.0865 | 14.1082 | 110 | 92 | 5 | 30 | 82 | 90 | 78 |
| 0 | 13 | 3 | 437 | 100 | 0 | 30 | 55 | 41.0 | 71 | 74 | 30 | 8.8789 | 9.2776 | 13.4992 | 13.5265 | 110 | 92 | 5 | 30 | 82 | 78 | 72 |
| 0 | 14 | 3 | 437 | 100 | 0 | 29 | 50 | 41.0 | 72 | 76 | 30 | 8.3932 | 8.7805 | 13.6800 | 13.7115 | 110 | 92 | 5 | 30 | 82 | 82 | 73 |
| 0 | 15 | 3 | 437 | 100 | 0 | 28 | 55 | 42.0 | 72 | 76 | 20 | 8.4241 | 8.7300 | 13.7995 | 13.8255 | 110 | 92 | 5 | 30 | 82 | 84 | 74 |
| 0 | 16 | 3 | 437 | 100 | 0 | 28 | 50 | 41.8 | 73 | 77 | 20 | 8.5719 | 8.8988 | 12.8082 | 12.8362 | 110 | 92 | 5 | 30 | 82 | 85 | 74 |

| TEST DATE | RUN NO. | SHAPE NO. | RPM | BED MASS | BLK | H1 | H2 | P3 | T3 | T4 | TIME | IWI | FWI | IWO | FWO | P1 | P2 | P4 | P5 | P6 | T1 | T2 |
|---|---|---|---|---|---|---|---|---|---|---|---|---|---|---|---|---|---|---|---|---|---|---|
| 11471 | 0 | 0 | 0 | 0 | 1 | 0 | 0 | 0 | 0 | 0 | 0 | 9.0054 | 9.0445 | 13.9000 | 13.9660 | 0 | 0 | 0 | 0 | 0 | 0 | 0 |
| 0 | 0 | 0 | 0 | 0 | 1 | 0 | 0 | 0 | 0 | 0 | 0 | 8.9775 | 9.0214 | 14.2215 | 14.2862 | 0 | 0 | 0 | 0 | 0 | 0 | 0 |
| 0 | 0 | 0 | 0 | 0 | 1 | 0 | 0 | 0 | 0 | 0 | 0 | 8.9554 | 8.9955 | 13.8464 | 13.9105 | 0 | 0 | 0 | 0 | 0 | 0 | 0 |
| 0 | 0 | 0 | 0 | 0 | 1 | 0 | 0 | 0 | 0 | 0 | 0 | 8.8827 | 8.9266 | 13.6525 | 13.7191 | 0 | 0 | 0 | 0 | 0 | 0 | 0 |
| 0 | 0 | 0 | 0 | 0 | 1 | 0 | 0 | 0 | 0 | 0 | 0 | 9.1657 | 9.2124 | 13.1428 | 13.2096 | 0 | 0 | 0 | 0 | 0 | 0 | 0 |
| 11471 | 1 | 3 | 437 | 100 | 0 | 30 | 300 | 41.5 | 72 | 76 | 20 | 8.9382 | 9.0896 | 13.8960 | 13.9832 | 110 | 92 | 5 | 30 | 82 | 82 | 72 |
| 0 | 2 | 3 | 437 | 100 | 0 | 30 | 300 | 41.5 | 73 | 78 | 20 | 8.9181 | 9.0864 | 13.7470 | 13.8263 | 110 | 92 | 5 | 30 | 82 | 86 | 76 |
| 0 | 3 | 3 | 437 | 100 | 0 | 30 | 300 | 41.5 | 74 | 78 | 20 | 8.9550 | 9.1200 | 14.3505 | 14.4314 | 110 | 92 | 5 | 30 | 82 | 89 | 77 |
| 0 | 4 | 3 | 787 | 100 | 0 | 29 | 300 | 64.0 | 75 | 80 | 30 | 8.8852 | 9.0538 | 13.9072 | 14.0257 | 110 | 92 | 5 | 30 | 102 | 89 | 78 |
| 0 | 5 | 3 | 787 | 100 | 0 | 29 | 305 | 64.0 | 75 | 82 | 30 | 8.9993 | 9.1862 | 14.3475 | 14.4460 | 110 | 92 | 5 | 30 | 102 | 90 | 80 |
| 0 | 6 | 3 | 787 | 100 | 0 | 28 | 305 | 64.0 | 75 | 82 | 30 | 8.8701 | 9.0588 | 13.8538 | 13.9452 | 110 | 92 | 5 | 30 | 102 | 92 | 80 |
| 0 | 7 | 3 | 787 | 100 | 0 | 29 | 500 | 64.0 | 72 | 78 | 30 | 9.0538 | 9.2103 | 14.4607 | 14.5651 | 110 | 92 | 5 | 30 | 102 | 85 | 75 |
| 0 | 8 | 3 | 787 | 100 | 0 | 28 | 500 | 64.0 | 74 | 81 | 30 | 8.8344 | 8.9944 | 13.8714 | 13.9670 | 110 | 92 | 5 | 30 | 102 | 90 | 79 |
| 0 | 9 | 3 | 787 | 100 | 0 | 28 | 500 | 64.0 | 76 | 82 | 30 | 8.8997 | 9.0650 | 14.3698 | 14.4630 | 110 | 92 | 5 | 30 | 102 | 94 | 82 |
| 0 | 10 | 3 | 900 | 100 | 0 | 28 | 305 | 74.0 | 76 | 82 | 30 | 8.8922 | 9.1198 | 14.0185 | 14.1357 | 122 | 92 | 5 | 30 | 120 | 93 | 80 |
| 0 | 11 | 3 | 900 | 100 | 0 | 27 | 305 | 74.0 | 76 | 83 | 30 | 8.9445 | 9.1770 | 13.8767 | 13.9885 | 122 | 92 | 5 | 30 | 120 | 94 | 82 |
| 0 | 12 | 3 | 900 | 100 | 0 | 26 | 305 | 74.0 | 76 | 83 | 30 | 8.7900 | 9.0176 | 13.0330 | 13.1227 | 122 | 92 | 5 | 30 | 120 | 95 | 82 |
| 0 | 13 | 3 | 0 | 0 | 0 | 31 | 505 | 33.0 | 75 | 80 | 11 | 8.9742 | 9.0868 | 13.0147 | 13.1110 | 122 | 92 | 5 | 30 | 72 | 92 | 76 |
| 0 | 14 | 3 | 0 | 0 | 0 | 30 | 495 | 33.0 | 75 | 80 | 10 | 8.9182 | 9.0323 | 13.9790 | 14.0809 | 122 | 92 | 5 | 30 | 72 | 95 | 80 |
| 0 | 15 | 3 | 0 | 0 | 0 | 30 | 500 | 33.0 | 76 | 80 | 10 | 8.5967 | 8.7035 | 13.8183 | 13.9176 | 122 | 92 | 5 | 30 | 72 | 97 | 82 |

| TEST DATE | RUN NO. | SHAPE NO. | RPM | BED MASS | BLK | H1 | H2 | P3 | T3 | T4 | TIME | IWI | FWI | IWO | FWO | P1 | P2 | P4 | P5 | P6 | T1 | T2 |
|---|---|---|---|---|---|---|---|---|---|---|---|---|---|---|---|---|---|---|---|---|---|---|
| 11671 | 0 | 0 | 0 | 0 | 1 | 0 | 0 | 0 | 0 | 0 | 0 | 8.6783 | 8.7736 | 13.6709 | 13.7383 | 0 | 0 | 0 | 0 | 0 | 0 | 0 |
| 0 | 0 | 0 | 0 | 0 | 1 | 0 | 0 | 0 | 0 | 0 | 0 | 8.5405 | 8.5948 | 12.9752 | 13.0440 | 0 | 0 | 0 | 0 | 0 | 0 | 0 |
| 0 | 0 | 0 | 0 | 0 | 1 | 0 | 0 | 0 | 0 | 0 | 0 | 8.3919 | 8.4440 | 13.5598 | 13.6302 | 0 | 0 | 0 | 0 | 0 | 0 | 0 |
| 0 | 0 | 0 | 0 | 0 | 1 | 0 | 0 | 0 | 0 | 0 | 0 | 8.3612 | 8.4123 | 13.0270 | 13.0943 | 0 | 0 | 0 | 0 | 0 | 0 | 0 |
| 11671 | 1 | 3 | 900 | 100 | 0 | 30 | 505 | 74.0 | 74 | 80 | 30 | 8.8984 | 9.0692 | 13.0923 | 13.2440 | 122 | 92 | 5 | 30 | 120 | 88 | 77 |
| 0 | 2 | 3 | 900 | 100 | 0 | 30 | 505 | 74.0 | 76 | 83 | 30 | 8.9789 | 9.1652 | 13.2214 | 13.3535 | 122 | 92 | 5 | 30 | 120 | 95 | 83 |
| 0 | 3 | 3 | 900 | 100 | 0 | 30 | 505 | 74.0 | 78 | 84 | 30 | 8.8274 | 9.0138 | 13.2964 | 13.4010 | 122 | 92 | 5 | 30 | 120 | 98 | 85 |
| 0 | 4 | 1 | 437 | 100 | 0 | 33 | 50 | 42.0 | 73 | 78 | 30 | 8.9933 | 9.4547 | 13.0595 | 13.1505 | 122 | 65 | 5 | 30 | 82 | 82 | 74 |
| 0 | 5 | 1 | 437 | 100 | 0 | 32 | 50 | 42.0 | 74 | 79 | 30 | 8.6221 | 9.0856 | 13.0669 | 13.1580 | 122 | 65 | 5 | 30 | 82 | 86 | 76 |
| 0 | 6 | 1 | 437 | 100 | 0 | 33 | 50 | 42.0 | 75 | 80 | 20 | 8.5473 | 8.9300 | 12.9812 | 13.0655 | 122 | 65 | 5 | 30 | 82 | 87 | 77 |
| 0 | 7 | 1 | 437 | 100 | 0 | 32 | 50 | 42.0 | 75 | 80 | 20 | 8.5329 | 8.8945 | 13.1359 | 13.2220 | 122 | 65 | 5 | 30 | 82 | 88 | 77 |
| 0 | 8 | 1 | 437 | 100 | 0 | 32 | 300 | 42.0 | 75 | 80 | 20 | 8.5406 | 8.7250 | 13.3485 | 13.4510 | 122 | 65 | 5 | 30 | 82 | 90 | 77 |
| 0 | 9 | 1 | 437 | 100 | 0 | 32 | 300 | 41.5 | 76 | 82 | 20 | 8.3034 | 8.4943 | 13.0525 | 13.1422 | 122 | 65 | 5 | 30 | 82 | 94 | 80 |
| 0 | 10 | 1 | 437 | 100 | 0 | 32 | 295 | 41.0 | 77 | 82 | 20 | 8.5719 | 8.7690 | 12.6605 | 12.7446 | 122 | 65 | 5 | 30 | 82 | 96 | 82 |
| 0 | 11 | 1 | 787 | 100 | 0 | 30 | 305 | 67.0 | 76 | 81 | 30 | 8.5209 | 8.7300 | 13.3006 | 13.3992 | 122 | 82 | 5 | 30 | 105 | 93 | 80 |
| 0 | 12 | 1 | 787 | 100 | 0 | 30 | 305 | 67.0 | 78 | 84 | 30 | 8.5270 | 8.7388 | 13.2865 | 13.3709 | 122 | 82 | 5 | 30 | 105 | 96 | 83 |
| 0 | 13 | 1 | 787 | 100 | 0 | 29 | 300 | 67.0 | 78 | 84 | 30 | 8.5370 | 8.7459 | 13.3309 | 13.4126 | 122 | 82 | 5 | 30 | 105 | 96 | 84 |
| 0 | 14 | 1 | 0 | 0 | 0 | 31 | 495 | 33.0 | 77 | 82 | 10 | 8.4280 | 8.5378 | 13.7767 | 13.8823 | 122 | 82 | 5 | 30 | 73 | 94 | 79 |
| 0 | 15 | 1 | 0 | 0 | 0 | 32 | 500 | 33.5 | 77 | 82 | 10 | 8.4678 | 8.5878 | 13.8650 | 13.9732 | 122 | 82 | 5 | 30 | 73 | 97 | 84 |
| 0 | 16 | 1 | 0 | 0 | 0 | 31 | 500 | 33.5 | 79 | 82 | 10 | 8.5853 | 8.7118 | 13.7641 | 13.8707 | 122 | 82 | 5 | 30 | 73 | 98 | 85 |

| TEST DATE | RUN NO. | SHAPE NO. | RPM | BED MASS | BLK | H1 | H2 | P3 | T3 | T4 | TIME | IWI | FWI | IWO | FWO | P1 | P2 | P4 | P5 | P6 | T1 | T2 |
|---|---|---|---|---|---|---|---|---|---|---|---|---|---|---|---|---|---|---|---|---|---|---|
| 11771 | 0 | 0 | 0 | 0 | 1 | 0 | 0 | 0 | 0 | 0 | 0 | 9.2615 | 9.2959 | 14.4799 | 14.5296 | 0 | 0 | 0 | 0 | 0 | 0 | 0 |
| 0 | 0 | 0 | 0 | 0 | 1 | 0 | 0 | 0 | 0 | 0 | 0 | 9.3745 | 9.4107 | 15.0251 | 15.0750 | 0 | 0 | 0 | 0 | 0 | 0 | 0 |
| 0 | 0 | 0 | 0 | 0 | 1 | 0 | 0 | 0 | 0 | 0 | 0 | 9.1939 | 9.2282 | 14.4545 | 14.5044 | 0 | 0 | 0 | 0 | 0 | 0 | 0 |
| 0 | 0 | 0 | 0 | 0 | 1 | 0 | 0 | 0 | 0 | 0 | 0 | 9.2265 | 9.2607 | 14.8993 | 14.9492 | 0 | 0 | 0 | 0 | 0 | 0 | 0 |
| 0 | 0 | 0 | 0 | 0 | 1 | 0 | 0 | 0 | 0 | 0 | 0 | 9.2871 | 9.3214 | 14.5846 | 14.6325 | 0 | 0 | 0 | 0 | 0 | 0 | 0 |
| 0 | 2 | 1 | 787 | 100 | 0 | 32 | 500 | 67.0 | 79 | 85 | 30 | 9.7173 | 9.4843 | 14.3039 | 14.3825 | 122 | 85 | 5 | 30 | 107 | 98 | 85 |
| 0 | 3 | 1 | 787 | 100 | 0 | 32 | 500 | 66.5 | 80 | 87 | 30 | 9.3275 | 9.4984 | 14.9008 | 14.9745 | 122 | 85 | 5 | 30 | 107 | 102 | 88 |
| 0 | 4 | 1 | 900 | 100 | 0 | 32 | 500 | 78.5 | 78 | 84 | 30 | 9.2614 | 9.4314 | 14.4607 | 14.5526 | 122 | 87 | 5 | 30 | 120 | 97 | 85 |
| 0 | 5 | 1 | 900 | 100 | 0 | 32 | 505 | 78.5 | 80 | 87 | 30 | 9.3996 | 9.5735 | 14.9397 | 15.0260 | 122 | 90 | 5 | 30 | 120 | 101 | 87 |
| 0 | 6 | 1 | 900 | 100 | 0 | 32 | 505 | 76.0 | 81 | 88 | 30 | 9.2554 | 9.4282 | 14.4245 | 14.5013 | 122 | 90 | 5 | 30 | 120 | 103 | 88 |

# APPENDIX B

# SAMPLE CALCULATIONS

## Sample Calculations

Sample calculations are provided to demonstrate the procedures used to arrive at numerical values of filtration efficiency. Ten steps are involved and are illustrated using the data from 12-29-70.

Step 1. Determine the average weight change for the inlet blank filters (Corr 1) and the outlet blank filters (Corr 2).

$$\text{Corr 1} = \sum_{1}^{6} (\text{FWI} - \text{IWI})/6 \quad \text{(grams)}$$

$$\text{Corr 2} = \sum_{1}^{6} (\text{FWO} - \text{IWO})/6 \quad \text{(grams)}$$

| FWI (grams) | IWI (grams) | Corr 1 (grams) | FWO (grams) | IWO (grams) | Corr 2 (grams) |
|---|---|---|---|---|---|
| 8.4040 | 8.4073 | | 13.1797 | 13.1797 | |
| 8.5140 | 8.5160 | | 13.0656 | 13.0654 | |
| 8.6399 | 8.6427 | -0.0022 | 13.2724 | 13.2728 | -0.0004 |
| 8.3677 | 8.3706 | | 13.0086 | 13.0093 | |
| 8.5300 | 8.5316 | | 13.1790 | 13.1796 | |
| 8.4550 | 8.4554 | | 13.0283 | 13.0294 | |

Step. 2. Determine the volumetric flow rate through the inlet sampling system and the outlet sampling system for each test run. To do this, use the manometer readings H1 and H2 with the appropriate orifice calibration curves (see p. 128 and 129).

| Run no. | H1 (0.1 in) | Inlet flow rate (l/min) | H2 (0.01 in) | Outlet flow rate (l/min) |
|---|---|---|---|---|
| 4 | 31 | 338 | 55 | 276 |
| 5 | 29 | 328 | 55 | 276 |
| 6 | 30 | 333 | 50 | 258 |
| 7 | 31 | 338 | 55 | 276 |
| 8 | 30 | 333 | 55 | 276 |
| 9 | 29 | 328 | 50 | 258 |

Step 3. Correct the volumetric flow rates for temperature (correct to 20°C).

Corrected Inlet Flow Rate = Flow rate (528/(460 + T3)) (l/min)

Corrected Outlet Flow Rate = Flow rate (528/(460 + T4)) (l/min)

| Run no. | Inlet flow (l/min) | T3 (°F) | Corr. flow (l/min) | Outlet flow (l/min) | T4 (°F) | Corr. flow (l/min) |
|---|---|---|---|---|---|---|
| 4 | 338 | 73 | 335 | 276 | 76 | 272 |
| 5 | 328 | 75 | 324 | 276 | 77 | 271 |
| 6 | 333 | 75 | 329 | 258 | 78 | 253 |
| 7 | 338 | 75 | 334 | 276 | 77 | 271 |
| 8 | 333 | 74 | 329 | 276 | 77 | 271 |
| 9 | 328 | 75 | 324 | 258 | 78 | 253 |

Step 4. Calculate the total volume of gas flowing through each sampling system for each test.

Total Volume = Corr. Flow Rate (l/min) x Time (min)

| Run no. | Corr. inlet flow (l/min) | Time (min) | Total vol. (l) | Corr. outlet flow (l/min) | Time (min) | Total vol. (l) |
|---|---|---|---|---|---|---|
| 4 | 335 | 30 | 10,050 | 272 | 30 | 8,160 |
| 5 | 324 | 30 | 9,720 | 271 | 30 | 8,130 |
| 6 | 329 | 30 | 9,870 | 253 | 30 | 7,590 |
| 7 | 334 | 10 | 3,340 | 271 | 10 | 2,710 |
| 8 | 329 | 10 | 3,290 | 271 | 10 | 2,710 |
| 9 | 324 | 10 | 3,240 | 253 | 10 | 2,530 |

Step 5. Calculate the change in the inlet and outlet sampling filter weights corrected for the changes in the blank filters (see Step 1).

Inlet Filter Corrected Weight Change = FWI - IWI - Corr. 1 (grams)

Outlet Filter Corrected Weight Change = FWO - IWO - Corr. 2 (grams)

| Run no. | FWI (grams) | IWI (grams) | Corr 1 (grams) | Inlet weight change (grams) | FWO (grams) | IWO (grams) | Corr 2 (grams) | Outlet weight change (grams) |
|---|---|---|---|---|---|---|---|---|
| 4 | 8.5431 | 8.4491 | -0.0022 | 0.0962 | 13.1712 | 13.1609 | -0.0004 | 0.0107 |
| 5 | 8.8581 | 8.7574 | | 0.1058 | 13.5512 | 13.5450 | | 0.0066 |
| 6 | 8.6400 | 8.5300 | | 0.1122 | 13.0228 | 13.0187 | | 0.0045 |
| 7 | 8.4275 | 8.3650 | | 0.0647 | 13.8521 | 13.8182 | | 0.0343 |
| 8 | 8.5933 | 8.5320 | | 0.0635 | 13.3004 | 13.2702 | | 0.0306 |
| 9 | 8.4827 | 8.4239 | | 0.0610 | 13.5008 | 13.4728 | | 0.0284 |

Step 6. Calculate the concentration of aerosols entering and leaving the fluidized bed.

$$\text{Conc.} = \frac{\text{Corr. Wt. Change (grams)} \times 10^6 \text{ (micro-grams)}}{\text{Total Volume Sampled (liters)} \qquad \text{(gram)}}$$

| Run no. | Inlet weight change (grams) | Volume samp. (l) | Inlet aerosol conc. (micro-grams/l) | Outlet weight change (grams) | Volume samp. (l) | Outlet aerosol conc. (micro-grams/l) |
|---|---|---|---|---|---|---|
| 4 | 0.0962 | 10,050 | 9.572 | 0.0107 | 8,160 | 1.311 |
| 5 | 0.1058 | 9,720 | 10.885 | 0.0066 | 8,130 | 0.812 |
| 6 | 0.1122 | 9,870 | 11.368 | 0.0045 | 7,590 | 0.593 |
| 7 | 0.0647 | 3,340 | 19,371 | 0.0343 | 2,710 | 12.650 |
| 8 | 0.0635 | 3,290 | 19.300 | 0.0306 | 2,710 | 11.292 |
| 9 | 0.0610 | 3,240 | 18.827 | 0.0284 | 2,530 | 11.225 |

Step 7. Calculate the aerosol filtration efficiency of the system.

$$\text{Eff.} = 100 \times \left(\frac{\text{Inlet conc. (micro-grams/l)} - \text{Outlet conc. (micro-grams/l)}}{\text{Inlet conc. (micro-grams/l)}}\right)$$

| Run no. | Inlet conc. (micro-grams/l) | Outlet conc. (micro-grams/l) | Filtr. eff. (%) |
|---|---|---|---|
| 4 | 9.572 | 1.311 | 86.30 |
| 5 | 10.885 | 0.812 | 92.54 |
| 6 | 11.368 | 0.593 | 94.78 |
| 7 | 19.371 | 12.657 | 34.66 |
| 8 | 19.300 | 11.292 | 41.49 |
| 9 | 18.827 | 11.225 | 40.38 |

Step 8. Calculate the average filtration efficiency of the system when no bed material is present. This situation exists for runs 7, 8, and 9 of 12-29-70 for Shape II at Flow Level I.

$$\text{Average Filtr. Eff.} = \frac{34.66 + 41.49 + 40.38}{3.0} = 38.84\%$$

Step 9. Calculate filtration efficiencies for the fluidized bed using the average filtration efficiency obtained in Step 8.

Fluid. Bed Filt. Eff. = Tot. System Eff. (%) - Eff. Without Bed Mat'l (%)

| Run no. | Entire system filtr. eff. (%) | Filtr. eff. without bed material (%) | Fluidized bed filtr. eff. (%) |
|---|---|---|---|
| 4 | 86.30 | 38.84 | 47.46 |
| 5 | 92.54 | 38.84 | 53.70 |
| 6 | 94.78 | 38.84 | 55.94 |

Step 10. Calculate the average filtration efficiency of the fluidized bed for each condition of bed shape and flow level. The example given is for Shape II and Flow Level I.

$$\text{Average Filtr. Eff.} = \frac{47.46 + 53.70 + 55.94}{3.0} = 52.3 \ (\%)$$

# APPENDIX C

# ORIFICE CALIBRATION CURVES

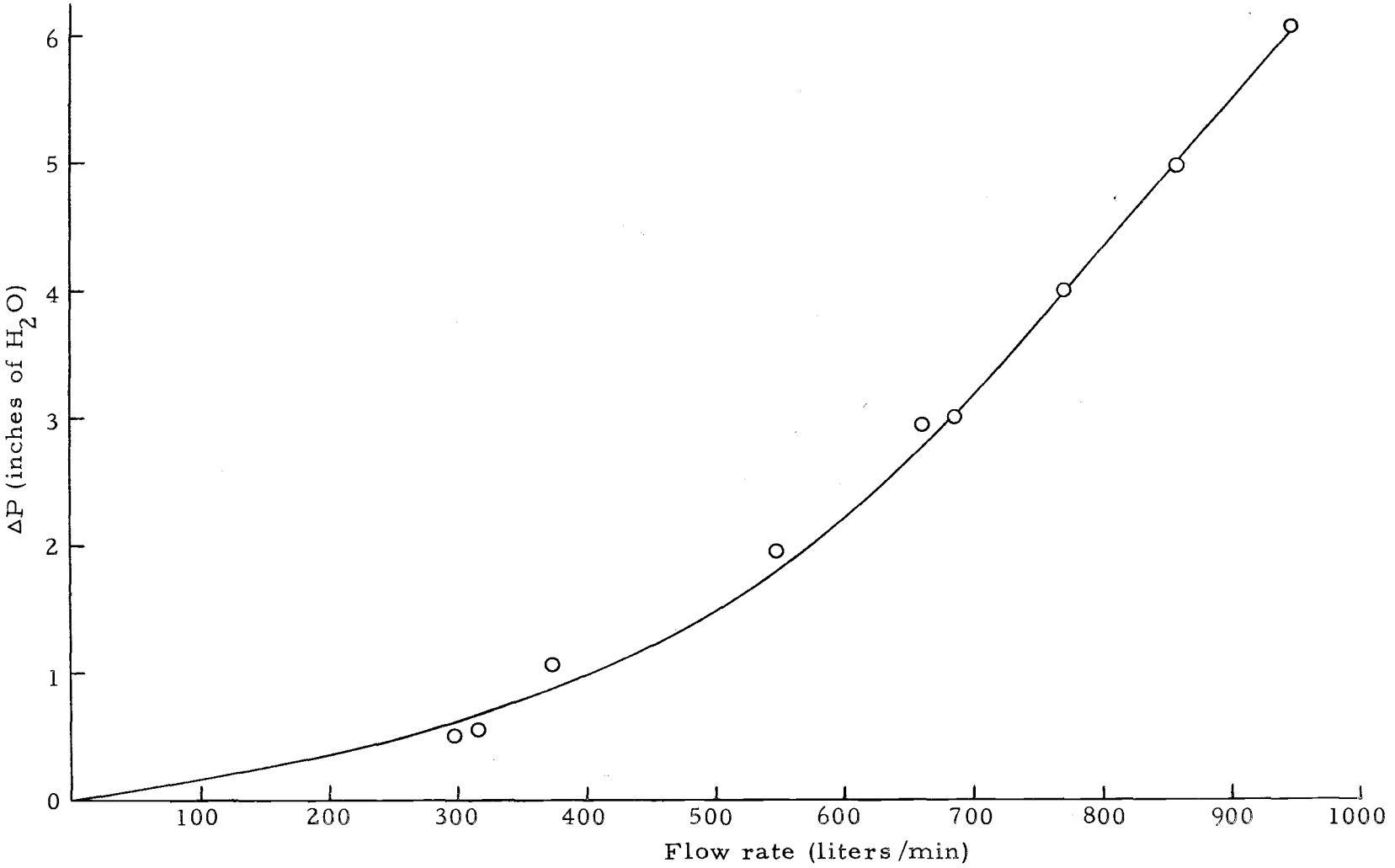


Discharge sampler orifice calibration curve; 11/16" Ø orifice measured with inlet pressure = 30 PSIG and corrected for temperature to 68°F.

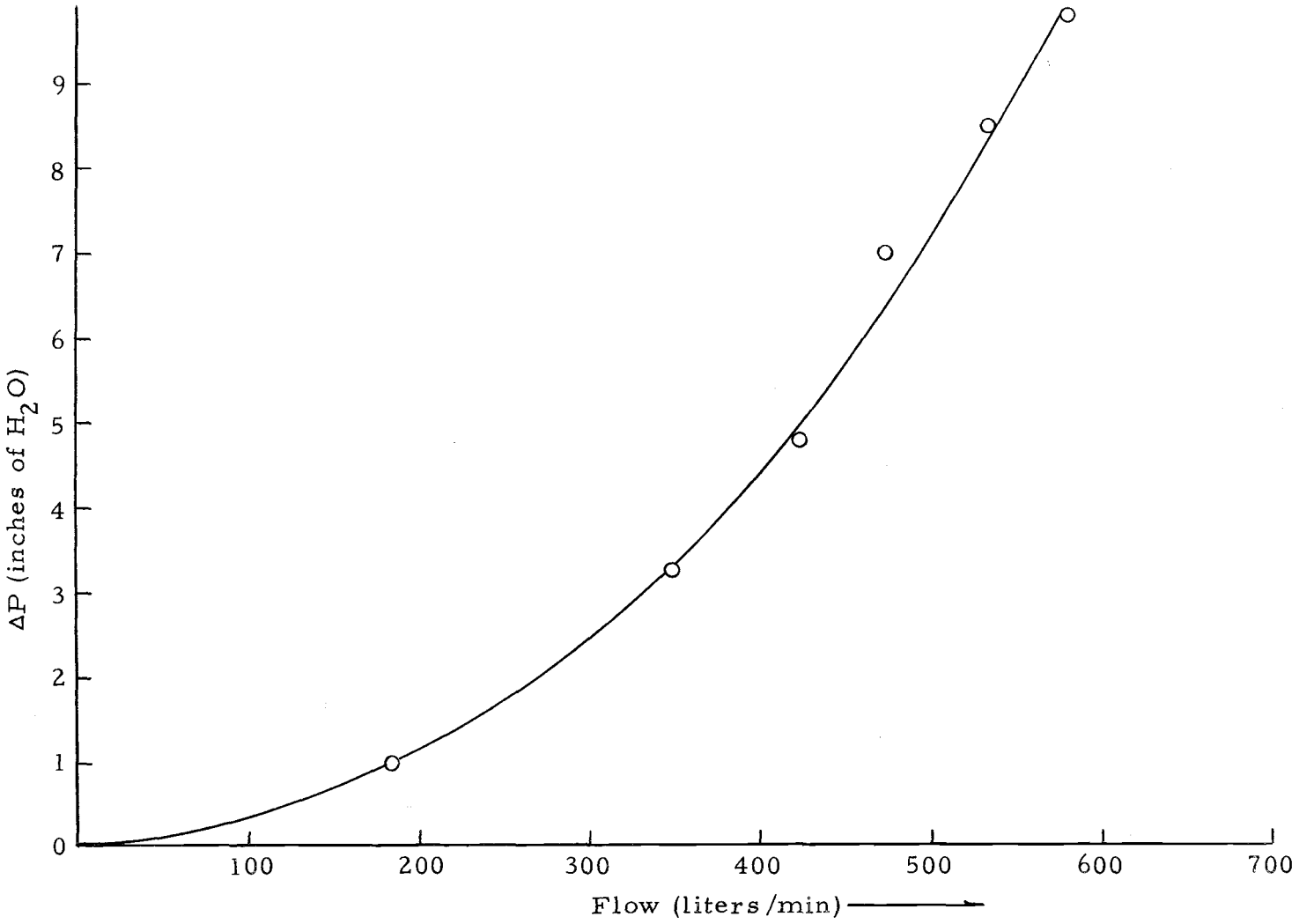


Inlet sampler orifice calibration curve; 1/2" Ø orifice measured with inlet pressure = 5 PSIG and corrected for temperature to 68°F.

# APPENDIX D

## BOOKS AND JOURNALS RELATED TO FLUIDIZATION ENGINEERING

Books and Journals Dealing with Fluidization
Which are Available

Black, C. H. Effectiveness of a fluidized bed in filtration of air-borne particulate of sub-micron size. Doctoral Dissertation, Oregon State University, 1967.

Fluidization, Chemical Engineering Progress Symposium Series, no. 38, Vol. 58, 1962.

Fluidized bed technology, Chemical Engineering Progress Symposium Series, no. 67, Vol. 62, 1966.

Fluid particle technology, Chemical Engineering Progress Symposium Series, no. 62, Vol. 62, 1966.

Hatch, L. P. Brookhaven National Laboratory fluidized bed studies, Brookhaven National Laboratory, Upton, L. I., New York

Kunii, D. and O. Levenspiel. Fluidization engineering. New York, John Wiley and Sons, 1969. 534 p.

Leva, Max. Fluidization. New York, McGraw-Hill, 1959. 327 p.

Othmer, D. F. Fluidization. New York, Reinhold, 1956. 231 p.

Symposium on the interaction between fluids and particles. London, Institution of Chemical Engineers, 1962.

Zabrodsky, S. S. Hydrodynamics and heat transfer in fluidized beds. Originally published in Russian by Fizmatgiz, Moscow-Leningrad, 1963. 379 p. Translated by Scripta Technica, Inc., Copyright 1966 by the Massachusetts Institute of Technology.

Zenz, F. and D. F. Othmer. Fluidization and fluid-particle systems, New York, Reinhold, 1960. 513 p.